GASIFICATION OF MUNICIPAL SOLID WASTE AND ITS IMPACT ON ENVIRONMENT

A Thesis

Submitted in Fulfillment of the Requirements for

The award of the Degree of

DOCTOR OF PHILOSOPHY

By

Raj Kumar Singh

University Enrollment No. Ph.D-74/08

Department of Mechanical Engineering
Faculty of Technology
University of Delhi

December 2012

CERTIFICATE

Certified that the thesis entitled "GASIFICATION OF MUNICIPAL SOLID WASTE AND ITS IMPACT ON ENVIRONMENT" being submitted by Mr. Raj Kumar Singh [Enrollment Number - 74/08] to Faculty of Technology, University of Delhi, in the fulfillment of the requirement for the award of the degree of Doctor of Philosophy from University of Delhi, is an authentic record of candidate's own research work carried out by him under our guidance and supervision. It is also certified that this research work being submitted herein has attained the standard required for a Ph.D. degree from the University of Delhi. Moreover, the results embodied in this thesis have not been submitted in part or full to any other University/Institute for award of any degree or diploma/certificate.

S. Maji
Supervisor
Professor
Department of Mechanical Engineering
Delhi Technological University
Delhi

Sanjeev Kumar Makin
Joint Supervisor
Professor
Department of Chemistry
DCR University of Science & Technology
Murthal, Haryana

Raj Senani
Professor & Head
Department of Mechanical Engineering
Faculty of Technology
University of Delhi
Delhi

Avdhesh Kumar Sharma
Joint Supervisor
Associate Professor
Department of Mechanical Engineering
DCR University of Science & Technology
Murthal, Haryana

DECLARATION

It is hereby to declare that the Ph.D. thesis entitled "GASIFICATION OF MUNICIPAL SOLID WASTE AND ITS IMPACT ON ENVIRONMENT" which has been submitted to the Faculty of Technology (Department of Mechanical Engineering), University of Delhi, in fulfillment for the award of the Degree of Doctor of Philosophy, is an authentic record of my own work (Raj Kumar Singh, Enrollment Number – 74/08). This research work has been carried out by me under the guidance of my supervisors Dr. S. Maji, Dr. Sanjeev Maken and Dr.Avdhesh Kr. Sharma. It is also to certify that the results embodied in this thesis have not been submitted in part or full to any other University/Institute for award of any degree or diploma/certificate.

Raj Kumar Singh
Ph.D. Scholar
Enrollment Number - 74/2008
Department of Mechanical Engineering
Faculty of Technology
University of Delhi.

Acknowledgements

During the course of this Ph.D, the guidance and support of several people has greatly assisted in carrying the work forward. I am deeply indebted to my supervisors Dr. S. Maji, Dr.Sanjeev Maken and Dr. Avadhesh Kr. Sharma for their guidance and clear sighted, objective thinking throughout the project. I am deeply grateful to Dr. B.D.Pathak for his encouragement and support.

Dr.L.N.das, Dr.Amit Pal, Dr. Praveen, Mr H. Das, Mr. Anoop Gupta and Mr.Roshan also provided significant help. I wish to express my heartfelt thanks to my friends, students, staff and family for their goodwill and support that helped me a lot in successful completion of this project.

Raj Kumar Singh

ABSTRACT

Management of municipal solid waste (MSW) is a serious problem, the world over. Presently, landfilling practice is one of the most common ways of MSW disposal in metropolitan cities. In Delhi itself, there are three major dumping grounds for MSW disposal, which are either exhausted or are on the verge of exhaustion. Developing new landfill is not only a difficult task but also a costly affair (as land is a scarce commodity in Delhi), and thereby a lot of importance is being given to find out cost effective and cleaner alternative for MSW disposal problem. High temperature energy recovery from MSW, usually known as Waste-To-Energy (WTE), is a promising technology for energy recovery, landfill materials reduction, preventing air and water contamination, safe waste disposal, improves recycling rate and lessens the dependence on fossil fuel. Gasification technology via thermochemical route is a kind of WTE technology. For gasification, even a pre-treated MSW or refuse derived fuel (RDF) is a problematic fuel (with low calorific value, high moisture and ash content compounded with unfavourable ash behaviour). Utilization of such feedstock in conventional fixed bed gasification systems poses additional challenges, whereas, MSW is seen as potential alternative solid fuel to the woody biomass. Moreover, from the past unfavorable experiences of MSW based thermal treatment (incinerator) plant at Timarpur in Delhi, a careful and comprehensive solid waste analysis is essential for making correct choice and successfulness of WTE technologies.

This work, therefore, focuses on characterization of physical, chemical and thermal properties of MSW/RDF received from three major landfill sites in Delhi namely Bhalaswa, Gazipur and Okhla. The aim of this study is to perform a thorough waste characterization (influence of season and location on MSW composition) of MSW in Delhi. The tests were performed to classify the raw MSW and to investigate physical and chemical composition of MSW, RDF and residual ash. It is revealed that organic component is relatively high, fuel and inert components are around 24% each, and recyclables are very low in Delhi waste. The processing or pretreatment of raw MSW is necessary before utilization in WTE technologies. Furthermore, experiments were performed on 10 kWe downdraft biomass gasifier using a mixture of RDF pellets and wood biomass of desired size in proportion of 1:1. The 10 kW converted engine (single fuel mode)

with an electric generator, coupled with the gasifier, was used to produce electric power. Exhaust emissions from gasifier-engine system and pollutants in re-circulated spray water over hot syngas for cooling have been measured as a function electric load. The emissions from engine exhaust are observed to be within the safe emission limits, while level of pollutants in re-circulated water was found to be higher than prescribed limits of Central Pollution Control Board (CPCB) of India.

Computational efforts for predicting syngas composition and landfill gas (LFG) emissions are also employed. An equilibrium and kinetic modeling was developed to predict steady state performance of downdraft gasifier in terms of syngas composition. The predictions were compared against experiments for validation. A 2-dimensional numerical model for a 10 kWe downdraft gasifier was also built employing a CFD code Fluent 6.2 followed by Gambit 2.4 (for geometrical treatment) to predict temperature and flow fields in reduction zone, where as the governing equations were solved using inbuilt FDM by assigning appropriate properties of species and solid biomass. The turbulence-chemistry interactions were taken into account by using the eddy dissipation concept (EDC) model together with in-situ adaptive tabulation (ISAT) algorithm to dynamically tabulate the chemistry mapping and to reduce the time of solution. The initial and boundary conditions of the gasifier were applied carefully to verify the distribution of temperature and gas composition at outlet of the reduction zone against measurements.

Air pollutants from landfill sites pose adverse impact on the environment. The computations are performed using commercially available software LandGEM to predict LFG emissions for three major landfill sites in Delhi. The policy options proposed in waste management policy were analysed under two possible scenarios first when MSW is continuously dumped at landfill sites till 2020 and in second case if MSW, instead of getting dumped into landfills is utilized in gasifier-engine systems from 2012 onwards to produce electricity. Forecasting for baseline scenario revealed that Delhi will produce 2.134×10^{5} Mg/year methane emission in 2021. The treatment capacity enhancement by introducing WTE, for producing 55MW electricity from RDF would reduce methane emission by 368236 Mg in next 20 years. The production of electricity by using WTE technology is expected to replace the fossil fuel.

Principal recommendation for utilization of processed MSW in conventional downdraft gasifiers is thorough characterization, processing raw MSW for enriching energy density (like RDF), careful apportionment of RDF and woody biomass feedstock, specific selection of gasifier design configuration and matching of thermal system response; such coupled gasifier-engine-systems for power production application can be seen as feasible solution for depleting resources of fossil fuel along with MSW disposal problem and degrading environment leading to climate change.

TABLE OF CONTENTS

Nomenclature

a	Absorption Coefficient
$a_{\in,i}$	The weighting factor depends on temperature
$\bar{a}_p$	Average of the momentum equation coefficients for the cells on either side of the face
A'	Pre-exponential Factor in Arrhenius Formula
A	Surface Area
b	Temperature Exponent in Arrhenius Formula
$b_{\in,i,j}$	The emissivity gas temperature polynomial coefficients
c_i	Concentration of Species *i*
C_p	Specific Heat Capacity at Constant Pressure
$C_{1\varepsilon}$, $C_{2\varepsilon}$	Constants of Standard k-ε Model
C_i	Vapor Concentration
C_D	Drag Coefficient
C_{RF}	Char reactivity factor
CV	Control volume
d_p	Particle Diameter
$\Delta G_j^0(T)$	Gibbs function
D	Diffusivity
$D_{i,m}$	Mass Diffusion Coefficient
D_f	transport due to the diffusion through the face f
$D_{T,i}$	Coefficient of thermal diffusion
E	Total Energy
E_p	Equivalent Particle Emission

E_a	Activation energy
f_{pn}	Scattering Factor of Particle n
F	Lorentzian Broadening Factor
$\vec{F}$	Force Vector
$\vec{F}_D$	Drag Force
ϕ_f	A first-order upwind scheme indicating that the face value f
g	Gravitational Acceleration
G	Incident Radiation
G_k	Production of Turbulent Kinetic Energy
Γ_ϕ	The diffusion coefficient
h	Species Enthalpy
$\bar{h}_I$	Sensible enthalpy change
h	Convective Heat Transfer Coefficient
$h_j^0(T_{\partial ref})$	Enthalpy of formation species j at reference temperature
h_{fg}	Latent Heat of Evaporation
H	Total Enthalpy
Hlat,ref	Latent Heat at Reference Condition
Hv	Net heat (lower heating values) of combustion of reactants
ΔH_j^0	Enthalpy change of reaction at standard conditions
I	Radiation Intensity
$\vec{J}_i$	Diffusion Flux
J_f	The mass flow is rate through the face f
k	Turbulent Kinetic Energy
$-k_{eff} A.\nabla T$	Axial heat transports
K_{eq}	Equilibrium constant

k_{eff} effective thermal conductivity

$\boldsymbol{K_{eq\,j}}$ Equilibrium constant for reaction j

k_f , $\boldsymbol{k_r}$ Rate Constant for Forward / Reverse Reactions

k∞ Thermal Conductivity of Continuous Phase

k_∞ high pressure limit

k_0 low pressure limit

Le Lewis Number

LHV Lower Heating Value

m Mass

$\dot{m}$ Mass Flow Rate

$\boldsymbol{\dot{m}_{char}}$ Inflow and outflow rates in each control volume

Mw,i Molecular Weight of Species i

$n_{i,f}$, $n_{i,r}$ Reaction Orders of Forward / Reverse Reactions

$\boldsymbol{n_{kl}}$ Molar flow rate of species k

N Number of Chemical Species

Nu Nusselt Number

$\nabla.\left(\rho\overline{\vec{v}'\vec{v}'}\right)$ Fluctuation in turbulent flows

p Pressure

P_e The Peclet number

σ_k Prandtl Number

σ_ε Scattering coefficients

q_r substituted into the energy equation to account for heat sources (or sinks) due to radiation

Qrad Radiative Heat Flux

$\dot{Q}_{loss}$ Heat loss rate from I^{th} CV to the surrounding

$\dot{Q}_{reac}$ Endothermic heat absorption rate

Q_{CH4} Annual methane generation in the year of the calculation

R Universal Gas Constant

Re Reynolds Number

R_i Production of i^{th} species due to chemical reaction

Re_{ij} Reynolds Stresses

Rt_k Net production rate of species k in the control volume

S Source Term

S_i Other source term

Sij Mean Rate-of-Strain Tensor

S_{ct} Turbulent Schmidt Number

Sh Sherwood Number

S_ϕ The source of ϕ per unit volume

S_m the mass added to the continuous phase from the dispersed second phase

ΔS_j^0 Entropy change of reaction at standard conditions

t Time

t_{cross} Particle Eddy Crossing Time

T Temperature

Tbp Boiling Temperature

Tvap Evaporation Temperature

Tw Gasifier Wall Temperature

$\bar{\tau}$ Stress tensor

u_i Velocity Magnitude

$u = \bar{u} + u'(t)$ Instantaneous gas velocity

u_p Particle Velocity

v Overall Velocity Vector

v_i' The stoichiometric coefficients for reactants

ν_i''	The stoichiometric coefficients for products
V	Volume
$V_{CV,I}$	Volume of I^{th} control volume
x_i	Direction
χ_{eq}	Equilibrium mole fractions
Xi	Mole Fraction of Species i
Y_j	Mass Fraction of Species j
Zi	Mass Fraction of Element i
α	Bell-Evans-Polanyi Factor
δ	Delta Function
p_n	Emissivity of Particle n
$\rho\vec{g}$	The gravitational body force
ε	Turbulent Dissipation Rate
ζ	Normally Distributed Random Number
ηk	Kolmogorov Length Scale
θR	Radiation Temperature
λ	Air-Fuel Ratio
λ	Thermal Conductivity
λeff	Effective Thermal Conductivity
λt	Turbulent Thermal Conductivity
μ	Dynamic Viscosity
μt	Turbulent Viscosity
ν	Kinematic Viscosity
ξ*	Length Fraction of Fine Structures
ρ	Density
ρ∞	Density of the Oxidizer Stream

σ	Stefan-Boltzmann Constant
σp	Equivalent Particle Scattering Coefficient
σs	Scattering Coefficient
τ	Time Scale
$\tau *$	Time Scale of Fine Structures
χ	Scalar Dissipation Rate
ωk	Angular Velocity
Δt	Time Step
ϕ	Phase Function
Ω'	Solid Angle
Ωij	Mean Rate-of-Rotation Tensor

List of Figures

List of Tables

List of Abbreviations

AMG	Algebraic multi grid
BHTGS	Battelle high throughput gasification system
CAA	Clean Air Act
CFB	Circulating fluidized bed
CFD	Computational fluid dyanamics
CGE	Cold gas efficiency
CPCB	Central pollution control board
CRF	Char reactivity factor
C_{RF}	Char reactivity factor
CV	Control volume
DPM	Discrete phase model
DRW	Discrete random walk
EDS	Energy dispersive X-ray spectrometry
EIA	Environmental Impact Assessment
EDC	Eddy dissipation concept
EPI	Energy Products of Idaho
GHGs	Green house gases
HTR	High temperature recycling
HAPs	hazardous air pollutants
IGCC	Integrated gasification combined cycle
IMD	India Meteorological Department
IPCC	Intergovernmental panel on climate change
ISAT	in-situ adaptive tabulation
LCI	Life-cycle inventory
LFG	Landfill Gas
MCD	Municipality Corporation Delhi
MEET	Multi-staged enthalpy extraction technology
Mg	Mega gram
MT	Metric ton
MTCI	Manufacturing and technology conversion international, Inc

MSW	Munispality solid waste
NDMC	New Delhi Municipality Corporation
NEERI	National environmental engineering research institute Nagpur India
NMOCs	Non-methane organic compounds
PPMV	Parts per million by volume
PTFV	Potential tar formation volume
RCBC	Rotary cascading bed combustor
RDF	Refuse derived fuel
TGA	Thermo gravimetric analysis
WSGGM	Weighted sum of gray gases model
WTE	Waste to energy
VOCs	Volatile organic compounds

Chapter 1

INTRODUCTION

1.1 Background

The quantity of MSW has increased exponentially in metropolitan cities of India. Its safe disposal is an alarming issue due to scarcity of space for dumping MSW in landfill sites. The disposal also creates an adverse environmental impact (Metin et al. 2003). In India, the metropolitan cities are generating increasing amounts of municipal solid waste (DPCC 2008; Gupta et al. 1998). An estimate (Sharholy et al. 2007) shows that Delhi contributed 2,172,138 MT MSW in the year 2011, where land-filling practice is the main option for solid waste disposal. In Delhi, there are three major landfills for MSW disposal namely at Bhalaswa, Gazipur and Okhla. All these three landfills have already exhausted their capacity (City Development Plan Delhi 2006). The conventional waste disposal model through landfills requires a huge space which is highly uneconomical (He et al. 1997). Moreover, it has serious environmental impacts as it results in the release of harmful greenhouse gases (GHGs), volatile organic compounds etc., and leachable toxic heavy metals which contaminate the nearby river water as well as underground water (IPCC 2001; Kjeldsen et al. 2002; Shin et al. 2005).

On the other hand MSW can be considered as a source of valuable solid fuel which can be utilised for energy and power generation applications, and for other industrial purposes (Kwak et al. 2006; Advanced Energy Strategies 2004; Belgiorno et al. 2003; Arena 2011; Bjorklund et al. 2001). The MSW consists of heterogeneous materials whose chemical composition, size and shape vary significantly depending upon the location, local policy, the origin of waste, consumption pattern etc. MSW generated in

Delhi has significantly low heating value (Manual on Municipal Solid Waste Management 2000) and it has a high inert content along with a high degree of non-homogeneity that poses difficulty for its thermal treatment in addition to serious environmental impact (McKay 2002). For instance, the use of unprocessed MSW in direct combustion and incineration process discharges extremely hazardous compounds such as dioxins and furans (Littarru 2006). Some researchers proposed that raw MSW having low heating value due to high inert component and moisture content can be transformed into better form RDF by separating the non-combustible portion from MSW (Eighmy et al. 1996). The RDF is relatively rich in energy content (i.e., heating value in the range 6.3-13.4 MJ/kg) and has lower ash content than raw MSW (Jidapa 2007; Gendebien 2003). This energy dense RDF, can be processed effectively by various WTE technologies including incineration, pyrolysis and gasification for recovering energy and disposal of MSW (Dalai et al. 2009). High temperature energy recovery from MSW is usually known as WTE technology (Morris 1998). On one hand, it reduces the pressure of MSW disposal at landfills and the dependence on fossil fuel (Dong et al. 2002); while on the other hand, it prevents air, water and soil contamination (Defra 2007). MSW dumped in various landfills is generating contaminated air, water and soil in addition to formation of huge amount of gases mainly methane, which is a serious contributor to global warming. Under the business-as-usual scenario, the conventional model of waste disposal can not run in long run. With scarcity of land and environmental constraints of land-filling, cleaner and cost effective technologies for treatment and disposal of huge resources of MSW should be identified and need to be implemented in present context (Murphy 2006).

For the year 2011, Delhi itself generated 2,172,138 MT MSW (CPCB 2012). Gasification is one of the several technologies, which can use such huge stocks for thermal application, motive power or electricity generation in addition to safe disposal of MSW (Consonni 2010). The technology has been known for quite a long, and was used extensively in Germany, Britain and even in India during the Second World War when oil and gas became scarce. In the past few decades, many researchers have been working towards improvement in the technology and its commercialization, particularly for motive power generation applications (Sharma 2006). The technology

has a very high potential to serve rural and urban needs for energy and power applications (Malkow 2004). Safe disposal of MSW via thermochemical route poses more challenges both technically and otherwise. This forms the focus of present work, which could contribute in efficient utilization of MSW for energy and power needs of the society along with facilitating environmentally safe disposal of huge MSW volumes.

1.2 Technologies for processing of MSW

There are several technologies for treatment of MSW which include sorting, recovery of secondary materials from waste (i.e. recycling), biological and thermal treatment of waste for energy recovery (Bebar et al. 2002). Incineration and gasification are among the two most commercially viable options for large scale treatment of MSW (E4tech 2009; Bebar et al. 2005; Kwak et al. 2005). Over the years, incineration of combustible waste is used for reducing mass and volume of MSW and recovery of energy from such huge MSW stocks (Liu 2005). However, incineration practice of MSW generates fly and bottom ashes, release of leachable toxic heavy metals, and responsible for formation of extremely hazardous dioxins and furans, and volatile organic compounds (Park et al. 2005). Stringent environmental regulations are being imposed by the government to control the environmental impact of MSW and incinerator residues (Kennan 2006). Melting of these ashes at high temperature, known as vitrification can further shrink the volume up to 50%; it destroys more than 98% of polycyclic organic compounds and also provides less leachable heavy metals (Kiss 1994; Maken 2005; Hyun 2004). Melting of MSW ash at temperatures higher than 1400^{o}C modify the state of ash and transform it into a type of glass that is innocuous to the environment and is a valuable source of secondary raw material with applications in construction and road building industries (Hyun et al. 2004; Park et al. 2005; Ferraris et al. 2009). Unfavourably, the technology consumes a large amount of electric energy, and hence is not economically viable. Therefore, in long run, incineration can not be seen as volume and mass reduction process for dealing with MSW. Increasing space constraints for landfilling of MSW and public opposition to new incinerators for waste disposal has effectively eliminated such an option for the

near future in many countries (Porteous 2001). Thus, there is a need to consider MSW as a valuable, abundantly available feedstock for substituting the fossil fuels for urban power generation and for other industrial applications.

In recent years, several new technologies including gasification or combinations of pyrolysis, gasification and melting processes are currently being brought into the market for energy efficient, environment friendly and economically sound approaches to thermal treatment of different wastes (Kwak et al. 2006; Gomez 2009; Higman 2003). Gasification is a very efficient process for environmentally safe disposal of MSW that devolatilizes the solids feedstock to convert it into a syngas or fuel gas. Gasification has several advantages over traditional combustion of MSW (Granatstein 2003). MSW pyrolysis and in particular gasification is obviously very attractive to reduce and avoid corrosion and emissions by retaining alkali and heavy metals (except mercury and cadmium), sulphur and chlorine within the process residues, prevent largely PCDD/F (Kwak et al. 2006; Kim et al. 2007; Huang 2001) formation and suppresses thermal NO_x formation due to lower reaction temperatures followed by reduction reaction environment. Slagging may additionally provide for destructing hazardous compounds and vitrification of various residues (Jimbo 1996; Hyun 2004). Additionally, components of Cl and S (such as HCl and H_2S) may be present in the fuel gas. Favourably, gasification leads to production of smaller gas volume which requires smaller gas cleanups, saves investment in equipments costs (Kawaguchi 2002) etc. While utilization of oxygen fuel enriches the calorific value and prevents thermal NO_x formation, it increases the operating costs (Lee et al. 2005). The fuel gas can be used in various applications, for instance, lime and brick kilns, metallurgical furnaces, dryers, steam-raising boilers, gas-engines and gas-turbines, fuel cells etc. It can also be used as a raw material for synthetic natural gas, methanol synthesis, fuel production etc. Often, gas cooling and cleaning is required.

Recently, advanced thermal waste treatment technologies combining pyrolysis (themolysis), gasification and/or incineration in an integrated/modular approach are emerging from long lasting research with the primary aim of improving environmental compliance by effective destroying air pollutants and vitrification of

the solid process residues, and also to recover materials and energy, thus saving disposal costs but at the expense of overall energy output (Lombardi 2012). The conventional gasification technology, however, can be seen as a low cost alternative to treat MSW for safe disposal in addition to energy recovery.

1.2.1 Gasification technology

Gasification is a thermal upgrading process, which takes place in two stages. During the first stage, the feedstock thermally decomposes into char (a kind of solid residue) and volatile matter. During the second stage, the char and volatiles get converted into producer gas under the restricted supply of air. Producer gas as obtained from the gasification of charcoal or biomass is a low energy gas. The combustible constituents are primarily carbon monoxide and hydrogen, while small percentage of methane is also present in the gas. The non-combustibles include carbon dioxide and nitrogen. The calorific value of final gas obtained from wood generally varies from 3.5 to 5.7 MJ/Nm^3. The syngas/producer gas obtained can either be used for thermal application or mechanical/electrical power generation. For thermal applications viz. dryers, kilns, furnaces, boilers etc., the syngas/producer gas can be burnt in burners to generate thermal energy. For mechanical/electrical power generation applications, the producer gas is used in IC engines. The motive power from the engine can be used either directly for water pumping, flour mill etc. or it can be converted into electric power by coupling with an alternator. For use in I.C. engines, the tar and particulate matter in the gas must be removed and gas should be cooled properly before induction in the engine, otherwise they can seriously affect the life and performance of the gas-engines/gas-turbines (Sharma 2006). Thus in systems using syngas/producer gas for motive power generation, the gasifier should be coupled with a suitable cooling and cleaning unit. A typical power production plant using MSW can be schematically shown as in Fig. 1.1

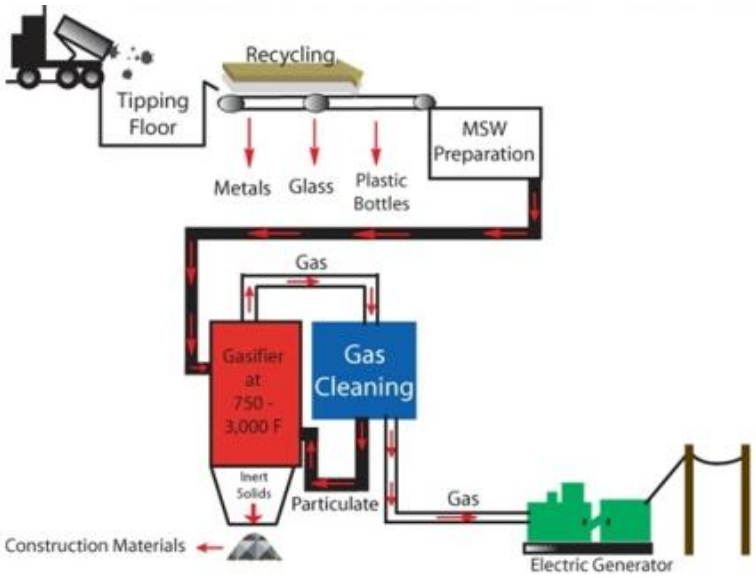

Fig. 1.1 Schematic of a typical Power Production Plant using MSW (Advanced Energy Strategies Inc. 2004)

Power production from MSW via gasification is accomplished in three stages including MSW handling and processing, conversion of MSW into a synthetic gas and electricity generation. During first stage, raw MSW is delivered through garbage trucks, commercial collection bins and by various other means. The feedstock is pre-processed up to the acceptable form for a gasifier. In next stage, processed MSW is heated in a gasifier under limited oxidant in order to facilitate thermochemical transformation of MSW into synthetic gas. In third stage, the synthetic gas is used for production of electricity.

(a) MSW handling and processing

MSW processing begins with "tipping" MSW onto a receiving floor. Unlike tipping facilities at many conventional MSW transfer stations, the tipping floor in a thermal MSW gasification power plant is fully enclosed inside the building where subsequent processing takes place. This largely eliminates the odors and litter often associated with conventional transfer stations. The MSW processing function depends on the requirements of the gasifier. The common elements of MSW processing include additional sorting, recycling, shredding, sizing and drying. Sorting and recycling

remove material from the MSW that cannot be gasified, such as metals, glass and other inert materials. Heating these inert materials in a gasifier would waste energy, reducing the efficiency of gasification. Metals and much of the glass that are sorted out of the MSW are recycled. Paper and plastic that are suitable for recycling can also be sorted out at this stage. All of the materials that are recycled in this step represent additional recycling that takes place after source recycling. The shredding and sizing functions reduce MSW to a size that allows it to be processed in the gasifier. Drying the MSW removes the moisture from feedstock for enhancing thermal efficiency of a gasifier.

(b) Conversion of MSW into syngas

In the second stage, the pre-processed MSW is transformed into a synthetic gas via thermal gasification. As described in earlier section, MSW is a non-homogeneous material with varying chemical composition, thus chemical reactor (i.e., gasifier) requires flexibility to handle such feedstock. Presently, there are three methods that can be employed for converting MSW into synthetic gas namely- pyrolysis, conventional gasification, and plasma gasification (Lemmens et al. 2007). All these methods involve high reaction temperatures and strict control of oxidant for favourable reaction rates. Product gas from the gasifier contains particulate matter in addition to heavy metals, ammonia, hydrogen chloride, hydrogen sulphide, and NO_x. The product gas requires further treatment. Treatment technologies employ educate cooling and cleaning arrangement including - scrubbers, baghouse filters, electrostatic precipitators, and cyclone separators.

(c) Electric generation

Power generating systems can be integrated with a MSW gasification system, for instance steam boilers, reciprocating engines, gas-turbines, combined cycle turbines and fuel cells (Holt 2005). Combustion boilers have the highest tolerance for tars and other impurities but are also the least efficient (~31%) from thermal energy conversion point of view. In contrast, combined cycle turbines, reciprocating engines and fuel cells offer operational efficiencies of 40%. For small power level range,

reciprocating engines are identified to be more economical, while steam/gas turbines are economical in large power range (Bridgewater 1995).

1.22 Waste-to-energy (WTE) technologies

In an incineration plant, the MSW is burned to produce heat which is utilized in boiler tubes to produce high potential steam, which is used to drive the turbine and hence the generator to produce electricity. Incineration plants typically include some pre-treatment and processing of the MSW in order to remove non-conforming wastes and recyclables. High moisture in MSW feedstock reduces the efficiency of the incinerator/boiler. A high level of pre-treatment is used to produce RDF. The Table 1.1 presents a review of early developments using waste gasification/ pyrolysis (Niessen 1996; Baggio 2008**)**.

1.23 Lesson from failure of Timarpur (Delhi) plant

A thermal treatment pilot plant of capacity 300 tonnes/day was set up in 1987 at Timarpur, Delhi. The plant was based on the technology supplied on Turn-key basis by M/s Volund of Denmark, which was to produce 3.75MW electricity. A waste management system with adequate segregation is considered a pre requisite for any waste incineration project to be successful and effective. The plant was operational hardly for a few months. It subsequently closed down due to a mismatch of the incoming refuse quality with the plant requirement (i.e., 1460 kcal/kg of net calorific value MSW). The reasons for the 'failure' are reported to be low heat value and high ash contents of Delhi's MSW (Manual on Municipal Solid Waste Management, 2000). Therefore careful and comprehensive solid waste analysis is a necessary condition for the correct choice and success of waste-to-energy technologies.

Table 1.1 Assessment of thermochemical conversion systems using biomass/MSW/RDF.

Designation	Gasification/ Pyrolysis	Reactor Technology	Waste fuel	Product (gas/liquid)	Operation
Voest Alpine	Gasification	Atmospheric Fixed Bed	RDF	Gas LHV	Abandoned (1991)
University of Sherbrooke	Gasification	Atmospheric Fluidized Bubbling	RDF	Gas LHV	Pilot Plant (1978)
TPS	Gasification	Atmospheric Fast fluidized+ CFB cracker	RDF	Gas LHV	Pilot Plant(Demo Gasifier Greve Ansaldo) (late 1980's)
Sofresid/ /Caliqua	Gasification	Atmospheric Updraft-fixed bed	RDF, MSW	Gas LHV	Commercial(early 70's)
Battelle	Gasification	Atmospheric Fluidized, bubbling	RDF	Gas MHV	Pilot plant (1980)
Lurgi	Gasification	Atmospheric Fast fluidized	RDF, MSW (shredded for metals)	Gas LHV	Commercial(mid 80's)
Purox	Gasification	Fixed Bed	MSW	Gas	Demo (mid 70's)
Pyrogas	Gasification	Fixed Bed	MSW	Gas+ Liquid	Demo(1974)
Destrugas	Pyrolysis	Fixed Bed	MSW	Char	Pilot plant (1970)
Landgard	Gasification	Moving Bed	MSW	Gas	Demo (mid 70's)
Garret Occidental	Pyrolysis	Fixed Bed	Shredded	Liquid	Demo (mid 70's)
Energy Product of Idaho	Gasification	Fluidized bubbling	Wastes	Gas	Demo
IGCC	Gasification, gas turbine, steam cycle		MSW	Gas	
Semass RDF Combustion			Shredded RDF	Gas	
Mass Burn WTE			MSW	Gas	
ThermoChem MTCI	Gasification	Atmospheric Fluidized, bubbling	RDF	Gas MHV	Demo
Daewoo	Gasification	Fixed Bed	MSW		
Proler		Rotary Reactor	MSW	Gas	
Pedco		Mechanically fluidized bed		Gas	
Ebara	Pyrolysis	Fluidized Bed	RDF	Gas	Abandoned (early 70's)
ERCO	Gasification	Fluidized Bed	RDF	Gas	Abandoned (70's)
Ejaho	Gasification	Fixed Bed	RDF Pellets	Gas	Abandoned (1986)
Scanarc	Gasification	Fixed Bed	MSW	Gas	Pilot plant (early 80's)
Thermoselect	Gasification, Pyrolysis	Tube Reactor	MSW	Gas	Pilot plant
Kiener Siemens	Gasification, Pyrolysis	Rotating Drum	MSW	Gas	Commercial (late 80's)
Daneco	Gasification	Fixed Bed	RDF	Gas	Actively Marketed

1.24 Statement of the problem

The present work aims at:

1. Collecting MSW from typical landfill site and preparing it for sampling.
2. Characterizing the MSW/RDF for physical, thermal and chemical properties
3. Equilibrium and CFD modelling of downdraft gasifier using mixture of MSW/RDF with wood chips.
4. Modelling of landfill emissions, especially Methane.
5. Conducting experiments on a downdraft gasifier- engine system using a mixture of wood and RDF for verification of Equilibrium and CFD modelling, and for assessing the impact on the environment.
6. Carrying parametric studies for identifying the feasibility of MSW/RDF treatment in conventional gasification systems as compared to present Landfill practice for waste disposal.

1.25 Layout of the thesis

The thesis has been divided into 5 chapters. The first chapter gives the background of the problem. Chapter 2 discusses past work relevant to the problem and scope of the present work. Chapter 3 presents the tests and experiments for characterization of MSW/RDF of Delhi, and experimental work on gasifier-engine system operated on single fuel mode using RDF and wood chips. The analysis of results has been presented in this chapter. Chapter 4 presents the mathematical modelling of downdraft gasification process using RDF and wood chips, and the emissions from landfills are also modelled. The results of gasifier model with its validation and parametric studies, and its impact on environment are presented in this chapter. Finally, Chapter 5 discusses the conclusions and scope of the future work.

Chapter 2

LITERATURE REVIEW

In the present work, the focus is on characterization of MSW/RDF and its utilization in conventional downdraft gasifiers for energy recovery and on its environmental impact. Thus, the literature presented falls under three broad categories. For the first one, the general literature on MSW/RDF/biomass characterization, state-of-arts and laboratory-scale experimental study using MSW/RDF/biomass gasification is discussed. In the second category, literature on modeling of downdraft gasifier (thermodynamic and CFD model) is reviwed. Lastly, the literature on modeling landfill emissions with focus on methane and carbon dioxide has been reviwed.

Apart from being review of existing literature this chapter also reviews the current technology WTE is used across the world while taking into account the underline fundamentals

2.1 Characterization and utilization of MSW/RDF

2.1.1 Characterization of MSW/RDF

The physical and chemical characterization of the MSW stream is one of the highest priorities in the waste management regulatory regime (EPA US 1996). The composition of MSW as received at the landfill site varies considerably with seasonal changes and the location of landfill. For evaluating the thermal performance and environmental impact due to power production using MSW, the characterization of MSW and biomass for physical, thermal and chemical properties is essential.

Numerous studies are reported on characteristics of local MSW and its by-products i.e., synthesized fuel and energy (Chang et al. 2007; Frey et al. 2003). Tchobanoglous et al. (2002) and Gawaikar (2006) highlighted the importance of source specific quantification and thermochemical characterization of MSW for design and operation of appropriate solid waste management systems for environmentally safe disposal of MSW. Chang and Eric (2008) and Alamgir et al. (2007) investigated the physical and chemical characteristics of MSW to illuminate the role of management policies with greater regional relevancy. Alamgir et al. (2007) characterize MSW from six major cities in Bangladesh. Mor et al. (2006) studied various physico-chemical properties of the MSW to characterize the waste from Gazipur landfill site, Delhi (India). The environmental impact assessment (EIA) for human health and the environment from the potential hazards of waste reuse, recycling, recovery, treatment, and disposal needs the support of a waste characterization database (Forteza et al. 2004).

NEERI characterized the waste from Delhi in 1996. However, this study could not provide complete classification/categorization of waste components. In Delhi, the earliest landfill was started in 1975 and two other landfills were started at Timarpur and Kailash Nagar in 1978. Seventeen landfill sites have been exhausted and closed till date (Mor et al. 2006; City Development Plan Delhi 2006).

2.1.2 Utilization of MSW/RDF

(a) Gasification Systems

The gasification process takes place in gasifiers. It is a partial combustion process where the lignocellulosic feedstock is subjected to drying, pyrolysis, oxidation and reduction in a controlled supply of oxygen. Gasification process yields combustible gas known as producer gas/syngas with carbon-monoxide and hydrogen as prime combustible constituents.

Under high temperature conditions, the solid feedstock loses its moisture and is then subjected to pyrolysis resulting in its decomposition into char and volatiles. The volatile products are a mixture of a large number of short chain hydrocarbons which may crack further to yield compounds like, carbon monoxide, hydrogen, carbon dioxide, water vapour and tar. These pyrolytic yields react with oxygen in high temperature combustion zone where oxidation and reduction reactions yield producer gas. The principal chemical reactions taking place in the oxidation and reduction reaction zones of the reactor are given as (Pinto et al. 2001).

(i) $C + O_2 = CO_2$

(ii) $C + CO_2 = 2CO$

(iii) $C + H_2O \rightarrow CO + H_2$

(iv) $C + 2H_2O \rightarrow CO_2 + 2H_2$

(v) $CO + H_2O \rightarrow CO_2 + H_2$

(vi) $C + 2H_2 \rightarrow CH_4$

The reaction (ii) is called Boudouard reaction and reactions (iii) and (iv) are known as primary and secondary water gas reactions, respectively. The forward reactions in the above are endothermic in nature and takes place at temperature of about 900°C. The excess moisture content in feedstock is unfavourable since it causes the secondary water gas reaction (iv) and water gas shift reaction (v) to proceed in the forward direction and thus reduces the calorific value of the gas. Most of the hydrogen produced in the reduction zone remains free. Only some of it combines with carbon to form methane. However, beyond the temperature of 1000°C, methane does not exit. The reactions (ii), (iii) and (vi) take place in reduction zone to convert char into gaseous products. These are highly endothermic and reversible reactions and high temperature favours the forward reactions

Fixed bed gasifiers typically have a grate to support the feed and maintain a stationary reaction zone, while fluidized bed gasifier keeps bed moving. Bridgewater (1995)

provides a neat classification of the various gasifiers. A brief description of a few technologies is presented here.

Updraft gasifier

The simplest gasifier is updraft or counter-current type, in which air enters at the bottom and the gas is drawn at the top. Fuel is fed in at the top and moves downward as shown in Fig. 2.1(a). This design has small pressure drop, good thermal efficiency and high calorific value of the gas. These design exhibits high tendency of slag formation and higher tar in final gas in addition to long starting time. Their role is limited for thermal applications.

Downdraft gasifier

Here solid fuel is fed in at the top and flow of air and gas is in downward direction. Hence flow of air and fuel is in same direction (Fig 2.1b). The drying zone is at the top followed by the pyrolysis zone, combustion zone and reduction zone. The gasifier is designed so that tar is given off in the pyrolysis zone where a high amount will be cracked and reduced to non-condensable gaseous products before leaving the gasifier. In most of the gasifiers, the internal diameter is reduced in the combustion zone to have a throat. Air inlet nozzles are commonly set radially round the throat to distribute air uniformly. Relatively tar-free gas can be obtained, but gas contains significant quantities of ash particle and soot. Also higher exit gas temperature is a problem in these gasifiers that affect, the conversion efficiency. Usually downdraft reactors are preferred for engine applications due to the cleaner nature of gas.

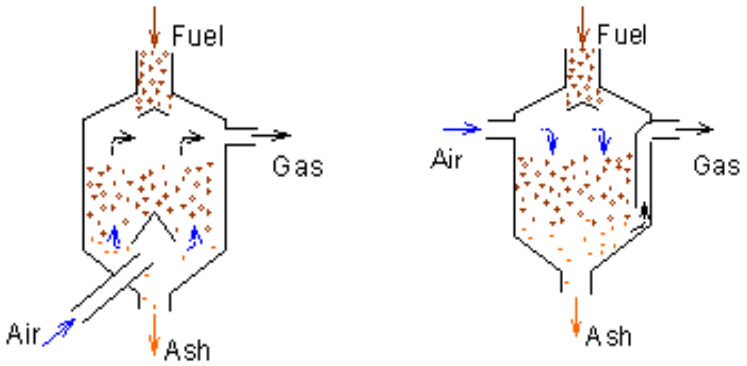

(a) **(b)**

Fig. 2.1 Fixed bed gasifier configurations (a) Updraft (b) Downdraft

Fluidized bed gasifier

Fluidized beds offer the best vessel design for the gasification of MSW. In this gasifier, air is blown upwards through an alumina sand bed at sufficient velocity to keep it in a state of suspension, and thus behaving like a fluid. Initially the bed is heated by an external fuel source; as it reaches at sufficiently high temperature, the waste in the form of small particles is introduced on the top through a feed chute or into the bed through an auger. The fluidized-bed gasifier is most suited for low-density materials. Fluidized bed technology is more suitable for generators with capacities greater than 10 MW because it can be used with different fuels, requires relatively compact combustion chambers and allows for good operational control (Morris 1998). Better control over temperature, multi-fuel capability and no slag/clinker formation are the main advantages of this system. Poor load-following characteristics, high tar, ash and unburned carbon particle content in the gas are the disadvantages associated with this design. Klein and Themelis (2003) provide an overview of fluidized bed gasifiers used for power generation applications.

Bubbling Fluidized Bed

In this design, the gas velocity must be high enough so that the solid particles, comprising the bed material, are lifted, thus expanding the bed and causing it to bubble like a liquid as shown in Fig. 2.2(a). A bubbling fluidized bed reactor typically

has a cylindrical or rectangular chamber designed so that contact between the gas and solids facilitates drying and size reduction (attrition). The large mass of sand (thermal inertia) in comparison with the gas stabilizes the bed temperature. The bed temperature is controlled to attain complete combustion while maintaining temperatures below the fusion temperature of the ash produced by combustion. As waste is introduced into the bed, most of the organics vaporize pyrolytically and are partially combusted in the bed. The exothermic combustion provides the heat to maintain the bed at temperature and to volatilize additional waste. The bed can be designed and operated by setting the feed rate high relative to the air supply. Under these conditions, the product gas and solids leave the bed containing unreacted fuel. Typical desired operating temperatures range from 900°C to 1000°C. Bubbling fluidized-bed boilers are normally designed for complete ash carryover, necessitating the use of cyclones and electrostatic precipitators or baghouses for particulate control.

Circulating Fluidized Bed

As the gas velocity increases in a turbulent fluidized chamber, the bed of solids continues to expand, and an increasing fraction of the particles is blown out of the bed. A low efficiency particle collector can be used to capture the larger particles that are then returned to the bed. This suspended-combustion concept is a called a circulating fluid bed (Fig. 2.2b). A circulating fluid bed is differentiated from a bubbling fluid bed in that there is no distinct separation between the dense solids zone and the dilute solids zone. Circulating fluid bed densities are on the order of 560 kg/m, as compared to the bubbling bed density of about 720 kg/m (Babcock and Wilcox 1992). To achieve the lower bed density, air rates are increased from 1.5-3.7 m/s of bubbling beds to about 9.1 m/s (30 ft/s) (Hollenbacher 1992). The particle size distribution, attrition rate of the solids and the gas velocity determine the optimal residence time of the solids in a circulating fluid bed. A major advantage of circulating fluid bed boilers is their capacity to process different feedstocks with varying compositions and moisture contents. As with bubbling-bed boilers, bed agglomeration is a concern. High alkaline content fuels cause particles in the bed to agglomerate, eventually defluidizing the system. In general, gasification technology is

selected on the basis of available fuel quality, capacity range, and gas quality conditions.

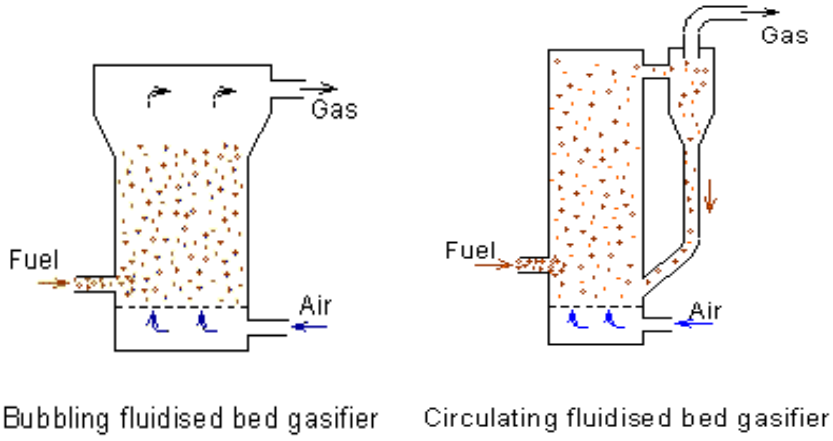

(a) **(b)**

Fig. 2.2 Fluidized bed gasifiers (a) Bubbling fluidized bed (b) Circulating fluidized bed

Table 2.1 shows the thermal capacity range of the main gasifier designs. Larger capacity gasifiers are preferable for treatment of MSW as they allow variable fuel feed, uniform process temperatures due to highly turbulent flow through the bed, good interaction between gas and solid phase, and due to high carbon conversion.

Table 2.1 Thermal Capacity range of Different Gasifier Designs (Klein and Themelis 2003)

Gasifier Design	Fuel Capacity
Downdraft	1KW – 1MW
Updraft	1-12MW
Bubbling fluidized bed	1-50MW
Circulating fluidized bed	10-200MW

The costing of power generation from solid fuels coal, biomass and solid waste including woody biomass, agricultural wastes, municipal solid waste, refuse-derived fuel, scrap tires and tire-derived fuel) was studied by Niessen et al. (1996). The power

technologies include pulverized coal and natural gas/combined cycle power plants, co-firing with coal, coal-fired utility boilers, direct combustion in dedicated mass burn, stoker and fluidized bed boilers, and wood gasification/combined cycle power plants.

Larsona et al. (1996) studied the production of clean transportation fuels (methanol or hydrogen) from MSW. Dong et al. (2008) analysed the energy potential of the RDF obtained from combustible solid waste was evaluated for Korea; they reported that utilization of 50% or 100% of the RDF as fuel, the industrial city can save disposal costs approximately 17.6% or 35.2%.

Yoshikawa (2004) developed a small-scale gasification and power generation systems for solid wastes (a 20 tons/day scale slagging MSW gasifier combined with 900 kW dual-fuelled diesel engines). The combustion of RDF in the cement industry was analysed by Gronli (1996) in a study on a Norcem plant in Norway. The study showed that the use of poor quality fuels such as RDF resulted in lower production levels, emissions problems and worsening chlorine salt build-up cycles due to high chlorine content of the fuel. They concluded that the upper limit for fuel substitution with RDF is 30% and that there is no economical advantage in burning RDF in cement manufacture without subsidy due to the initial cost of investment in equipment and operation costs.

Zubtsov et al. (2005) studied the aspects of using the advanced, high-temperature air/steam-blown gasification and pyrolysis technologies for converting solid fuels into syngas. He summarizes the present R&D status of Multi-staged Enthalpy Extraction Technology (MEET), which employs high-temperature air and steam as oxidizer agents for converting the solid fuels into syngas and has many features that are advantageous for power generation. The low-cost gasifier/pyrolyzer is extremely compact and flexible, capable of operating efficiently on a wide range of low-caloric-value fuels. Choy et al**.** (2004) assessed the feasibility of installing a small-scale MSW gasifier on a university campus.

(b) Gasification and WTE Process

Thermal treatment of biomass and waste with energy recovery is a one of the choice for its safe disposal. Research activities are going on in many countries including India to workout efficient, cost effective and reliable gasification systems for biomass and wastes.

Gang et al. (2008) studied five kinds of organic components (i.e. wood, paper, kitchen garbage, plastic and textile) and simulated three types of MSW in a fluidized-bed gasifier. Li (2002) developed a model to compare the life-cycle inventory (LCI) of gasification and WTE facility utilizing MSW for energy production.

Calaminus (1998) reported the Thermoselect High Temperature Recycling (HTR) process for waste treatment by eliminating the major problems of traditional techniques like landfills or ashes, filter dust and emission producing processes. The heat of reaction leading to temperatures up to about 2000°C in the core of the lower HTR section acts to also smelt the metal and mineral components of the waste. Chlorinated hydrocarbons such as dioxins and furans are reliably destroyed along with other organic compounds in the gaseous and the liquid phase. The synthesis gas is purified before use as combustible or primary material.

Lee (2006) determined the gasification characteristics of combustible wastes in a 5 ton/day fixed bed gasifier. Kikuchi et al. (2005) performed a semi-pilot scale test for production of hydrogen-rich fuel gas from different wastes by means of a gasification and smelting process with oxygen multi-blowing. Bain (2008) experimentally updates the technical & economic performance of an integrated hydrogen production process based on biomass steam gasification. He et al. (2009) investigated the catalytic steam gasification of MSW to produce hydrogen-rich gas or syngas with calcined dolomite as a catalyst in a bench-scale downstream fixed bed reactor. Gang et al. (2007) carried out experiments to recover energy and materials from waste tire efficiently from a low-temperature gasification in a lab-scale fluidized bed. Thamavithya et al. (2008)

present the experimental results of MSW gasification in a spout-fluid bed reactor. Three scenarios (primary air, secondary air and effect of the recirculation) were investigated in this study.

Milne and Evans (1998) reviewed the formation of Tar in gasifier its nature and Conversion. “Tar” is the most cumbersome and problematic parameter in any gasification commercialization effort.

Yassina et al. (2008) studied the techno-economic performance of energy-from-waste fluidized bed combustion and gasification processes in the UK context. Mass and energy balances of the processes were performed and the cost effectiveness of the different waste treatment options, for the generation of electric power, was assessed using a discounted cash flow analysis.

Yang et al. (2007) attempted to convert moving-grate incineration from combustion to gasification. In this study, burning characteristics, including burning rate, gas composition, temperature and burning efficiency as a function of operating parameters are investigated using advanced, mathematical models. Detailed comparisons between the combustion mode and gasification mode are made.

Hamel (2005) demonstrated that in order to increase the efficiency of waste utilization in thermal conversion processes, pre-treatment is advantageous. The dried and homogenized waste-derived Stabilats fuel has a relatively high calorific value and contains high volatile matter which makes it suitable for gasification. As a result of extensive mechanical treatment, the Stabilats produced is of a fluffy appearance with a low density.

Arena (2011) proposes a critical assessment of MSW gasification. The analysis indicates that gasification is a technically viable option for the solid waste conversion, including residual waste from separate collection of MSW. It is able to meet existing emission norms and can remarkably reduce the landfill option.

Niessen et al. (1996) summarize the state of the art for seven technologies involving gasification and other innovative thermal processing technologies for MSW. Although, the technologies are at the level of "incipient commercial availability", they have passed through the "idea" stage. A company “Advanced Energy Strategies” (2004) studied three technologies namely pyrolysis, conventional gasification, and plasma gasification for thermal processing of MSW, while Murphy (2004) has comparatively analysed incineration, gasification, generation and utilisation of biogas in a combined heat and power (CHP) plant.

The researchers (Malkow 2004; Collin 2004) also studied the existing WTE technologies for thermal treatment of MSW. A brief review is given below

Sofresid/Caliqua process (ANDCO-TORRAX)

The air gasification is carried out in a fixed bed updraft reactor. MSW can be handled without separation for even hazardous hospital wastes. By preheating the air to some 1000°C, the gasification temperature can be maintained well above 1200°C in the bottom of the shaft and the countercurrent gas can leave the reactor at high temperature. Combustion air is added before the combustion unit and the flue gases will have immediate temperature of order of more than 1200°C. Steam is produced in a conventional boiler and after an electrostatic precipitator the flue gases are discharged to the atmosphere. The slag from the gasifier as well as from the combustor is quenched by circulating water and collected as granules. Output of this process is only power and steam (hot water) for district heating.

Motala Pyrogas, Sweden

Motala Pyrogas was an atmospheric air-blown updraft fixed bed gasifier coupled to a boiler in a rubber and tyre manufacturing plant. The fuel was waste rubber, MSW (without any pre-treatment) and coal. The co-gasification with coal was used to stabilize the lower char layer in the bed. To be able to feed the MSW stream, a new robust lock hopper cell with 1 m^3 volume was designed and installed. The lower part of the reactor was cooled, and produced steam to moderate the ash temperature, thus limiting clinkering formation. A two-stage design was used to control the tar

condensation in the gas pipeline of the boiler. A lower hot gas exit has been mixed with the cool top gas which forced to pass through an electrostatic filter. The recovered tar was fired in a separate burner in the boiler.

Purox process

The Purox process is a high temperature oxygen gasification process. The MSW is stored and shredded before feeding through the top of the high temperature updraft shaft furnace operated on oxygen. Molten slag is quenched with water and constitutes a material that can easily be deposited. The raw product gas is cleaned by conventional techniques, for instance, in the chemical industry. A small part of the product gas is fed to the reactor to ensure high reaction temperature and the rest is a "clean fuel". The thermal efficiency has been reported to be more than 60%.

Landgard process (Monsanto)

MSW is shredded and fed to a rotary kiln where it meets hot gases from an oil burner. At a maximum temperature of 1000°C, a solid residue is collected in the lower part of the kiln while pyrolysis gases exit at the upper end (feed inlet of MSW). The gases are directly burned with steam production and the flue gases are scrubbed before exhausting in the atmosphere.

Destrugas process

In a downdraft (concurrent) with indirect heating (retort) reactor shredded MSW is fed at the top. The shredded MSW flows downwards in the shaft while it is indirectly heated to about 1000°C. The energy required to obtain 900-1050°C in the shaft is supplied indirectly through the walls and is originally formed by combustion of some of the gas. The gas is further cleansed in a scrubber where the water (at that time) was considered no more polluted that it could be sent to the communal sewage treatment. About 50 % of the energy in the MSW is obtained as gas.

Omnifuel process (Eco-fuel, University of Sherbrooke)

The raw material can be fed either from the middle or at the lower half of the reactor. Fluidized bed consists of inert material. Gas and solids leave the reactor top where a cyclone separates the solids to be recycled to the reactor. The gas is further cleaned in another cyclone. The thermal efficiency achieved, based on cold and hot conditions has been nearly 75 % and 90%, respectively.

Ebara process

It utilizes the concept of two fluidized sand beds, one for combustion and one for steam gasification, with circulating sand as the heat carrier between the two beds. The energy supply is carried out in the combustion reactor where residual char is burnt. The heat is transferred to the pyrolysis reactor by means of the fluidized bed material (sand), which flows between the reactors. The energy balance requires some extra fuel to match deficiencies. In the pyrolysis reactor RDF is pyrolysed by means of the hot bed material in the temperature range of 650-750°C. In all fluidized systems certain homogeneity of the feed is vital. The outgoing raw gas from the pyrolysis unit contains tar and char and has to be cleaned before exhaust. The resulting gas has a high heating value and the overall thermal efficiency is reported in the range of 50 - 60 %.

Flash Pyrolysis process (Garrett - Occidental)

The flash pyrolysis process was developed for coal, and also as part of a more general separation system for MSW. RDF is fed to a reactor. At a temperature range of 450-500°C and a short residence time (few seconds) and a slight over-pressure, nearly 40 % of pyrolytic oil or tar is formed. This tar is in the vapour phase and the gases are separated from the char in a cyclone. Upon cooling tar condensates and it is separated from the lighter gases. The lighter gas is used as fuel together with the solid char to provide the necessary heating for the process.

Erco/Power recovery system process

This process is a complete process from MSW to power generation. The MSW is upgraded into RDF and fed to the fluidized bed where it is primarily gasified by air at

temperatures of 760-820°C. In waste gasifications a "reactive" bed material is used instead of sand. The "reactive" material is claimed to include an adsorbent for SO_2. The solids are separated from the gas in one or two cyclones. The gas is further cleaned in a multistage system including scrubbing and mist elimination. Solid – tars are returned to the gasification and the rest is treated in the water. When the gas is to be used in an engine for power production a fabric filter is also used in the gas cleaning. The thermal efficiency is reported up to 75%.

Elajo/Tornegaard/Komako, Sweden

The Elajo gasifier is a downdraft bed gasifier operated on air as oxidant. The intention was to combust the gas and then applying wet/dry flue gas cleaning with a fabric filter. The raw material was initially RDF Fluff, and after testing only RDF pellets a small scale modular unit was planned as standard. In the presented design, a rotating movable grate should allow control of pressure drop and ash discharge. Gas cooling/heat exchanger decreases the temperature up to 500°C. The gasifier was directly coupled to a boiler. A bottom ash that could be partly treated and recycled was anticipated, heavy metals retained in the ash, and dioxin formation should be low.

Voest Alpine process

The Voest Alpine process involves a fixed bed, updraft reactor where the gasification is carried out at high temperature (more than 1500°C). This high temperature is obtained with air as gasification medium by means of a fuel mixture to some extent including materials with high heat contents. With the high temperature a molten slag is quenched and collected in the bottom of the reactor. The specific feature giving Voest Alpine a special character is a coke bed through which the gas is cleaned from certain components. This coke bed is built into the gasification reactor.

In the pilot plant reactor a mixture of about a third of waste oil (including a part of fuel oil), a little more than half of RDF and some ten percent of coke is used as fuel. These different parts are introduced at various positions: the oils at the bottom of the shaft, the RDF in the middle and the coke at the top in a special shaft through which the top gas passes. The hot coke bed acts as a catalytic bed where tar and other tar components are broken down. After combustion they are less than 1 mg/m^3 flue gas;

for Cd, Hg, Ti, As, Co, Ni and Se less than 0.01 mg /m3. Although, the gas was cleaned for use in IC engine, yet further gas cleaning is still suggested. For the molten slag, approximately 1 m^3 of water for quenching per ton of fuel is used. The energy efficiency of the process is reported 83 % and RDF as well as shredded car waste has been used.

Scanarc (Plasma) process

To produce reducing gas for iron manufacture, plasma was introduced in the bottom of the shaft producing H_2 and CO from air and coal. Two of these processes were installed full-scale: the PlasmaZinc and the PlasmaChrome for handling Zinc dust and Chrome materials. The Scanarc (former "SKF Plasma") process is a fixed bed, high temperature process with a molten slag in similarity to the Andco-Torrax and Voest Alpine processes. In line, the gasification is also carried out in an updraft shaft. In the ScanArc process the gas cleaning is obtained in plasma, where the gas is heated to very high temperatures causing a decomposition of tar, chlorinated hydrocarbons and ammonia. The ScanArc process uses a shaft reactor outlined as simple as possible and fed with a mixture of air and oxygen in the bottom, or in the middle. Oxygen is needed when the effective heat content of the wastes is too low to result in a temperature of 1200°C or more. The raw gas is fed to a second reactor which in fact is more or less an empty shaft with a plasma generator on top. The electric plasma generates a theoretical temperature of more than 1500°C through which the gas is passed (lowering the temperature) into the shaft. The fuel to the plasma is composed of power and air for combustion (oxidation). After the second reactor, chlorine is present as Cl_2 or HCl, nitrogen as N_2, all organic compounds and several others are decomposed. The gas after the plasma reactor is cooled and washed. The molten slag is tapped from the bottom of the first reactor. The power consumption for the plasma is reported 200-400 kWh/ton of feed - depending on heat value of the feed.

Thermoselect process

In the Thermoselect process MSW is gasified and melted in two steps: first one is indirect drying/pyrolysis and second step belongs to high temperature oxygen-gasification. High temperature treatment effects molten slag and enables the process

to handle a large range of solid wastes. The high temperature gasification is achieved by oxygen and support fuel taken from the product gas but also - to some extent - by the preceding drying and pyrolysis of the wastes. This reaction is carried out in a compressing and feeding system attached directly to the high temperature gasifier. MSW are mechanically compressed and transported through a "tube" by a piston. In the indirectly heated tube reactor, the temperature is gradually raised to about 600°C facilitating the drying of the material and subsequently the pyrolysis. The pyrolysis solid residues are intermittently pushed into the gasifications shaft where the temperature is raised to 1200-2000°C by means of oxygen and extra fuel provided from the product gas. The gases and volatiles including tars are concurrently fed into the shaft together with the solids. Metals, minerals and other types of inorganic material in the wastes are melted in the gasifier and withdrawn as a liquid at temperature of 1800°C from the bottom. After cooling, a harmless solid residue is claimed which might even be used as a raw material source for certain metals but which is basically deposited. The exiting raw product gas consists to a large extent of carbon monoxide and hydrogen giving a fuel gas of medium heating value or what might be called a synthesis gas (Sumio et al. 2004).

Lurgi CFB processes (Oko-gas, Wikonex)

These processes are applications of the Lurgi CFB gasification operating at atmospheric pressure. The feed is biomass, RDF or similar raw materials and fluidized by oxygen enriched air. The fluidized bed reactor requires a certain homogenity in the feed material. Thus, the municipal waste has to be sorted, milled and sometimes dried into a RDF before entering the CFB gasifier. In the fast fluidization shaft the material is gasified with air and oxygen in an inert bed. The temperature is about 900°C and the reaction time is few seconds. At the top unreacted material and other solids are separated in a cyclone and recycled to the fluidization shaft. From the bottom of the reactor ash is taken out, cooled and separated from metals. From the cyclone the raw product gas is fed to a “gas cracker" which operates at some 1400°C. The temperature is raised by oxygen in the raw (fuel) gas. At these elevated temperatures a cracking or rupture of dioxin like components is ensured. The gas is cooled in a waste heat boiler and further quenched by water. After a subsequent

scrubber where ammonia, metals, etc are removed, specific cleaning of sulphur and mercury are applied. A considerable amount of waste water has to be treated with precipitations and neutralizations. With the extensive gas treatment, a pure fuel gas with medium heat value may be distributed.

Kiener-Siemens process

Unsorted wastes of different types such as MSW, industrial waste and sludge are mixed homogeneously and then treated in a rotating pyrolysis drum with flue gases near 450°C temperatures. In the drum a drying and pyrolysis occur, producing gases (including tar) and solids. In the end of the drum the gases are fed directly to the air blown combustion unit running at high temperature; some 1300°C. The flue gases from the combustion are subjected to conventional flue gas cleaning.

DANECO

A 10 MW air-blown updraft gasifier is fed with RDF pellets from the top. Air is inducted through a rotation bottom grate. The raw gas is fed to a fixed bed cracker with recycled ashes and fuel gas cleaning residues (lime). The cracking temperature is around 800°C and soot is recycled to the gasifier. After gas cooling through air and steam heat exchangers to 600°C, the gas enters a recovery boiler. A wet dry lime system operating at approximately 250°C precedes a bag-house filter. After scrubbing/cooling the gas is sent to a dual fuel engine.

Energy Products of Idaho (EPI)

The EPI incineration system uses a bubbling-type fluid bed concept that accepts a prepared 10 cm top size RDF. Within the bed, RDF particles are exposed to a vigorously turbulent hot environment that promotes rapid drying, gasification, and char burnout. In the bed, EPI's proprietary design features provide continuous removal of oversized noncombustible materials. The hot gases from the bed are passed through a boiler to generate the high-pressure, superheated steam that is used either to produce electricity or for process applications.

Pedco Incorporated

The Pedco Rotary Cascading Bed Combustor (RCBC) is a robust solid-fuel burner and heat-recovery system (it is not a gasifier). The RCBC burner comprises a rotating, horizontal, cylindrical combustion chamber. A bundle of boiler tubes projects into one end of the chamber. The rotational speed of the chamber is high enough to keep a substantial fraction of the bed material continually airborne. This activity produces an environment similar to that of a fluid bed but, in this case, a mechanically fluidized bed. The hot falling solids cascade across the whole diameter so that the boiler tubes are submerged in hot fuel and bed material. The hot solids recycle preheats the combustion air, drying and igniting the incoming fuel. The RCBC burner could discharge into a boiler making superheated steam for electrical generation. As a fuel flexible burner, the RCBC system is intended to burn coals, coal waste, wood, chipped tires, RDF, and a variety of other fuels having the common denominator of low cost.

PROLER International Corporation

The PROLER SynGas Process is a patented technology that reforms hydrocarbon-containing wastes into a reactor gas. The process accepts preshredded material and produces a fuel gas suitable for power generation. The residue is discharged in the form of commercially useful vitrified by-products as well as wastes acceptable for landfills. The system, referred to as the Proler SynGas Process, is designed to produce recyclable solid by-products together with a clean fuel gas from ASR and other wastes, including MSW. The demonstration unit has a capacity of 1.9-Mg/h shredded MSW, equivalent to 2.6-Mg/h raw MSW. The unit includes a feeding system; a horizontal, rotary re-actor; a gas-cleaning train; and a compressor that supplies cleaned fuel gas to a dual-fuel-fired engine/ generator.

Battelle

The Battelle High Throughput Gasification System (BHTGS) is an indirectly heated, two-stage process that uses CFB reactors. In a high-throughput gasifier, RDF or other biomass feedstocks is gasified (using steam without oxygen as the fluidizing medium)

into a medium-heating-value gas (18.6 to 22.4 Nm^3). Residual char is consumed in an associated CFB combustor. A circulating-sand phase is the method for heat transfer between the separate reactors.

The Battelle biomass gasification process produces a medium-Btu product gas without the need for an oxygen plant. The process consists of two reactors and their integration into the overall gasification process. This process uses two physically separate reactors:

- A gasification reactor in which the biomass is converted into a medium-heating-level gas and residual char
- A combustion reactor that burns the residual char to provide heat for gasification.

Heat transfer between the reactors is accomplished by circulating sand between the gasifier and the combustor. The Battelle process provides a cooled, clean, 18.6- to 22.4 MJ/Nm^3 product gas. Waste heat in the flue gas from the combustor can be used to preheat incoming air and then to dry the incoming feedstock. The condensed, organic phase scrubbed from the product gas is separated from the water and injected into the combustor.

Thermo Chem

The Manufacturing and Technology Conversion International, Inc. (MTCI) Steam Reforming Process is an indirectly heated fluidized bed reactor using steam as the fluidizing medium. Pulse Enhanced^{TM} indirect heating combined with a fluid bed and steam reforming provides a process for converting organics to fuel gas while separating the inorganics without oxidation or melting. The heart of the process is the Pulsed Enhanced^{TM} heater, which is immersed in the fluidized bed. This pulsed heater, with unique aerovalves, generates an oscillating flow in a bundle of heat-transfer tubes that pass through the fluidized bed gasifier. The pulsed combustion phenomenon results in turbulent mixing and significantly enhanced heat transfer between the gases in the tube and the RDF. Part of the product gas is used in the pulsed heater as the energy source. The exhaust from the heater never enters the fluid-

bed steam reformer and does not dilute the product gas. The organic waste fed to the fluid-bed steam reformer reacts solely with the steam in a reducing atmosphere, producing the fuel gas.

TPS Termiska Processer-AB

The TPS technology uses a starved-air gasification process in a combined bubbling and circulating fluidized bed reactor operated at 850°C and near atmospheric pressure. RDF is fed to the fluidized bed. Air is used as the gasification/fluidizing agent. Part of the air is injected into the gasifier vessel through the bottom section and the remaining higher up in the vessel. This pattern of air distribution causes a density gradient in the vessel. The lower part maintains bubbling fluidization that allows coarse fuel particles adequate residence time for good gasification reactions. The remaining air introduced higher up in the vessel increases the superficial velocity of air through the reactor so that smaller, lighter particles are carried away in the gas flow. The process gas from each gasifier passes through two stages of solids separation before being fed to a furnace/boiler. The flue gas exiting the boiler is then cleaned in a three-stage dry scrubber before being exhausted through the stack. Alternatively, some of the raw gas stream can be sent to a nearby cement factory, without cleaning, to be used as fuel in the cement kilns. Immediately downstream of the gasification vessel, a dolomite (mixed magnesium-calcium carbonate) containing vessel catalyzes most of the tars formed in the gasification process and breaks them down into simpler compounds of lower molecular weights and melting points. The dolomite also will absorb acids in the flue gas, including HCl and sulphur oxides. The product gas can then be cooled and passed through conventional scrubbing systems without operational problems. After cooling, the syngas can be compressed and cleaned up to acceptable limits for a combined cycle turbine.

Essex County

The Essex County Mass Burn WTE facility is New Jersey's largest resource recovery facility and is owned and operated by American Ref-Fuel. The Essex facility combusts about 2800 tons of MSW per day and generates approximately 65 MW of electricity. The facility does not shred or processes MSW, so the sizes of the items

deposited to the combustion chamber can be large and the rates of mass transfer and oxidation are relatively slow. As a result a very large combustion chamber and grate are required and the intensity of combustion is correspondingly low. Energy is generated via steam production from waterwall tubes and a superheater. Flue gas is cleaned with three DBA electrostatic precipitators and dry scrubbing systems. The stack height is nearly 300 feet.

SEMASS RDF Combustion

In this process waste brought to the plant is loaded onto conveyors, shredded and exposed to overhead magnets that recover ferrous metals from the waste. The RDF is then sent into the combustion chambers through inclined chutes. A portion of the feed is burned in suspension, while the remainder falls onto a horizontal moving grate. The grate moves slowly and it takes materials approximately one hour to move from the front to the rear of the boiler. The feed rate can be adjusted automatically by installed temperature controls to provide maximum efficiency. Underfire and overfire air are introduced to enhance combustion. Waterwall tubes, a superheater and an economizer are used to recover heat for production of steam. Detailed operating data show that 650 kWh of electricity are generated per ton of MSW combusted. Of this, 100kWh are used in the plant operation.

Integrated Gasification Combined Cycle (IGCC)

IGCC concept is based on the combination of a gasification system with a gas turbine and a steam cycle and has the potential to provide thermal energy to power conversion efficiencies exceeding 40 %. Critical for the success of the IGCC is the maintenance of the gas turbine. The IGCC turbine's lifetime can be limited due to erosion and high temperature corrosion caused by impaction of particles and deposition of impurities such as alkali metals in the product gas.

Corrosion of the turbine blades is accelerated by formation of low melting eutectic salt mixtures, of which alkali sulfates are believed to be important constituents. Turbine manufactures have set specifications for the maximum tolerable alkali metal

concentration of the fuel gas to be less than 0.1 ppm of the fuel by weight. These specifications are often based on operating experience with fossil fuels.

(c) WTE Technologies

Combustion, gasification and pyrolysis belong to thermal conversion processes which can be used for thermal treatment of solid wastes. Different products are gained from the application of these processes and different energy and matter recovery systems can be used to treat these. The thermal treatment with heat recovery "WTE technologies" is prefered due to environmental consequences, energy generation and recycling of material. Several studies with achievements have been summarized as below,

Granatstein (2003) performed a case study on a waste-fuelled gasification project at Greve (Italy) using wide range of feedstocks. He observed poor gas quality, heavily contaminated with tar. Consonni and Federico (2012) investigated two gasification technologies with conventional WTE plants and found their energy performances are very similar to those of conventional plants. The potential benefits that may justify their adoption relate to material recovery and operation/emission control: recovery of metals in non-oxidized form; collection of ashes in inert, vitrified form; combustion control; lower generation of some pollutants.

Pyrolysis

Complex polymeric substances like MSW, coal, wood or biomass, plastic, black liquor, and distillery effluent decompose or depolymerize when heated at high temperature and release pyrolysis products largely in the form of gases.Danheux et al. (1997) compared the incineration with thermolysis.

Sanchez(2007) studied the energetic valorisation of the products. Owing to the specific characteristics of the plant, two products were obtained from the process: gas and carbonized solid. No liquid fraction was obtained, so the gas fraction is a greater percentage made up from both condensable and non-condensable compounds, while at the laboratory scale were obtained separately.

Liu (2009) studied the characteristics of oxygen-enriched air combustion of raw MSW by thermo gravimetric analysis. Experiments on oxidative pyrolysis of MSW were carried out under different atmospheres.

Yang et al. (2006) mathematically modeled the slow pyrolysis of segregated solid wastes in a packed-bed pyrolyser. It was found that packed-bed pyrolysis produces 30–100% more char compared to standard TGA tests and the local heating rate across the packed-bed reactor differs remarkably from the programmed wall-heating rate and varies greatly in both time and space.

Phan (2007) investigated the role of pyrolysis and found its importance in the thermal processing of municipal solid wastes, since it decomposes wastes into three types of intermediate products to be collected as fuel feedstock or to be gasified. In this study, the main products from slow pyrolysis of key segregated waste materials were characterised for mass yield, energy content, elemental composition and chemical compounds.

Baggio et al. (2008) studied the energy and the environmental impact analysis of an innovative system based on the pyrolysis of MSW which produces solid (char), liquid (tar) and gas (syngas) fuels used in a combined cycle for electric power generation.

Wang et al. (2005) experimentally studied the low-temperature pyrolysis of the mixture of nine typical components from municipal household garbage, in an externally heated fixed-bed pyrolyser, at temperatures ranging from 300°C to 700°C. The solid product yield decreases with the increase of temperature in the test temperature range, and reduces quickly at 300–550°C but very slowly at 550–700°c.

Incineration

The new generation of incineration plants are being designed and developed to meet strict emission limits. Comparing emission limits valid for waste incinerators and other large combustion plants it can be stated that new WTE systems are among the cleanest and most reliable sources of energy in the form of heat as well as electrical power.

Otoma (1997) demonstrated that using the heat from waste incineration to generate electricity requires the addition of generating equipment, while the manufacture,

construction, and operation of this equipment also use energy. It was found these are effective methods for energy recovery, and that the gas turbines combined with waste incinerators for repowering have an optimum size that will improve overall efficiency. Murphy (2004) found that the major current technology is based on direct combustion of wastes in a moving-grate furnace. However, general public opinion prefers non-direct burning technologies. Waste gasification is one of those nearest technologies available. Detailed comparisons between the combustion mode and gasification mode are made.

Magrinho (2008) analysed the recycling of packaging wastes and found that it may be compatible with incineration within integrated waste management systems. To study this, a mathematical model was used to calculate the fraction composition of residual MSW only as a function of the MSW fraction composition at source and recycling fractions of the different waste materials.
Shen et al. (2005) studied the influences of different catalysts on the ignition and combustion of MSW using thermo gravimetric (TG) analysis.

Plasma gasification

Plasma technology for waste treatment is now a viable alternative to other potential treatment/disposal options. Thermal plasma technology is expected to become commercially viable in the future.
Gomez et al. (2008) and Lemmens (2006) analysed the available scientific and technical literature on waste plasma treatment of a variety of hazardous wastes such as residues from municipal solid waste incineration, slag and dust from steel production, asbestos-containing wastes, health care wastes and organic liquid wastes. The principles of thermal plasma generation and the technologies available were outlined, together with potential applications for plasma vitrified products. Lemmens developed a test facility to evaluate the feasibility of plasma gasification and the impact of this process on the environment with aim: (1) to evaluate the technical feasibility of making a stable synthesis gas; (2) to characterize the composition of this synthesis gas; (3) to define a suitable after-treatment configuration for purification of the syngas and (4) to characterize the stability of the slag, i.e., its resistance to

leaching for use as a secondary building material. The tests illustrate that plasma gasification can result in a suitable syngas quality and slag with acceptable leachability.

Gasification of RDF pellets

Incineration has many drawbacks including producing hazardous emissions and harmful residues. To enhance the resource recovery from MSW, the RDF is considered as a better solution in industrialized countries. RDF obtained is a value added material with a higher calorific value, low moisture and a homogeneous particle size. The few relevant studies reported in past are quoted in this section.

Cristo (1999) researched the gasification of RDF pellets in different countries and analysed the performance of gasification of RDF pellets. Ravelli et al., (2008) carried out steam gasification of two different RDFs, differing slightly in composition as well as thermal stability, in a fixed-bed reactor at atmospheric pressure. The proximate and ultimate analyses reveal that the major components in RDFs are carbon and hydrogen. Rao et al. (2004) conducted air-blown gasification studies on a counter current fixed-bed gasifier for municipal residue-based RDF pellets and compared these with the mass and energy performance features of a gasifier with other biomass and residual fuels. The mass conversion efficiency and cold gas efficiency (CGE) of the gasifier were observed to be 83% and 73%, respectively for RDF pellets. The higher heating value and global energy content of the producer gas generated from gasification of RDF pellets was observed to be 5.58 MJ/Nm^3 and 12.2 MJ/kg, respectively. They reported that the tar content of gas from RDF pellets was dramatically less than (up to 45% less) that of wood chips. Dalai et al. (2008) studied steam gasification of RDF in a fixed bed reactor. They studied the steam gasification (fixed-bed reactor at atmospheric pressure) of two different RDFs and thermal stability. The proximate and ultimate analysis revealed that carbon and hydrogen are the major components in RDFs, while thermal analysis indicates the presence of cellulose and plastic based materials in RDFs. They reported that H_2 and CO are two major combustible products from gasification of RDFs.

Cleaning of Syngas and pollution

The emissions, dioxin and furan, are primary catalyst for political and environmental opposition to the WTE industry. Over the past decade, progress has been made in reducing dioxin/furan release from U.S. WTE plants lowering them from 4000 g/year in 1990 to 400 g/year in 1999. Klein (2002) states that "The most effective capturing techniques have been adsorption on activated carbon and the use of baghouse filters instead of electrostatic precipitators. Cunliffe et al. (2007) investigated the influence of temperature on the levels of pcdd and pcdf remaining in, and desorbed from, a municipal solid waste incinerator fly ash. Considerable desorption of pcdd/pcdf from the fly ash was seen at 275 ^{o}C and above. The results indicate that formation of pcdd /pcdf on fly ash deposits in the post-combustion plant of incinerators can result in the release of significant pcdd /pcdf.

Lasagni et al. (2008) performed a simultaneous study of the native carbon oxidation and formation of pcdd /f. The experimental study was carried out to gain information on the role of fly ash deposits in cold zones of municipal solid waste incinerators in pcdd /f formation reaction. Yokohama et al., (2007) investigated the gasification behaviour of pcdd and pcdf in fly ash by thermal treatment to estimate gas-particle partition in flue gas. For all samples, pcdd /f started to gasify at 350°C treatments, whereas 53-98% of pcdd /f homologs gasified at 400°C treatment, implying that gaseous pcdd /f are dominant in flue gas at temperatures in the range 350-400°C regardless of particle concentration.

Santisirisomboon et al. (2003) tested calcined limestone and calcined dolomite at bench scale to study their usefulness in cleaning hot raw gas from a fluidized bed gasifier of a synthetic or simulated RDF with a high (3 wt%) content in chlorine. Kusar et al. (2003) studied catalytic combustion for gas turbine application using a low heating-value gas derived from gasified waste. A selective catalytic oxidation for decreasing the NO_X formation from fuel-bound nitrogen was examined using two different approaches: fuel-lean and fuel-rich conditions.

Stehlik (2009) studied a number of recent advances in technologies and improvements in units for the thermal processing of MSW and various other types of waste. This study revealed achievements include low-NOx burners, improved efficiency, heat exchangers,

waste heat recovery systems, newly developed equipment for wet scrubbing, dioxin filters and systems for the treatment of sewage sludge.

Lee et al. (2006) studied the environmental aspects of gasification of Korean municipal solid waste in a pilot plant. Municipal solid waste was gasified via thermoselect process in a 3 ton/day capacity pilot plant with oxygen at a temperature of nearly 1200°C. A vitrified slag of dark brown colour with glassy shining and non-hazardous in nature was found, which can be used as natural raw material in cement and construction industry. Sangtongam et al. (2007) studied parameters influencing clean syngas production from biomass, solid waste, and coal during steam gasification.

2.2 Mathematical Modeling

2.2.1 Gasifier Modeling

(a) Thermodynamic modeling

Most gasifier models reported in literature can be classified as equilibrium, kinetic free, kinetic rate and diffusion controlled models. The equilibrium model assumes single control volume to describe the gasifier chemistry. The gasification reactions are assumed to be at thermodynamic equilibrium. However, in the kinetic free models, the reactor is subdivided into two or more separate reaction zones in which distinct processes occur viz., drying, pyrolysis, gasification, combustion. These models assume a fixed reaction temperature, pressure and either heterogeneous or homogeneous chemical equilibrium. Equilibrium and kinetic free models generally use algebraic equations to predict reaction temperatures and exit gas compositions. The equilibrium model has been used by many researchers to analyse the gasification process. These models are based either based on minimizing Gibbs free energy or equilibrium constant.

Equilibrium model has been developed by Zainal et al. (2001) to predict the performance of a downdraft gasifier using different biomass materials. They reported

that the calorific value of gas decreases with increase in moisture content in the raw material and gasification temperature in the range of temperatures investigated.

Hau et al (2008) studied thermodynamic model for gasification of solid waste. By solving the equilibrium reaction equations, the model describes pollutants formation and amounts of raw synthesis gas and in the slag. Mountouris et al. (2006) focused on the thermodynamic analysis of plasma gasification technology, which includes prediction of the produced synthesis gas, energy and exergy. Carnevale et al. (2012) analysed two alternative thermo-chemical processes from the thermodynamic point of view for waste treatment namely high temperature gasification and gasification associated to plasma process.

Jarungthammachote and Dutta (2006) investigated thermodynamic model and second law analysis of a downdraft waste gasifier. Buragohain et al. (2011) investigated the gasification of biomass mixtures using thermodynamic equilibrium and semi-equilibrium models. Ntshengedzeni et al. (2010) evaluated the conversion efficiency of the Johansson Biomass Gasifier by using analysis for gas profiles and temperature measurement system. Ratnadhariya and Channiwala (2009) investigated a three zone equilibrium and kinetic free modeling of biomass gasifier. Ratnadhariya and Channiwala (2003) studied parametric sensitivity of downdraft gasifier as predicted by three zone kinetic free (KF) model. Babu and Sheth (2005) reported interesting study on modeling & simulation of biomass gasifier in oxygen rich environment and study the steam-air ratio on gasifier performance.

(b) CFD modeling

CFD numerical models can be used to describe gasification processes because they have become an important analysis and design tool to visualize the flow, concentration and temperature contours. Wang et al. (2009), in their review critically presented and compared CFD modeling applications on biomass thermochemical conversion processes for modeling, design and optimization of thermochemical reactors. Mathematical equations governing the fluid flow, heat and mass transfer and chemical reactions in thermochemical systems are described and sub-models for individual processes are presented.

Giltrap et al. (2003) developed a model for the reduction zone of a downdraft biomass gasifier to predict the composition of producer gas under steady-state operation. Factors affecting the gas composition were the fraction of pyrolyzed gas in the initial gas entering the reduction zone of the biomass gasifier, air-to-fuel ratio, moisture content of biomass, bed temperature, and reactivity of char. Molar balance, energy balance, pressure gradient equation, and Arrhenius type of temperature dependence kinetic equation formed the set of first order differential equations, which were solved by finite difference method. The accuracy of the model was limited by the availability of data on the initial conditions at the top of the reduction zone. Moreover it was assumed that char reactivity factor (CRF), which represented the reactivity of char and the key variable in simulation, was constant throughout the reduction zone. Babu and Sheth (2006) modified Giltrap's model by using variable CRF along the reduction zone. The model was simulated with the finite difference method to predict the temperature and composition profiles in the reduction zone. A finite difference technique was successfully applied to solve such type of partial differential equations in other studies (Babu and Chaurasia 2004; Mathieu et al. 2002). Babu and Sheth (2006) presented the modeling and simulation study on reduction zone to predict the influence of air-fuel ratio. They also studied the effects of pyrolysis fraction on the outlet gas concentration in a downdraft biomass gasifier. Tilmans and Jeanmart (2007) investigated the reactions of pyrolysis gases in the combustion zone of the reactor in a downdraft gasifier. This model includes three average temperatures, which corresponds to solid particles surface, particles interior and the gas phase, respectively. Sivakumar et al. (2008) studied downdraft biomass gasifier with focus on reduction zone using Computational Fluid Dynamics.

Gerun et al. (2008) developed a two dimensional axis symmetric CFD model for oxidation zone in a two-stage downdraft gasifier. The simulations fit satisfactorily to the experimental data for temperature pattern and tar concentration.

Zhou et al. (2007) numerically modelled the combustion of straw in a bench-top stationary fixed bed with focus on NOx formation and reduction. Higman et al. (2003) employed a two-dimensional steady state model for straw combustion in a moving bed, while Kaer (2006) developed a numerical model of a 33 MW straw-fired grate boiler incorporating a stand-alone bed model using commercial CFD code for gas-

space computation. He concluded that poor mixing in the furnace is a key issue leading to high emission levels and relatively high amounts of unburnt carbon in the fly ash. The stand-alone bed model is based on a one-dimensional "walking-column" approach and included the energy equations for both the fuel and the gas accounting for heat transfer between the two phases.

Gomez-Barea and Leckner (2010) developed a CFD model for fluidized bed biomass gasifier. Special attention was paid to comprehensive fluidization models, where semi-empirical correlations were used to simplify the fluid-dynamics. For the CFD modelling of combustion processes in industrial-scale reactors the EDC is often used to couple chemical reaction mechanisms to the computed flow field (Rehm et al., 2008). Perkins and Sahajwalla (2007) modelled the heat and mass transport phenomena and chemical reaction in underground coal gasification using two-dimensional axi-symmetric computational fluid dynamic. The model is used to simulate the combined effects of heat and mass transport and chemical reaction during the gasification process. Silaen and Wang (2010) studied the role of turbulence and devolatilization models on simulation of entrained-flow coal gasifier. They employed Eulerian-Lagrangian approach to solve the Navier-Stokes equations and the particle dynamics. Hermansson (2011) performed a CFD modelling of bed shrinkage and channelling in the fixed-bed combustion. In this study, a two-dimensional model of the combustion of fixed fuel beds has been developed for studying the influence of heterogeneous fuel-bed properties on the conversion. Likewise, Porteiro et al. (2009) used CFD modeling on small-scale commercial biomass pellet boiler and reported that CFD computations can be used for design and optimization of biomass combustion systems. Wang and Yan (2008) employed a fluidized bed sewage sludge gasifier for prediction of syngas composition. The CFD code employs standard κ-ε turbulence model for the gas phase in an Eulerian framework, and the discrete phase model for the sludge particles in a Lagrangian framework, coupled with the non-premixed combustion model for chemical reactions. Pablo Cornejo and Oscar Farías (2011) developed a three-dimensional CFD model for describing coal gasification of fluidized-bed reactors. The commercial multi-purpose CFD code FLUENT 6.3 was employed, taking into account drying, volatilization, combustion and gasification processes. Miltner et al. (2007) used CFD-Model for optimisation of an innovative

combustion chamber for a solid stem-shaped bio-fuel in the form of compressed biomass bales. Carlsson et al. (2010) studied gas phase reaction schemes for black liquor gasification modeling. Blasi et al. (1999) developed a one-dimensional, unsteady-state model for biomass gasification in a stratified concurrent downdraft reactor. Heat and mass transfer across the bed were coupled with moisture evaporation, biomass pyrolysis, char combustion, and gasification, gas-phase combustion and thermal cracking of tars.

Fletcher et al. (2000) developed a detailed CFD model to simulate the flow and reaction in an entrained-flow biomass gasifier. Biomass particulate is modelled by using Lagrangian approach because it entered the gasifier, released its volatiles and finally underwent gasification. Transport equations were solved for the concentration of CH_4, H_2, CO, CO_2, H_2O and O_2 and heterogeneous reactions between fixed carbon and O_2, CO_2 and H_2O were modelled. The model provided detailed information on the gas composition and temperature at the outlet and allowed different operating scenarios to be examined in an efficient manner.

There are several modeling studies on packed-bed biomass combustion which are given in Table 2.3.

Table 2.3 Summary of CFD modeling attempts

Application	Code Dim	Turb. Model	Extra Model	Exp. validation	Authors
Two-stage downdraft gasifier	Fluen2-D	RNG k-ε	DOM	Satisfactory	Gerun (2008)
Entrained flow gasifier	CFX 2-D	Std k- ε	Langragian,DTRM	N/A	Ma et al. (2007)
Downdraft gasifier	Code 1-D	N/A	Porous	N/A	Sharma (2007)
Horizontal entrained flow	Fluen1-D	N/A	Langragian	Reasonable	Zhou (2006)
Moving packed bed	Fluen2-D	Std k- ε	DOM	N/A	Kaer (2004)
Cone calorimeter reactor	Code 1-D	N/A	Porous	N/A	Giltrap (2003)
Entrained flow	CFX4 2-D	Std k- ε	RSM, Langragian	Acceptable	Feltcher (2000)

2.3 Modeling landfill gas emissions

The decomposition of organic components produces methane, which is a significant contributor to global warming. There are numerous review papers on Landfill gas (LFG) emissions (Abushammala et al 2009; Staniunas and Burinskiene 2011). Abushammala et al. (2009) reported the dependency of LFG production rate on many factors controlling the quality of gas production needs to be accounted for in developing predictable models for LFG emission rates. Staniunas and Burinskiene (2011), on the other hand, studied the assessment of green house gases attributable to waste management sector in urban planning. The result of their study is a carbon dioxide equivalent that refers to waste management sector and possible measures of compensation. They quoted that Lithuania produces 407 kg of MSW per year which is equal to 1.7 tons of CO_2 (equivalent) in 20 years horizon. They recommended that for

small cities tree planting is feasible. Roughly 3 trees per person are needed as compensation while for big cities (i.e., districts) they suggested supplementary areas to be identified for tree plantation.

Methane emissions rates from LFG can be obtained through mathematical models, which are generally based on mass balance (Oonk 2010). There are numerous models; most of them are either based on a first-order decay model or a multi-phase model. Mor et al. (2006) have used the first-order decay model for estimating methane generation from Gazipur landfill site. Kumar et al. (2004) estimated CH_4 emissions from MSW landfills using *Default Methodology* and *Triangular model*, while Akolkar et al. (2008) employed *Flux Method* in addition to *Default Method* and *Triangular Method* for monitoring landfill gas emissions. Recently, other ways to deal with oxidation estimates are being developed. Jha et al. (2007) generated greenhouse gas emission inventory from landfills of Chennai by measuring the site specific emission factors in conjunction with relevant activity data as well as using the IPCC methodologies for CH_4 inventory preparation. CH_4 emission estimates were found to be about 0.12 Gg in Chennai from MSW management for the year 2000 which is lower than the value computed using (IPCC 1996). Chakraborty et al. (2011) estimated the methane emissions from municipal waste dumping sites in Delhi, namely three operational landfills Ghazipur, Bhalswa and Okhla. To get true landfills specific methane emissions, well recognized closed Perspex chamber based in-situ method were used and methane concentrations were analyzed by GC-FID. The in-situ methane measurements in Delhi's landfills revealed that the average methane emission flux was 1911±506, 2014±596 and 1041±307 mg/m^2h for Ghazipur, Bhalswa and Okhla landfill sites, respectively. Whereas, average emission factor (EF) for Delhi's landfills was reported to be 6.9±2.4 g/kg. To compare methane emissions developed by in-situ method, other available methods for CH_4 estimation viz. the IPCC (1996) Default Methodology (DM), IPCC First Order Decay (FOD) and Modified Triangular Method (MTM) have also been used.Using in-situ, DM, FOD and MTM methodologies it has been estimated that during 2008-09 periods, the three landfills in Delhi together emit 10 Gg, 46 Gg, 31 Gg, 41 Gg respectively. Chalvatzaki and Lazaridis (2010) compared the LandGEM and IPCC Methodology for prediction

of landfill emissions. They concluded that LandGEM modeling is more efficient than IPCC methodology.

Talyan et al. (2006) used system dynamics modeling approach to model methane emission from MSW disposal landfill site in Delhi during period 2005-2025 and proposed a waste management policy for Delhi. According to this waste management policy, the treatment capacity can be enhanced by introducing different available technologies, for instance, biomethanation, composting and refuse derived fuel, replacement of traditional open landfilling by sanitary landfilling having the facility to capture the landfill gas. The implementation of such policy may be expected to reduce the methane emission to the level of 2001 by the year 2025 despite an almost two-fold increase in waste generation.

Petrescu (2011) experimental study revealed the characteristics of gaseous emissions generated by a non-compliant municipal landfill of Radouti (Romania) after its closure. High concentrations of approximately 60% of CH_4 and 39% of CO_2 of the landfill gas captured in two different landfill sites revealed the polluting character of those emissions and also revealed that they directly affect the environment.

Gaur et al. (2010) upgraded LFG to pure methane using the adsorption and absorption processes by removing toxic compounds using granular activated carbon.They also conducted experiments to develop process for removing CO_2 from LFG (Gaur et al. 2011).

2.4 Scope of the present work

Numerous studies have been conducted in the past on biomass gasification with focus on mathematical and experimental modeling, and characterization of woody biomass. The studies on characterization of MSW/RDF, its utilization in conventional gasifier-engine systems for power generation applications and its impact on environment are scant in open literature. In view of above, the present work is focused on development of database, sampling and characterization of processed MSW or RDF (obtained from three landfill sites of Delhi). This work also deals with utilization of RDF in gasifier-engine system for power production, and evaluation of its impact on environment. Since, composition of MSW/RDF vary considerably with seasonal changes and the location of landfill, the tests and measurements have been planed to characterize its properties including calorific value, chemical composition, moisture and ash content etc. Several other characteristics need to be obtained such as ash sintering temperature, char yields, volatile and moisture release rate, moisture content and density of MSW/RDF. The thermograms for TG and DG analysis of RDF sample in reactive (air) environment (as per the conditions prevailed in a gasifier) are expected to be obtained and analyzed. Proximate and ultimate analysis of MSW/RDF, the pH value, potassium and sulphur content is planned and. characterization of residual ash for its composition, EDS analysis, ash deformation and fusion temperature need to be carried out.

For utilization of MSW, it can be upgraded into more energy rich form "RDF". This RDF can be compressed into briquetes of desired size. A mixture of RDF briquetes and wood chips are prepared in proportion of 1:1 as feedstock for conventional fixed bed downdraft gasifier system. An experimental test rig was developed by coupling the NETPRO downdraft biomass gasifier (capacity 10 kWe) with gas engine of capacity 10 kW convertd to operate with single fuel mode. Experiments were prformed on gasifier-engine system in order to study the syngas composition, exhaust emissions from engine and pollutant concentration in recirculating water used for spray over syngas cooling in order to identify the suitability of RDF in conventional fixed bed gasification systems.

Considerable efforts have been done on understanding the thermochemical conversion processes for efficient and cost effective utilization. A theoretical study was carried out to predict resulting gas composition from conventional downdraft biomass gasifier. A thermodynamic modeling was developed and a commercial CFD software has been adapted to predict the final syngas composition, temperature profile inside the downdraft gasifier operated on mixture of RDF (obtained from major landfill site in Delhi) and wood chips. Predicted syngas composition using equilibrium modeling and CFD software have been compared with experimental data for validation.

Presently, Landfilling practice is very common for MSW disposal. However, it releases volatile organic compounds with leachable toxic heavy metals and greenhouse gases including methane and carbon dioxide. The present work focused on the determination of emissions from the three major landfill site located in Delhi. LandGEM model was employed to compute the landfill gas production. Finally, the potential of energy recovery and greenhouses gases reduction was studied in context of power production through gasifier-engine system utilizing the huge stocks of MSW dumped at various landfill sites.

Chapter 3

CHARACTERIZATION OF MSW/RDF AND EXPERIMENTAL STUDIES ON GASIFIER-ENGINE SYSTEM

3.1 Introduction

For successful gasifier operation with solid fuels like MSW, the heating or calorific value, ash sintering temperature, char yields, volatile and moisture release rate, moisture content and density of solid fuel are very important parameters. The heating value of solid MSW feedstock depends on several factors including chemical composition, moisture and ash content. Several other characteristics are also needed to describe the technical and environmental aspects of the solid fuel. In the subsequent sections the characterization of MSW/RDF and experimental studies on gasifier-engine system are carried out in order to identify the suitability of MSW/RDF in conventional fixed bed gasification systems.

The per capita solid waste generated in Delhi lies in the range of 150 - 600 g per day depending upon the economic status of the community involved. It mainly includes waste from households, industry and medical establishments (City Development Plan 2006). There are three large landfill sites functioning at present in Delhi - Ghazipur, Okhla and Bhalswa. These are spread over the area of 66.42 hectors as shown in Fig. 3.1. The Gazipur landfill site is operational since 1983 and covers an area of 73 acres (3.0×10^5 m^2). Bhalswa landfill receives MSW from Nazafgarh, Rohini, Civil Line, Karol Bagh, Southern Paharganj and West Zone. Ghazipur site receives MSW from Shahdara south, Shahdara north, city zone, and NDMC. Okhla receives MSW from

south zone, central zone, and city zone, Nazafgarh and NDMC (Table 3.1). The waste coming to these landfill sites mainly comprises of the waste from slaughterhouse, hospitals, roads/streets, residences, commercial & industrial establishments, construction and demolition waste, dairy waste etc (City Development Plan 2006).

Fig. 3.1 Waste Disposal Sites in Delhi

Table 3.1 Zonal description of landfill sites

S.No.	Name of Site	Location	Area (Ha)	Year started	Zones supplying waste
1.	Bhalswa	North Delhi	21.06	1993	Civil Lines, Karol Bagh, Rohini, Narela, Najafgarh and West Delhi.
2.	Ghazipur	East Delhi	29.16	1984	Shahdara (south and north), City, Sadar Paharganj and NDMC.
3.	Okhla	South Delhi	16.20	1994	Central, Najafgarh, South and Cantonment Board.

3.2 Characterization of MSW/RDF

Waste stream analysis can be defined as any program which involves a logical and systematic approach for obtaining and analyzing data on one or more waste streams or sub-streams. It also provides an estimate of solid waste quantity and its composition referred to as waste characterisation (EPA-USA 1996; EPA-USA 1999; EPA-Ireland 1996). Presently, there is no any agreed international standard for waste characterisation, although India has developed its own manual on MSW management in 2000 for MSW characterisation (Expert Committee Delhi 2000). In the present study, the waste is quantified on the basis of total waste received at the landfill sites and composting plants in the city. Some important physical, chemical and thermal properties of Delhi MSW were evaluated and characterized based on field and laboratory investigations (Jeevanrao 1993; Characterization of New York City's Solid Waste Streams 2000).

3.2.1 Physical characterization

Quantification

The quantity of waste (to be managed) is an important aspect of solid waste management, which can be determined in terms of its size, number of functional units and equipment required for managing the waste through a suitable technology. The quantity of MSW can be measured in terms of weight and volume. The weight is a fairly constant quantity for a given set of discarded objects whereas volume is a variable parameter. Waste quantity is usually estimated from past records. Tchobanoglous (2002) reported three methods commonly used to assess the quantities namely load count analysis, weight volume analysis and material balance analysis.

To study the waste quantification of Delhi landfill sites, data was obtained from MCD. Data collected on daily basis gives the weightof material collected on each land fill. The original data was from weight-scale readings at the landfill site in operation. The data of MSW received at the landfill sites in New Delhi is listed in Table 3.2 and

Table 3.3. Table 3.2 gives the amount of MSW received (month-wise) at Bhalswa, Ghazipur and Okhla Phase-1 landfill sites from April 2005 to March 2011 in Delhi. Table 3.3 shows the amount of MSW (month wise) dumped at the three sites individually from April 2009 to March 2010.

Table 3.2 Amount of MSW received (month-wise) at Landfill sites (Delhi) from 2005-06 to 2010-11

		Weight (MT)					
S.No.	**Month**	**2005-06**	**2006-07**	**2007-08**	**2008-09**	**2009-10**	**2010-11**
1	Apr	164368	161489	133358	128915.6	149195.5	173492
2	May	173397	181210	138452	88332.97	145043.7	182417.3
3	June	150578	159233	127377	141007.7	141155.5	167820.3
4	July	202534	170903	142178	154073.4	163349.6	185834.3
5	Aug	190903	175509	139974	146975.9	152330.2	181013.2
6	Sept	199830	177393	134588	161048	161558.4	180466.6
7	Oct	209327	192265	136705	165336.8	167902.8	192953.8
8	Nov	191031	188628	133933	184671.1	159856.5	183503.2
9	Dec	186315	171588	153749	157533.2	167793.9	180653
10	Jan	167613	145755	127090	147979.5	158483.1	187123.9
11	Feb	159191	129142	119531	139637.7	155078.4	173650.1
12	Mar	161937	138770	128634	147653.1	165900.4	183211
Year-wise total		**2157024**	**1991885**	**1615569**	**1763165**	**1887648**	**2172139**

Table 3.3 Amount of MSW received (month-wise) at landfill sites Bhalswa, Ghazipur & Okhla Phase-1 during 2009-10

			Weight (MT)	
Sites	**Bhalswa**	**Ghazipur**	**Okhla P-1**	**Total (MT)**
Apr 2009	64839.82	50179.24	34176.45	149195.5
May 2009	60543.44	50389.61	34110.67	145043.7
Jun 2009	58425.27	49452.37	33277.84	141155.5
Jul 2009	68235.6	55196.79	39917.21	163349.6
Aug 2009	60759.03	54565.53	37005.64	152330.2
Sep 2009	69031.09	55454.08	37073.24	161558.4
Oct 2009	73402.49	56962.19	37538.11	167902.8
Nov 2009	64274.54	57172.97	38409.00	159856.5
Dec 2009	70660.08	56393.37	40740.47	167793.9
Jan 2010	65241.39	54174.43	39067.27	158483.1
Feb 2010	61555.66	56375.76	37146.97	155078.4
Mar 2010	65351.86	60467.04	40081.52	165900.4
Total	**782320.2**	**656783.3**	**448544.4**	**1887648**

MSW characteristics depend on a number of factors, such as food habits, cultural traditions, socio-economic and climatic conditions (Chang and Davila 2008). It varies not only from city to city but also within the same city. The simplest way for MSW characterization is “Sampling”. There are two methods of sampling. In first one, the sampling is carried out directly at waste generation sources, while in the other; the samples are obtained from trucks arriving at the disposal sites (Crowe and Carty 2006). Sampling for the present study was designed to handle seasonal variations and influence of location on waste composition. Ideally, waste analysis should be carried out at an interval of three months; however, it is also acceptable to carry out a minimum of two surveys within year (Gawaikar 2006; Maclaven et al. 1995). Sampling should, however, be avoided during big festivals and public holidays (EPA Ireland 1996). In this work, one year is sub-divided into the four seasons. The data collected from 16 December 2008 to 30 March 2009 is assigned for Season-1; from 1 April 2009 to 30 June 2009 for Season-2; from 1 July 2009 to 30 September 2009 for Season-3, while Season-4 corresponds to data collected from 1 October 2009 to 15

December 2009, respectively. For present work, a total of three hundred samples were collected during the year of 2008-09.

The equipment used for conducting the waste composition survey are listed as

1. Vehicle
2. Weighbridge
3. Mechanical shovel, or other device (for mixing the sample) and hand shovels
4. One 60 kg precision scale (minimum precision 10g)
5. One box sieve with a 20 mm round mesh
6. One tray for fines recovery
7. Containers (boxes or bags) for storing and weighing separated fractions
8. Brooms, disinfectant, gloves, masks, magnet (for distinguishing between ferrous and non-ferrous metals)
9. First aid kit

It should be noted here that selection of representative sample is a very important task associated with a waste stream analysis. It is of critical importance that the sample collected, be representative of the waste management unit under study (AIT 1991).

Sample size

According to a study carried out in USA with a sample ranging from 100 kg to 1000 kg, it was found that a 100 kg sample provide as much accuracy as compared to a 1000 kg sample (Alamgir 2007). If the material collected at a point is too small to complete a sample (say of 100 kg), in such situation, a smaller sample could also be collected for analysis. Repetitive sampling and analysis provide a more representative data. Smaller the sample weight the greater the variance of the waste sample composition (Klee 1980). Klee noted that as the sample weight is decreased from approximately 91 kg, the sample variance increases rapidly, but above it a sample size is more than 140 kg, the variance decreases. Thus according to Klee's recommendations the sample weight should be in the range of 91-140 kg. In the present work, the target sample weight was taken around 100 kg (EPA Ireland 1996).

Representative sample

If the collected sample is too large, the cone and quartering size reduction will not yield a representative sample for sorting. This is why it is recommended that the collected sample be restricted to less than 5,000 kg. The sample for sorting is obtained by reducing the sample collected to between 100 and 200 kg using a cone and quartering technique as described below (Visvanathan et al. 2004).

Sample size reduction

The sample should be reduced to a more manageable size as the actual classification of materials will be carried out by hand. The ideal sample size for characterisation is between 100-200 kg (minimum 100 kg) and the size reduction is achieved by a 'coning and quartering technique' as:

1. The sample is placed on the floor and thoroughly mixed by shovel.
2. The sample is then placed in a uniform pile of approximately 0.8 m high.
3. The pile is divided into four quarters using straight lines perpendicular to each other.
4. Either pair of opposite corners is removed to leave half the original sample.
5. The process is repeated until the desired sample size i.e. 100-200 kg is obtained.

The surplus 'two-quarters' from the last size reduction should be retained for analysis of moisture content and bulk density. Care should be exercised to avoid selection of larger sized particles to reduce sample bias (EPA Ireland 1996).

Collection of samples

For characterization of MSW going to three landfill sites, *Dhalao* (situated in different types of areas - residential, slum, commercial and industrial) were identified. Trucks coming from these areas were also identified at the landfill sites. Samples were collected from *dhalaos*. 10 kg sub-samples of MSW were collected from ten different points from outside and inside of any one solid waste heap. Similar exercises were

carried out at 5 different *dhalaos* or trucks leading to landfill sites. Consequently around 500 kg of MSW is mixed thoroughly to make one representative sample and it is then reduced to around 100 kg by coning and quartering method (as described earlier). On similar grounds, total 5 representative samples were collected from MSW leading to each landfill site for one season. Hence, total 15 samples in all were collected from different representative profile of the MSW, five each for three land fill sites per season. Thus total 60 samples were collected for final characterisation.

Sample analysis

Jeevanrao and Shantaram (1993) detailed the characterization methods, which recommend that sorting area should be accessible to vehicles and protected from winds and precipitation. Basic sorting sequences can be initiated when collection of sample is complete as:

1. A copy of data form;
2. Sample is unloaded onto the surface of sorting area;
3. Large items and bags containing single waste category are removed from the sample and set aside for weighing, bypassing the sorting box; any unclassified material should be allocated as "combustible" or "incombustible".
4. The waste is segregated into different components in the container; and
5. The containers are brought to scale, checked for accuracy of sorting and then weighed.

The above procedure is followed with due regard to safety precautions. Standard personnel safety procedures need to be followed during the sorting process such as wearing gloves, apron, safety glasses and boots, etc.

Classification of the waste stream

After measuring the weight of collected waste samples, they were transported to the designated sheds for sorting. The collected samples were sorted into twenty-four targeted categories on a sorting platform. Individual components were separated and weighed. The weights are then expressed in percentage basis of original sample. In the present study the twenty four targeted sub categories were clubbed into five broad

groups namely fuel, organics, inert, recyclables, and miscellaneous (Classification of Solid Waste and Monitoring Methodology for Hong Kong 2000; Chang and Chang 2008).

Sorting into 24 targeted categories was done for four seasons namely Season-1, Season-2, Season-3 and Season-4 for each of the three landfill sites as described earlier. In any given season the sorting was done on five different dates for each of the landfill sites.

Table 3.4 Physical characterization of MSW

S.No.	Waste components
A-Fuel	
1	Wooden Pieces
2	Paper / Card board
3	Textiles / Cotton
4	Coconut Shell
5	Polythene Bag
6	School Bag
7	Plastics
8	Straw & Hay
9	Thermocole
10	Dry leaves/dry matter
B-Organic	
1	Green Matter (Leaves/cuttings from trees)
2	Vegetable peels
3	Kitchen waste
4	Vegetable
C-Inert	
1	Concrete/ Stone
2	Ceramics
3	Lime /sand /mud/ Soil
4	Bricks / Broken Tiles
D-Recyclables	
1	Glass
2	Rubber/Leather/Tyre
3	Metal (ferrous and non ferrous)
	Type of waste
E-Miscellaneous	
1	Hazardous waste (Medical waste)
2	Moist and Muddy vegetable waste

Moisture content and bulk density

The surplus 'two-quarters' from the last cone and quartering step were set aside for analysis. The two quarters were combined and a further cone and quartering was performed. Each pair of opposite quarters were then be combined to form two samples (i.e. A and B). Sample A was then used for obtaining moisture content, while Sample B analyzed for bulk density (Manual on Municipal Solid Waste Management 2000).

In order to measure the bulk density of a sample, a procedure was followed, according to which solid waste was taken in a box of 0.028 m^3, from different parts of the heap of waste, and then weighed with the help of spring balance. After weighing, contents of this box were emptied in to a bigger 1 m^3 box and the weight of the waste poured into the bigger box was noted. This was repeated till the larger box got filled to the top. Care was taken that the waste did not get compacted by pressure. The 1 m^3 box was filled three times and the average bulk density was computed. Thus the weight per cubic meter was obtained (Manual on Municipal Solid Waste Management 2000).

Moisture content of the sample is determined by establishing the weight loss data when heated under rigidly controlled conditions of temperature, time and atmosphere, sample weight, and equipment specifications (IS 1350:PART1:1984 Reaffirm 2001).

3.2.2 Thermo-chemical characterization of MSW/RDF

One of the important processes in characterization of a solid fuel is to understand its weight loss rate when subjected to a particular heating rate. The thermo-gravimetric (TG) analysis provides information of the rate of devolatilization and weight loss of solid fuel sample.

The method based on thermogravimetry produces information related to combustion and gasification. Therefore, TG and DG thermograms for RDF sample were obtained

using thermo-gravimetric analyzer (Perkin-Elmer). Analyzer enables continuous recording of weight loss of sample as a function of time and temperature with specified heating rate and flow rate of sweeping gas. The TG Anaysis can be carried out in reactive and inert environments. In this work, the tests were performed in oxidant environment (air) maintaining air flow rate of 40 ml/min. The weight of RDF samples was 1.661 g. For better correspondence of result, the data from analyzer are divided into four groups: temperature, time, weight loss thermo-gravimetric (TG) and first derivative of weight loss with respect to time (DTG). The data of TG and DTG are defined (Shen and Qinlei 2006) as

$$TG = \alpha = \frac{w - w_0}{w - w_\infty} \tag{3.2}$$

$$DTG = \frac{d\alpha}{dt} \tag{3.3}$$

Here w_0 is sample initial weight; w and w_∞ are sample weight at time t and final weight of the sample.

The RDF sample was used to obtain weight loss from 50°C to 900°C in reactive ambient in presence of air at slow heating rate i.e., 20°C/min (suitable conditions for conventional gasification). The first indication in weight loss is due to release of moisture from RDF test sample. The next sharp weight loss is attributed to primary thermal decomposition of RDF. The next weight loss is attributed due to secondary thermal decomposition of RDF. DG thermogram is used to obtain weight loss rate.

Chemical analysis

Important chemical properties including the pH value, potassium and sulphur content, proximate and ultimate analysis were carried out to find out the suitability of MSW for thermochemical conversion. Through coning and quartering technique a 1 kg sample was identified from a 100 kg sample. This sample was further dried and grounded in a ball mill.

The pH value

The pH value was determined following Peterson (Ragland et al. 1991). A mixture of waste sample and water is prepared in proportion of waste to water ratio of 1:2.5. For this work, a mixture of waste in 250 ml of water was prepared and kept for 24 hours. The pH was then measured on pH meter (HACH (USA) HQ 40 d 18).

Potassium and phosphorous content

The potassium content was obtained using flame photometry, while phosphorus was determined by gravimetric methods.

Proximate analysis

A fair idea of major components of pyrolysis products (viz., fixed carbon, volatile maters and residual ash) is obtained from proximate analysis. The procedure for proximate analysis was adopted as prescribed by Grover et al. (1988). Proximate analysis of MSW and RDF provides proxy information of moisture, fixed carbon (non-volatile carbon), volatile maters and residual ash.

Chemical composition of MSW/RDF

Ultimate analysis was performed on Euro Vector elemental CHNSO analyser (2400 Perkin Elmer), which gives elemental composition (% by weight) of the sample.

Heating value

The higher heating value of the oven dried MSW and RDF samples were measured on a Parr-6100 bomb calorimeter (precision of 0.02 %) following the ASTM D2075-77 standards. The lower heating value or calorific value of MSW and RDF can be obtained in terms of hydrogen and moisture quantity using Du Long equation as

$$Lhv = Hhv - 600(M + 9H) \tag{3.4}$$

where, H and M are the weight percentage of hydrogen and moisture, respectively.

3.2.3 Characterization of ash

The ash deformation and fusion temperatures can be used as an indicator of sintering and deposition tendency of ash that may hamper the process operation. In this article, ash deformation and fusion temperature of RDF sample is measured in the laboratory by ASTM method D-1857. The ash sample obtained from proximate analysis was then finely ground. A solution containing 10 % dextrin, 0.1 % salicylic acid and 89.9 % water (by weight) was mixed to the ash and prepared to form a stiff paste pressed into small cone-shaped molds. After drying, these cones were inserted in a high temperature muffle furnace and heated at 800°C. After an interval of 15 minutes, the temperature of the sample was increased by 50°C. During each interval of 15 minutes, the shape of the cone was observed. The oven temperature at which the cone first deformed was recorded as ash deformation temperature. The softening temperature, hemispherical and fluid temperature were also recorded. As the temperature of sample was increased further, the sample showed the tendency to fuse into a hemispherical lump. This temperature was recorded for ash fusion temperature.

Materials and compounds containing the metal elements were detected by energy dispersive X-ray spectrometry (EDS). The EDS images of ash sample from MSW were obtained in the present work.

3.3 Experimental studies on gasifier-engine system

3.3.1 Description of experimental setup

Experiments on gasifier system were taken up primarily to validate the CFD model predictions and to analyze the environmental impact of gasification-engine system for electric power applications. As described in earlier section, the thermo-physical properties of RDF are not conducive for successful operation of conventional gasifier systems, therefore, in the present work, feed is prepared by mixing RDF with woody biomass in the proportion of 1:1.

In the reactor, both gas and biomass feedstock move downward as the reaction proceeds. While mixture of woody biomass and RDF flows downward due to gravity, the part of air intake is induced through the reactor open top and through the air tuyers (distributed across the circumference of oxidation zone) due to suction created either by blower arrangement or engine itself. The feedstock slowly moves down along with air passing through the drying, pyrolysis, oxidation and reduction zones of the downdraft reactor and gets converted into producer gas which leaves the reactor at the bottom through the screw grate. The system has a provision for using a part of the heat of the producer gas for preheating the biomass. The producer gas, thus, passes from the bottom of the reactor to the annular region around the top of the reactor, through a duct followed by a cyclone. Cooling of producer gas exiting the reactor is carried out by the combination of two spray towers. The cooled producer gas is then allowed to pass through a chiller in order to remove the moisture and tar content of the gas. The properly cooled gas is then allowed to pass through the sand bed filters. Finally, the gas is allowed to pass through the fabric filter. This two-stage filtering ensures that the gas is cleaned to the desired level for use in the engines. The various sub-assemblies of tipical gasifier are described schematically in Fig. 3.2.

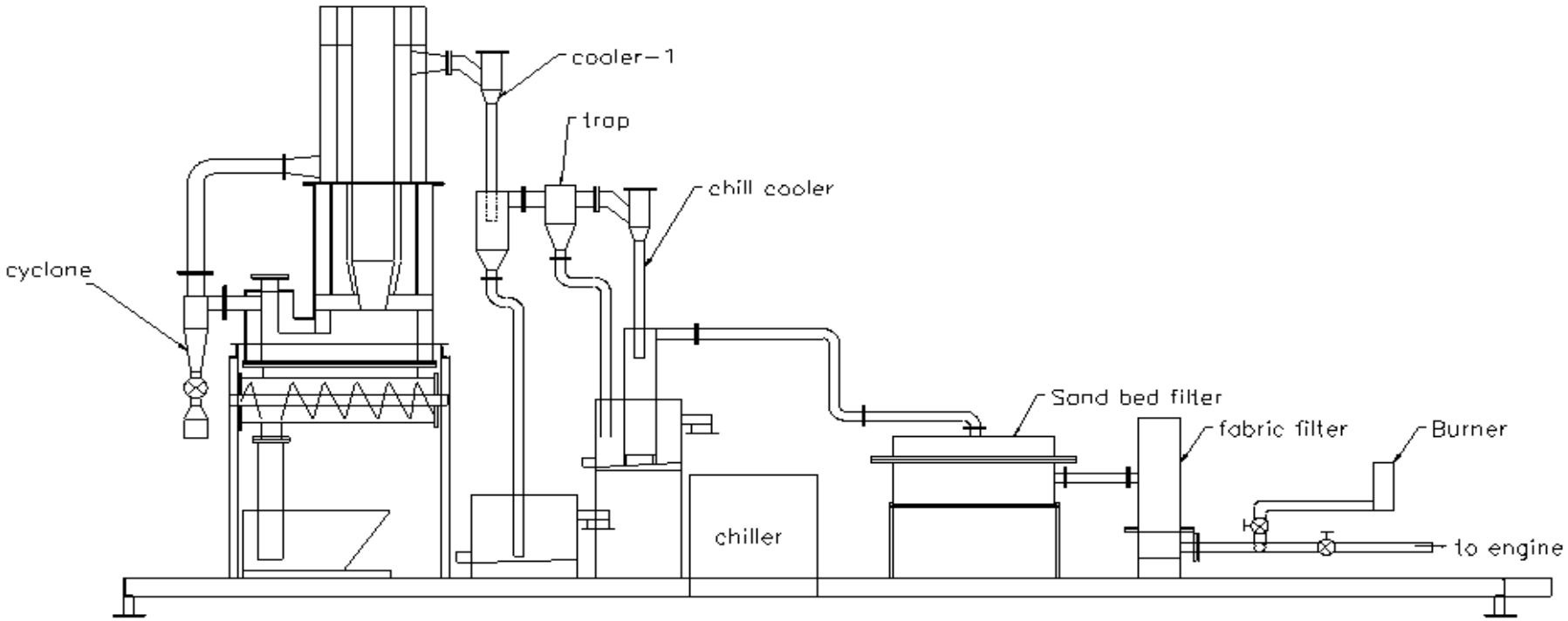

Fig. 3.2 Gasifier system including cooling-cleaning train

3.3.2 Reactor

NETPRO downdraft biomass gasifier of capacity 10 kWe was used in present work. The schematic view of the gasifier is given in Fig. 3.3. The reactor is a twin shell arrangement with ash extraction at the bottom and gas exit at bottom side. The bottom shell is made of MS plate casing with inner insulation and ceramic tile lining. The top shell is double walled stainless steel shell having an annular spacing in which hot gas passes, transferring a part of sensible heat to the incoming biomass. The bottom and top shells are interconnected by cyclone and interconnecting duct. There is a screw based ash extraction system provided at the bottom to hold the charge, with a handle for extraction and a bin for collecting the extracted ash and char. The cyclone helps in particulate removal.

Fig. 3.3 Downdraft gasifier (capacity 10 kWe)

3.3.3 Cooling and cleaning system

Cooling of final gas is obtained through water cooler followed by chill cooler as well. It is made of stainless steel. The hot gas comes in contact with the cold water and the gas temperature comes down to ambient. There is a small dump provided at the bottom, which forms the exit for the cooler, for separating the gas and water (Fig. 3.3). The gas after the cooler passes through a moisture trap where the moisture carryover is partly eliminated which is again made up of stainless steel.

The gas passes through a chill water scrubber which reduces the gas temperature below the ambient thereby reducing the levels of moisture, tar and particulates. The chill water flows in a recirculation mode and chilling is assisted by a chiller of capacity 0.3 TR. The entire system is insulated to prevent heat loss to surroundings. The gas before entering the engine passes through a sand bed filter and a 5 micron non-woven fabric filter. This filter acts as a final security filter.

3.3.4 Flare

This is provided to check the initial quality of the combustible gas. The gas is flared in the burner for few minutes prior to ‘change over’ to the engine.

3.3.5 Instrumentation

(a) Gasifier system

Before proceeding to the experiments, the experimental setup was properly instrumented. The gasifier-engine system was provided with water tube manometers at strategic locations for monitoring the health of the gasifier. The pressure indicated by the manometer at the reactor exit forms the basis for operating the ash extraction system. The pressure drop across the gasifier was measured. The manometer scale had a least count of 1 mm. K- type thermocouples were used for temperature measurement. The thermocouples were inserted from the open top of the gasifier into the fuel bed to the desired position in the bed. The flow rate of producer gas was measured using a venturimeter already provided in the system

by the manufacturer. For measurement of gas composition, Gas Chromatograph (NUCON 5765) was used. The sample of gas at various gas flow rates was collected in air tight sampling bags. The gas sample was injected into the column of GC with Argon as carrier gas. The detector was inserted into the gas stream at the end of the column, which records the time of the passage and the quantity of each component on a computer. The GC was calibrated using the calibrated producer gas sample of typical composition for CO: 19.2%, CH_4: 3.95%, CO_2: 11.57%, H_2: 20.45% and N_2: 45.1%. By comparing the areas of peaks for calibration gas and gas sample; the composition of gas sample was predicted by the computer software.

(b) Gas engine

For using producer gas in SI engine (capacity 10kW), the compression ratio of engine was fixed at 10. The details of engine specifications are given in Table 3.5.

Table 3.5 Engine specifications

Engine	Specifications
Gas engine generator set	CUMMINS.
No. of cylinders	03
Diameter (bore)	102 mm
Stroke length	115 mm
Ignition	23^0 b TDC
Compression ratio	10:1

The engine generator panel has an incomer from the generator and an outgoing feeder to the load. This also has a change over switch to facilitate gasifier operation during the start up where the gas engine is not operational. The change over switch should have connection from the grid to provide startup power and the same gets taken over by gas engine when it is made operational.

3.3.6 Initial startup

For gasifier start-up, the gasifier bed was initially filled with charcoal particles up to air tuyers and the remaining volume was loaded with mixture of wood and RDF. The gasifier was ignited with blower switched on and gasifier bed was ignited with the help of torching flame at the entry of the tuyers. The warm up and starting time was about 20 to 30 minutes after which combustible gas (suitable for engine use) starts getting generated. As the temperature rises, the self-sustaining exothermic reactions take place. Initially, the released gas have very little of CO or H_2 and therefore, was flared out to the burner to check for steady and colourless flame. Measurements with engine were started only after a steady, colourless flame was obtained.

3.3.7 Experiments

As the clean burning of the producer gas was obtained from gasifier, the gas side valve was opened gently and burner side valve was closed and engine was started. The load on engine was applied through electrical panel. Gas samples were collected and analyzed later.

Fig. 3.4 Wood Chips

Fig. 3.5 RDF Briquetes

An experiment was conducted and syngas produced was used to run a 10 kW 3- cylinder 100% producer gas generator for 3 hrs at different power levels (voltage remaining constant) and the exhaust gasses were measured by AVL-444 multi gas analyzer.

3.4 Results and Discussion

3.4.1 Physical classification of the waste stream

The representative samples were used to analyze the MSW at Gazipur landfill site in Delhi for all seasons. The raw MSW was available in terms of various components viz., fuel, organics, inert waste, recyclable and miscellaneous.

The results for gravimetric profiling of raw MSW at Gazipur landfill site for each season are listed in Table 3.6 and aso presented in Fig. 3.6.

Table 3.6 MSW Analysis (weight %) of Gazipur landfill site

Components	Season-1	Season-2	Season-3	Season-4
Fuel	22.12	27.53	34.19	27.95
Organics	38.91	34.36	32.55	35.28
Inert	25.52	31.94	23.99	27.15
Recyclable	1.01	1.79	1.57	1.46
Miscellaneous	12.44	4.37	7.70	8.17

Except season 3 it was observed that the organic components were highest in all other seasons ranging from 34.36-38.91 %. Amongst seasons organic components happened to be highest during Season-1 (16^{th} Dec. 2008 to 30^{th} March 2009). Fuel component of MSW peaks at 34.19 % during Season-3 (1^{st} July 2009 to 30^{th} Sept. 2009). It was observed to be minimum at 22.12 % during Season-1(16^{th} Dec 2008 to 30^{th} March 2009). Inert components were also a significant part of the MSW ranging from 23.99% during Season-3 to 31.94% during Season-2 (1^{st} April 2009 to 30^{th} June 2009). Recyclable were however very low ranging from 1.01% during (for Season 1) to 1.79% (for Season-2).

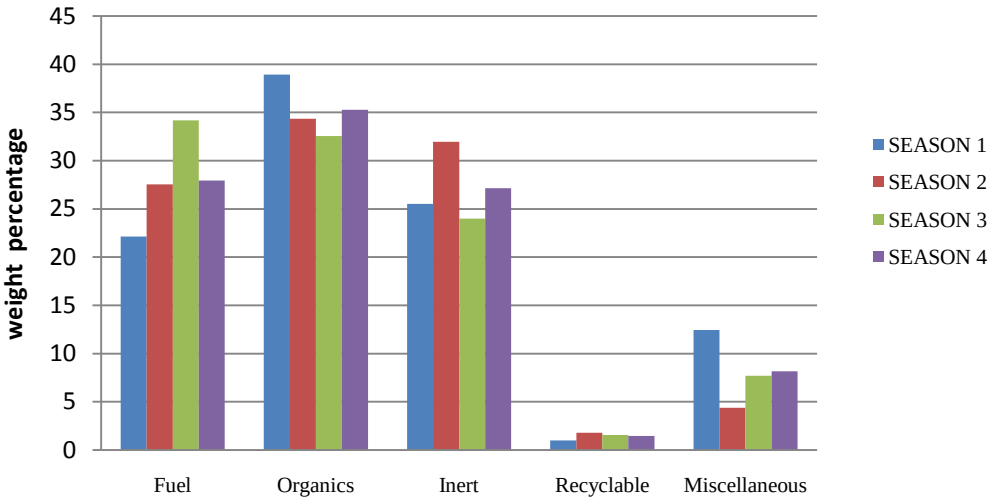

Fig. 3.6 Gravimetric profiling of raw MSW at Gazipur landfill site for each season.

The gravimetric profile of raw MSW with respect to Okhala landfill is shown in Table 3.7 and Fig. 3.7. The pattern for MSW at Okhala was similar to that at Gazipur landfill site. However the recyclable component was high ranging from 13.21% (for Season-3) to 19.37% (for Season-1). The inert component was relatively less, ranging from 12.82% (for Season-1) to 18.70 % (for Season-2).

Table 3.7 Analysis (weight %) of fresh MSW to be dumped at Okhala landfill

Name	Season-1	Season-2	Season-3	Season-4
Fuel	24.72	30.62	31.82	26.76
Organics	42.71	35.12	40.16	39.44
Inert	12.82	18.70	13.93	16.45
Recyclable	19.37	15.15	13.21	16.13
Miscellaneous	0.38	0.41	0.88	1.22

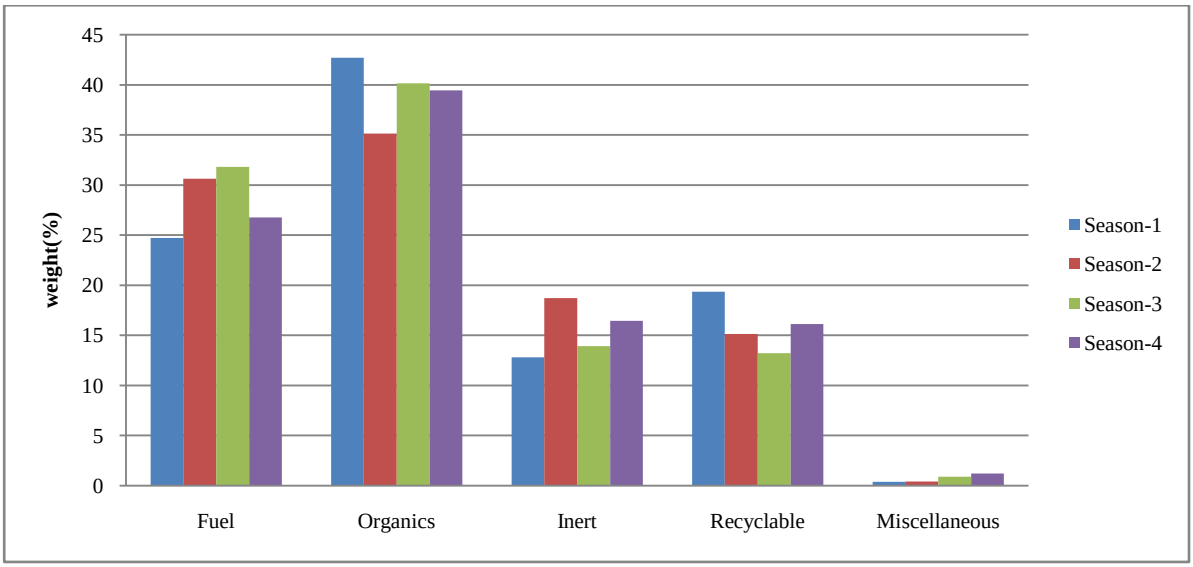

Fig. 3.7 Gravimetric profiling of fresh MSW at Okhala landfill site.

The five components of raw MSW along with seasonal variation are given Table 3.8 and Fig. 3.8. The fuel and organic components received with respect to Bhalswa landfill site follow the trend similar to Gazipur landfill site. The recyclable component is higher than Gazipur but lower than Okhla landfill site. The recyclable contribution varies from 4.07% (for Season-3 to 7.70% (for Season-2).

Table 3.8 Analysis (weight %) of fresh MSW at Bhalswa landfill site for year 2009-10

Name	Season-1	Season-2	Season-3	Season-4
Fuel	23.93	23.66	20.12	22.92
Organics	40.11	39.24	60.50	39.86
Inert	26.51	27.12	13.00	28.92
Recyclable	7.38	7.70	4.07	5.68
Miscellaneous	2.08	2.29	2.31	2.63

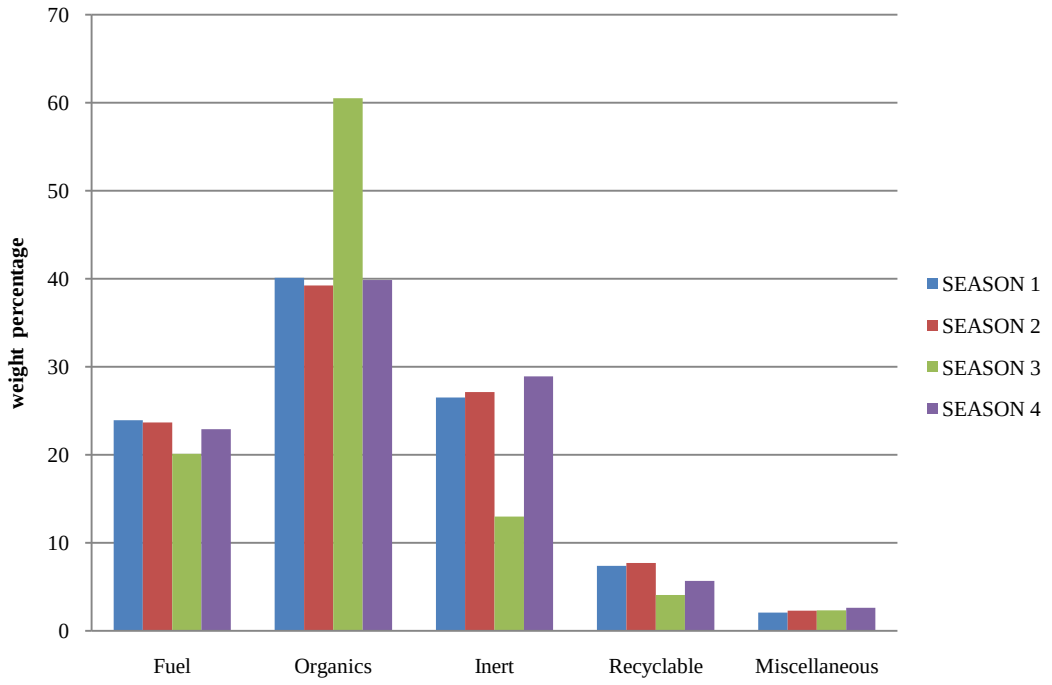

Fig. 3.8 Gravimetric profiling of fresh MSW at Bhalswa landfill site.

For comparative analysis, the details of five components along with further physical classification are tabulated in Table 3.9. It can be observed for fuel component of MSW, the "textile/cotton" waste were among the biggest contributor for both the seasons (i.e., Season-1 and Season-3) for all three landfill sites. For Season-1, the sub-components "paper" and "cardboard" were observed to be among the second biggest contributors in fuel component for all three landfill sites. For Season-3 straw and hay were among the second biggest sub-component at Gazipur and Okhla, whereas at Bhalswa, the second biggest contributor was again paper and cardboard. Amongst organics, the sub-component "green matter" was the main contributor at Gazipur and Okhla, while sub-component "vegetables" was observed to be the main contributor from Bhalswa landfill site.

Table 3.9 Physical classification of components and sub-components for all three landfills for two seasons (2009-10)

Particulars (Weight %)	Season 1: Gazipur	Season 3: Gazipur	Season1: Okhala	Season 3: Okhala	Season 1: Bhalswa	Season 3: Bhalswa
Fuel						
Wooden Pieces	1.34	3.2	1.44	2.98	1.3	0.85
Paper / Card board	3.35	4.03	3.36	3.74	3.3	3.1
Textiles / Cotton	6.27	8.56	8	7.96	7	6.1
Coconut Shell	2.12	2.94	2.1	2.58	2.34	2.14
Polythene Bag	2.52	2.4	2.5	2.03	2.33	2.12
School Bag	1.2	3.41	1.1	3.04	0.98	1.4
Plastics	2.4	2.6	2.3	2.38	2.1	2.5
Straw & Hay	2.17	6	2.2	5	1.9	1.18
Thermocole	0.17	0.53	0.1	0.4	0.2	0.01
Dry leaves/dry matter	2.75	0.52	1.62	1.71	2.48	0.72
Organic						
Green Matter (Leaves/ cuttings from trees)	15	13	16	15.3	15	20
Vegetable peels	1.91	1.85	2	1.64	2	7
Kitchen waste	10	6.87	14.72	13.8	7.11	10
Vegetable	12	10.83	10	9.42	16	23.5
Inert						
Concrete/ Stone	2.67	2.43	2.5	2.6	2.8	1.26
Ceramics	0.6	0.59	1.12	1.15	0.7	0.5
Lime /sand /mud/ Soil	22	18	8.6	9.5	22.2	10.54
Bricks / Broken Tiles	0.25	2.97	0.6	0.68	0.8	0.7
Recyclables						
Glass	0.16	0.25	5	2	3	0.5
Rubber / Leather / Tyre	0.55	0.6	11	8	3.02	0.7
Metal(ferrous and non ferrous)	0.3	0.72	3.37	3.21	1.35	2.87
Miscellaneous						
Hazardous waste(Medical waste)	5	2.2	0.11	0.05	0.3	0.11
Moist and Muddy vegetable waste	6.44	5.5	0.27	0.83	1.78	2.2

3.4.2 Moisture content and Bulk density

Sample A, was used for finding out the moisture content of MSW. The results for moisture contents in sample A for each landfill site for all four seasons are given in Table 3.10 and Fig. 3.9. Moisture content of the MSW was very high for all three landfill sites during all seasons. It ranged from 35.06% at Okhla during season 2 to 58.60% at Gazipur during season 3.

Table 3.10 Variation of moisture content in all seasons for each landfill site

Landfill site	Moisture content (wt %)			
	Season-1	Season-2	Season-3	Season-4
Gazipur	47.26	45.58	58.60	57.00
Okhala	41.69	35.06	50.56	47.53
Bhalswa	45.19	40.49	48.74	47.77

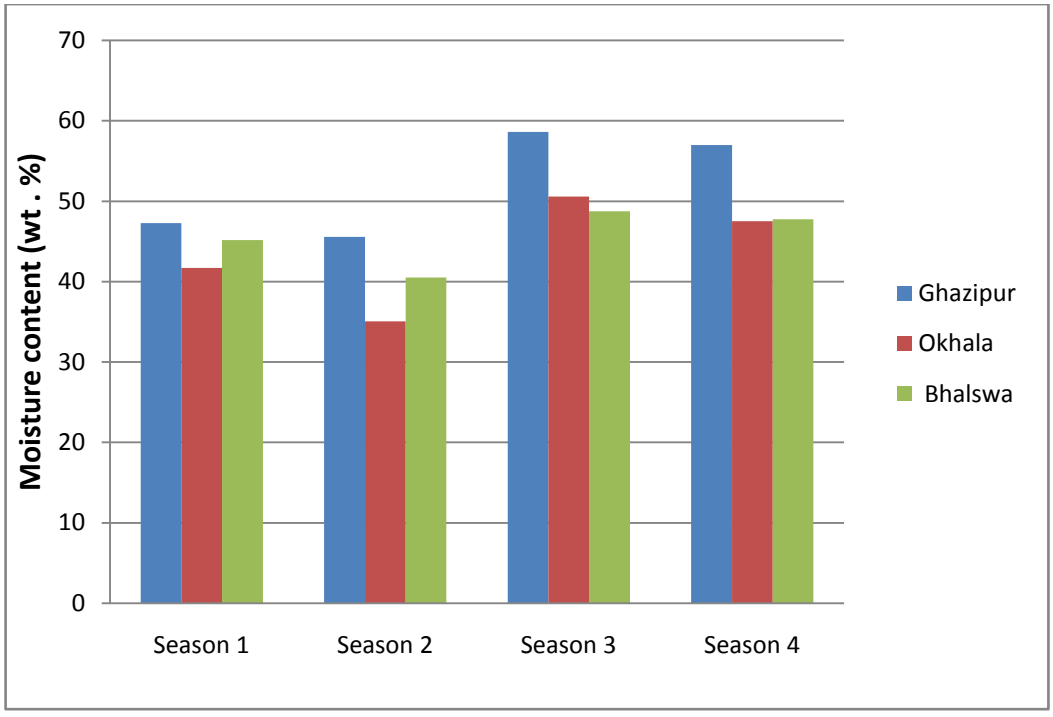

Fig. 3.9 Variation of moisture content in all seasons for each landfill site

Sample B, was used for finding out the bulk density of MSW. The results are given in Table 3.11 and shown in Fig. 3.10. Bulk density displayed considerable variations amongst sites and season. No general pattern can be observed. However at Gazipur it was more uniform varying from 593.80 kg/m^3 during season 2 to 804.47 kg/m^3 during season 3. At Okhla it varied from 680.07 kg/m^3 during season 2 to 794.98 kg/m^3 during season 1. At Bhalswa the variation was quite sharp. It ranged from 801.13 kg/m^3 during season 2 to 899.72 kg/m^3 during season 3.

Table 3.11 Variation in bulk density of raw MSW at each landfill site

Landfill site	Bulk Density (kg/m^3)			
	Season-1	**Season-2**	**Season-3**	**Season-4**
Gazipur	744.81	593.8	804.468	703.46
Okhala	794.98	680.068	763.08	741.12
Bhalswa	888.276	801.134	899.724	872.73

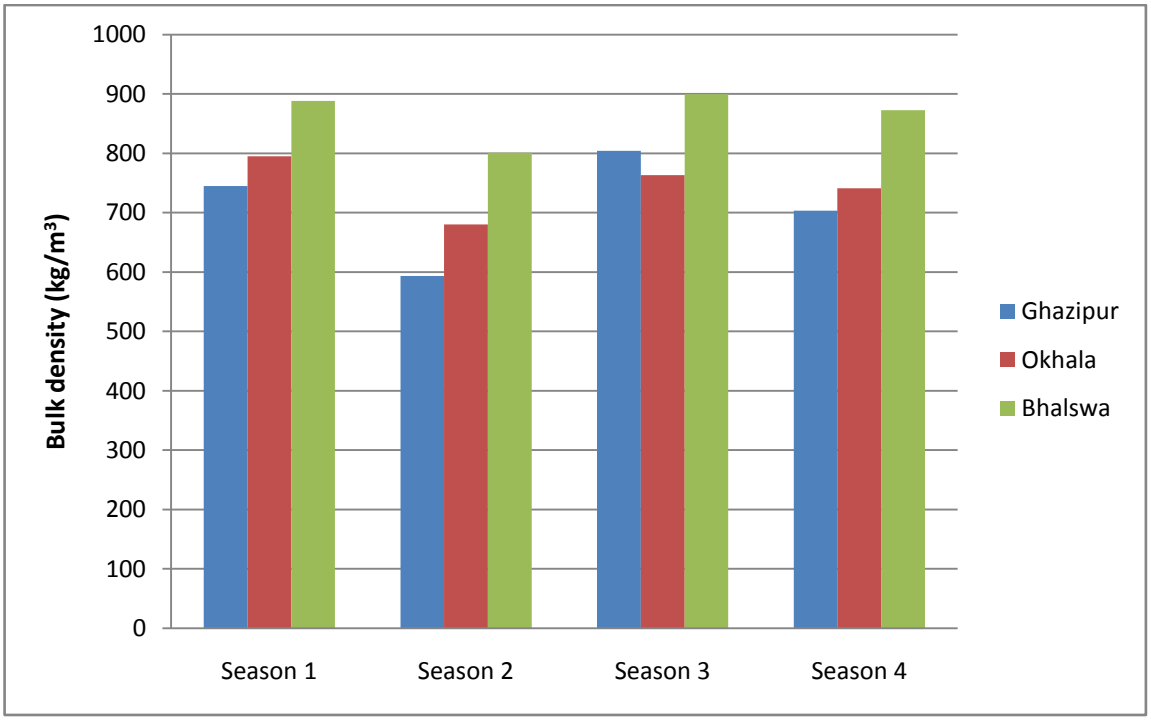

Fig. 3.10 Variation in bulk density of raw MSW at each landfill site

3.4.3 Thermal characterization of MSW/RDF

(a) Weight loss rate

Fig. 3.11 shows the loss in weight of RDF from 50°C to 900°C in reactive ambient in presence of air at slow heating rate i.e., 20°C/min (suitable conditions for conventional gasification). The initial mild weight loss of 4.8% up to the temperature of 190°C is due to release of moisture from RDF test sample. The next sharp weight loss around the temperature range of 190°C-436°C is attributed to primary thermal decomposition of RDF. It represents to 58 % weight loss, which indicates that RDF sample includes hemicellulose and cellulose constituents. This is an important phase where the volatile gases are released from the solid substrate "RDF". The next rapid weight loss around the temperature range of 436°C-523°C is attributed to secondary thermal decomposition of RDF. It covers 22.3 % weight loss. Further heating beyond 523°C, no significant weight loss can be observed. The solid residue left from RDF test sample beyond the temperature 523°C is only 13.6%. It shows the presence of solid substrate, ash and inert material presence. Fig. 3.12 shows the superimposed TG on DG thermogram (derivative weight loss in % weight loss /minutes). DG thermogram indicates the initiation of devolatilisation activity near 190°C, which maximize in the range of 225-310°C and completes at ~523°C. Major fraction of the volatile release below 325°C shows that the less formation of tar from the RDF test sample. Another TG and DG thermogram for RDF sample (in presence Nitrogen) also shown in Fig. 3.13. The distribution of volatiles released from RDF sample in different temperature ranges is given in Table 3.12.

Table 3.12 Distribution of volatiles released during devolatilization process

Sample	<180(°C)	180-320(°C)	320-500(°C)	500-650(°C)	Volatiles (with moisture)	%PTFV (320-500°C)
RDF	13.73	41.73	30.43	14.09	40	11.74

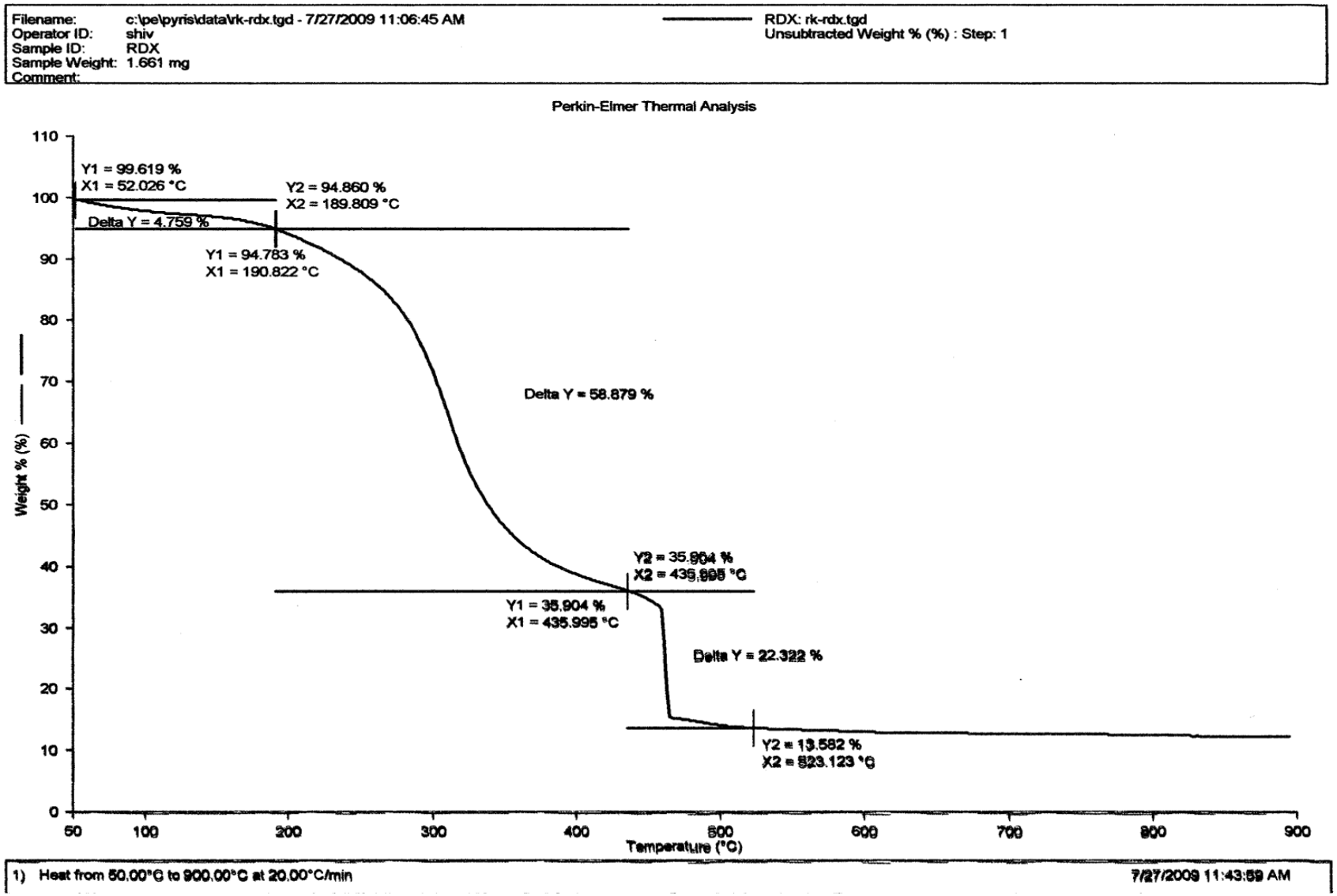

Fig. 3.11 TGA thermogram of RDF in oxidant (air) environment

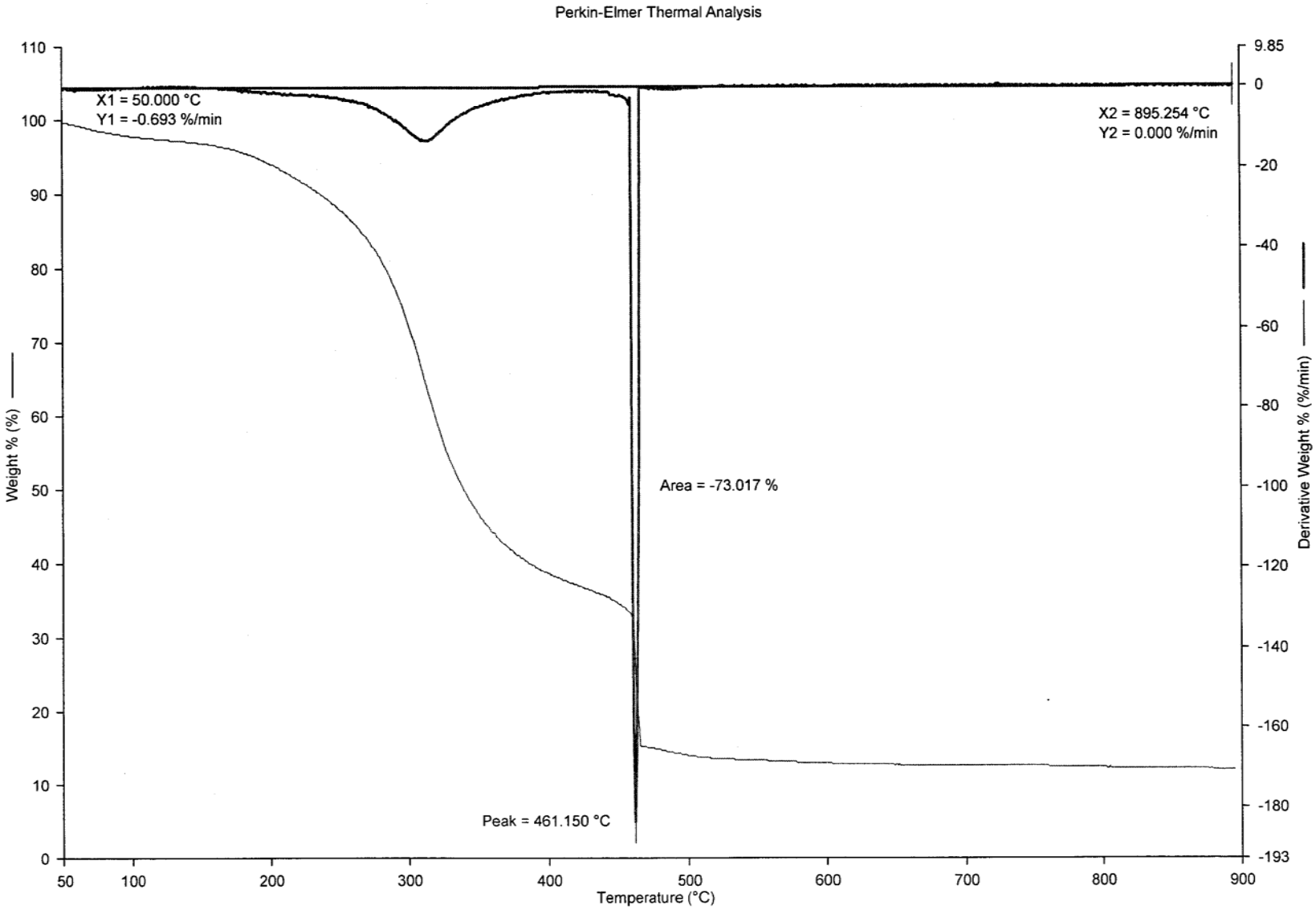

Fig. 3.12 TG and DG thermogram of RDF sample in the reactive (air) environment

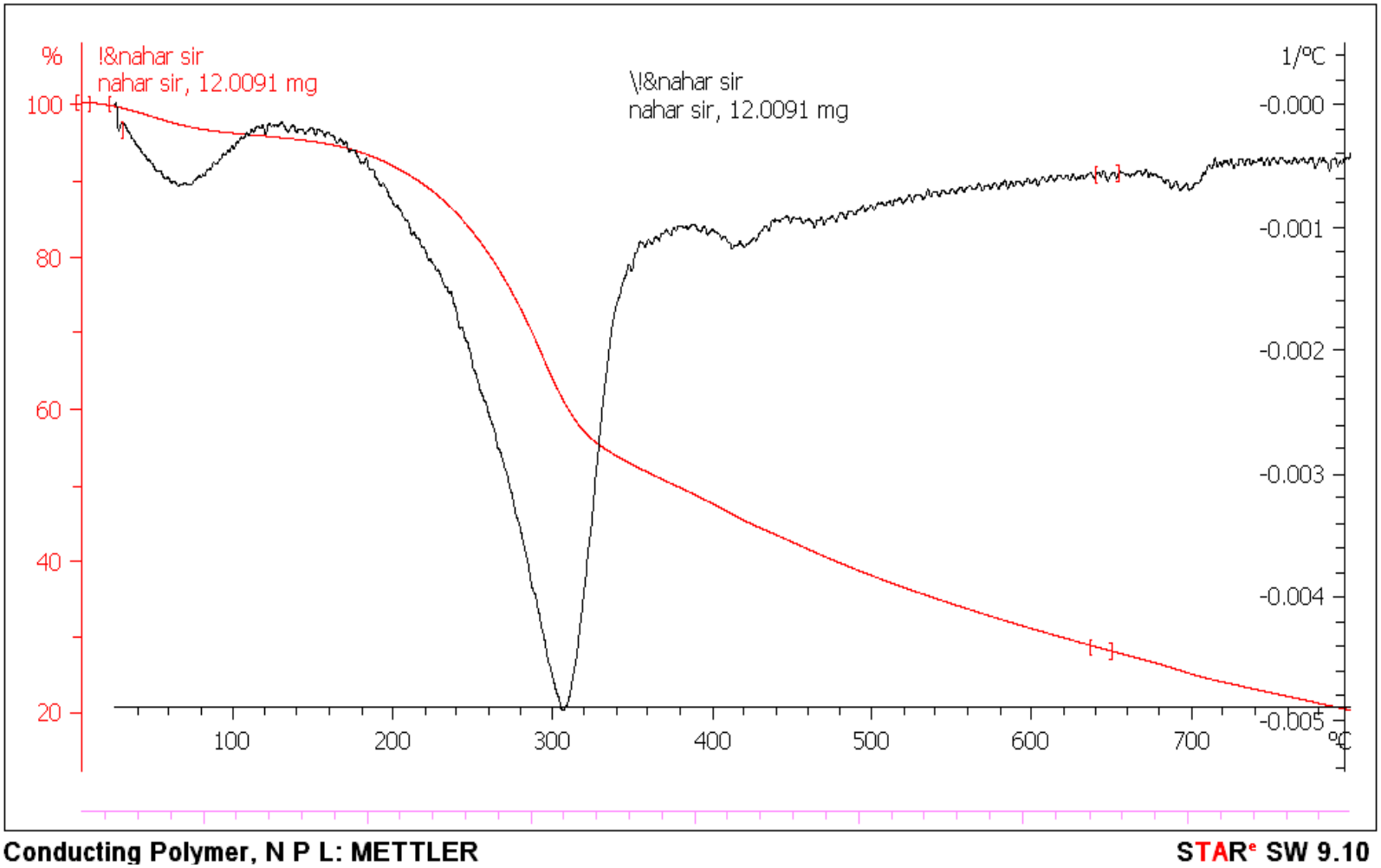

Fig. 3.13 TG and DG thermogram of RDF sample in the inert environment

(b) Chemical analysis

The pH value

The pH was measured on pH meter (HACH (USA) HQ 40 d 18) and its value is 7.5 as per IS: 3025(P 11) -1983.

Potassium and phosphorous content

The potassium and phosphorus contents of MSW are 3830 mg/kg and 431 mg/kg. as per IS 228:PART3:1987(Reaf.2002).

Proximate and ultimate analysis of MSW/RDF

Proximate analysis of RDF and MSW was carried out to obtain fixed carbon, volatile maters and residual ash. The results of proximate analysis of MSW and RDF in addition to heating value are listed in Table 3.13. Results show that MSW have high moisture and ash content than RDF, while safe limit of moisture content in wood for downdraft gasifier vary from 10-20% on dry basis, the ash content should not go beyond 5%. The fixed carbon is a very important issue for successful gasifier operation. In conventional gasifier systems fixed carbon of ~20(%) has been recommended. The carbon content is extremely low compared to wood, while the ash content is alarmingly high in MSW. Thus MSW can be upgraded into RDF for relatively better feedstock (Chang et al. 2008). For gasification systems, the fixed carbon and ash content of feedstock can be controlled using appropriate proportion of RDF and wood.

Table 3.13 Proximate analysis (wt. %) of air dried MSW and RDF

Proximate analysis	MSW	RDF
Moisture content	40.00	16.00
Ash content	25.10	20.00
Volatile matter	31.89	56.00
Fixed carbon	3.01	8.00
Calorific Value (kcal/kg.)	1175	2600

The exact idea of elemental composition of MSW and RDF sample can be obtained by using elemental C-H-N-S analyzer. The results of ultimate analysis of MSW and RDF are listed in Tables 3.14-3.15.

Table 3.14 Ultimate analysis of air dried MSW (wt. %)

Sample	C	H	N	S
1.	23.001	3.501	0.902	0.101
2.	22.991	3.478	0.896	0.091
3.	25.004	3.523	1.001	0.085
4.	26.010	3.438	1.005	0.112
5.	24.110	4.010	0.910	0.097
Average	**24.223**	**3.590**	**0.942**	**0.097**

Table 3.15 Ultimate analysis of RDF (wt. %)

Sample	C	H	N	S
1.	39.511	7.880	8.355	0.243
2.	40.503	6.500	8.350	0.368
3.	41.782	6.459	5.341	0.493
4.	31.039	5.693	8.051	0.375
5.	40.096	6.090	6.326	0.413
Average	**38.586**	**6.524**	**7.285**	**0.378**

The detailed proximate and ultimate analysis of MSW gave 40% of moisture, 25.1% ash and 31.89% volatile matter. The calorific value of the waste was 1175 kcal/kg. The amount of RDF can be obtained from the MSW collected at the sites was 751894 MT for the year 2010-11. The moisture content, ash and volatile matter as obtained for RDF is observed to be 16 %, 20 % and 56 %, respectively. The calorific value of the RDF sample was found to be 2600 kcal/kg.

(c) Ash analysis

Elemental analysis

These contained much larger amounts of Silica, oxides of Aluminium and Calcium, as shown in Table 3.16.

Table 3.16 Mineral analysis of ash from RDF sample

Description	Wt (%)
Silica	53.10
Aluminum	11.18
Iron oxide	4.87
Titanium oxide	0.89
Calcium oxide	13.15
Magnesium oxide	2.90
Sodium oxide	5.79
Potassium oxide	1.56
Sulphur trioxide	2.55
Phosphorous pentaoxide	1.43

EDS analysis

The materials and compounds detected by energy dispersive X-ray spectrometry (EDS) have been specified earlier in this chapter. The EDS images for analyzing the chemical composition of RDF are shown in Fig. 3.14. Figs. 3.15-3.16 show the SEM images of residual ash from RDF sample.

Deformation and fusion temperature of ash

Ash deformation and fusion temperatures of RDF sample are measured in the laboratory by ASTM method D-1857. The initial deformation and softening temperature of ash is observed to be 860˚C and 950˚C, respectively (hemispherical and fluid temperatures are 950˚C and 1100˚C), which are relatively lower than for ordinary wood. The data for ash characterization are listed in Table 3.17.

Table 3.17 Ash deformation and fusion temperatures

Physical condition	Temperature
Initial deformation temperature	860˚C
Softening temperature	950˚C
Hemispherical temperature	950˚C
Fluid temperature	1100˚C

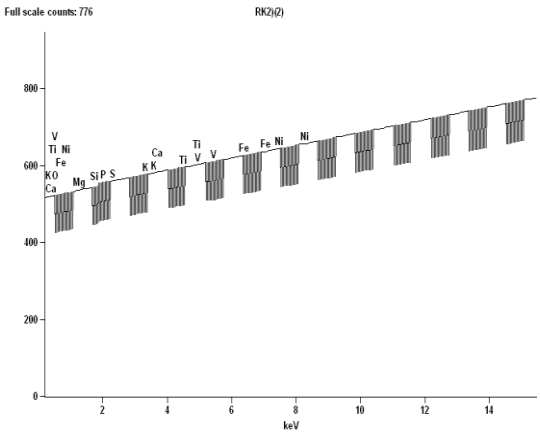

Fig. 3.14 EDS analysis of residual ash from RDF

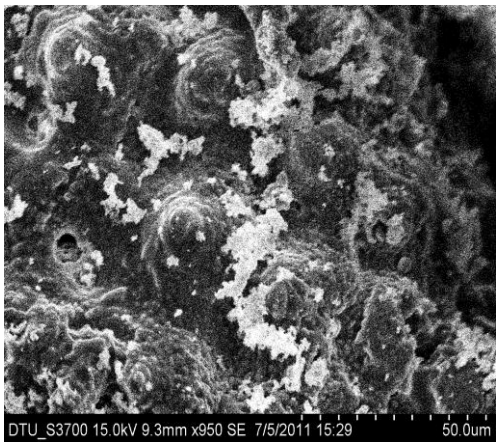

Fig. 3.15 SEM image of ash from RDF

Fig. 3.16 Enlarged SEM image of l ash from RDF

3.4.4 Experimental results

(a) Gasifier-engine system

As described earlier, the feed is prepared by mixing the RDF pellets with woody biomass in the proportion of 1:1. This feed was used in gasifier to produce syngas, which was used to run a 10 kW 3-cylinder engine operated on producer gas in single fuel mode. In order to produce electric power, the gasifier-engine system was coupled with a generator. The decentralized power production system was run for more than three hours. Experimental results along with curve fit trends of carbon monoxide, hydrocarbons, carbon dioxide and oxides of nitrogen (NO_x) at exhaust emissions are plotted in Figs. 3.17-3.20 along power output. These results are tabulated in Table 3.18. In Fig. 3.17, the curve-fit trend along with experimental data of CO emissions at engine exhaust is shown. The trends of CO emissions are increasing with power output. This is attributed t leaner mixture due to dilution at lower throttle opening. Fig. 3.18 gives the curve-fit trend along with experimental data of hydorcarbon emissions (HC) at engine exhaust. Initially these trends are increasing and then decreases after peaking near 4kW load. In Fig. 3.19, the trends CO_2 emissions are shown, which are observed to be increasing with power output.

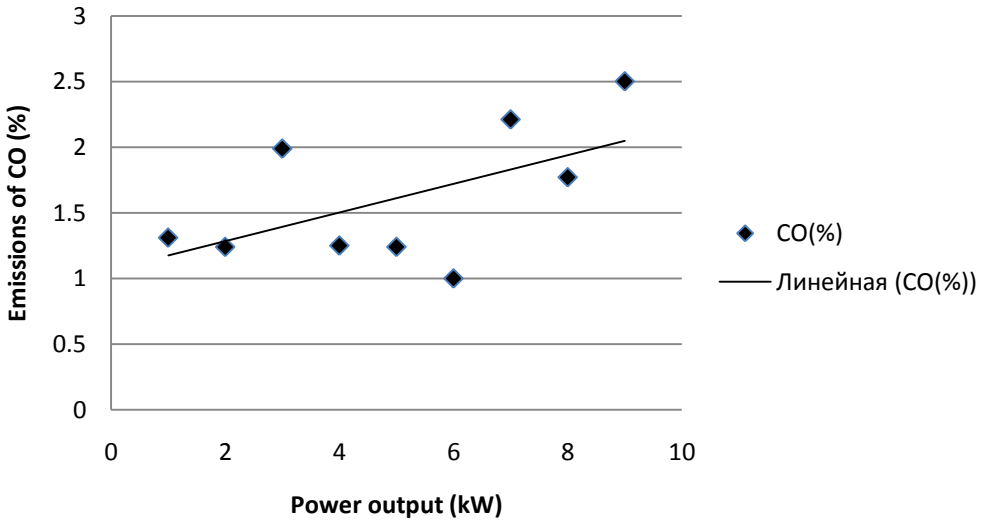

Fig. 3.17 Effect of power output on carbon monoxide (CO) emissions

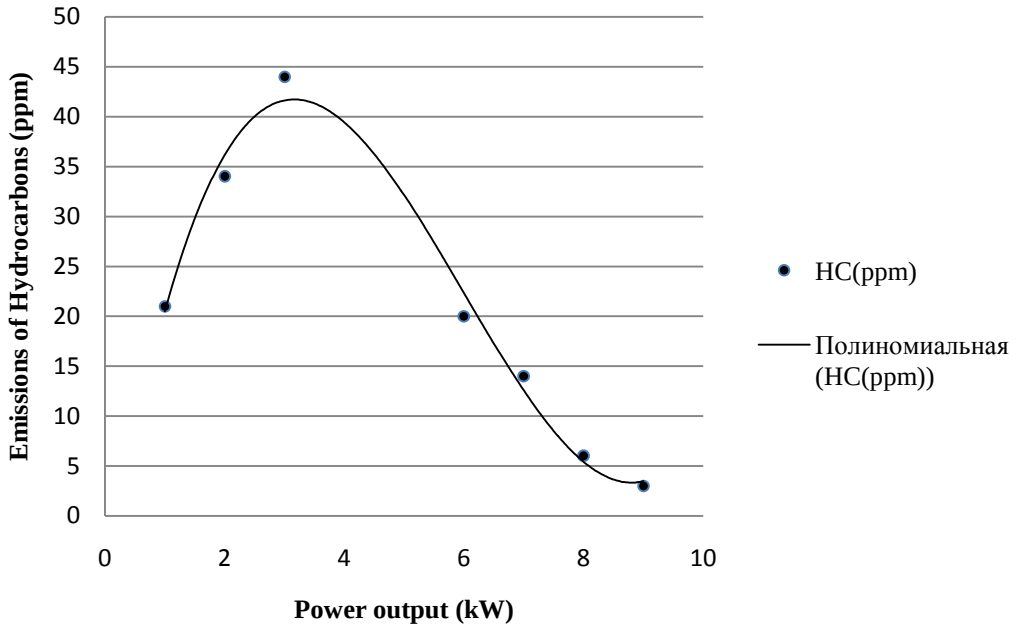

Fig. 3.18 Effect of power output on hydrocarbon (HC) emissions

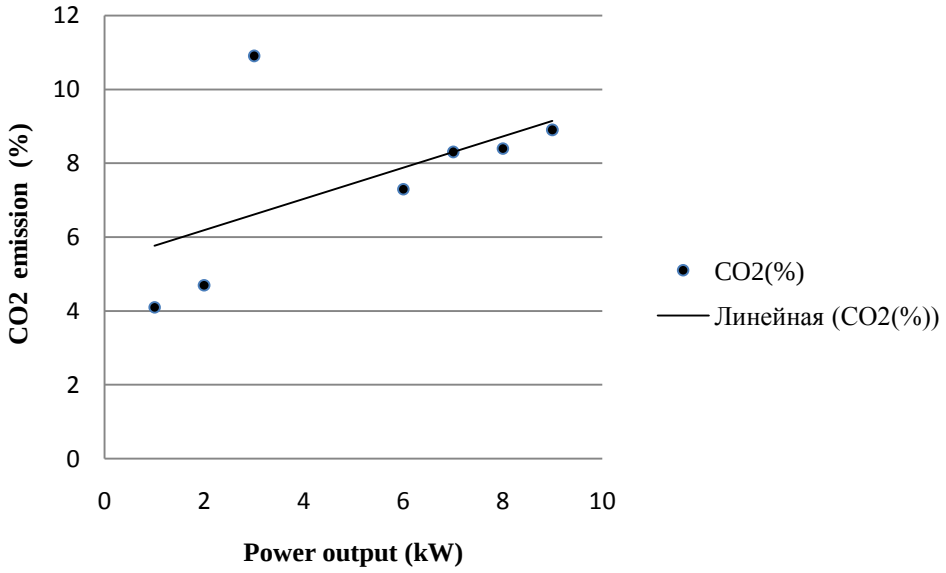

Fig. 3.19 Effect of power output on carbon dioxide (CO_2) emissions

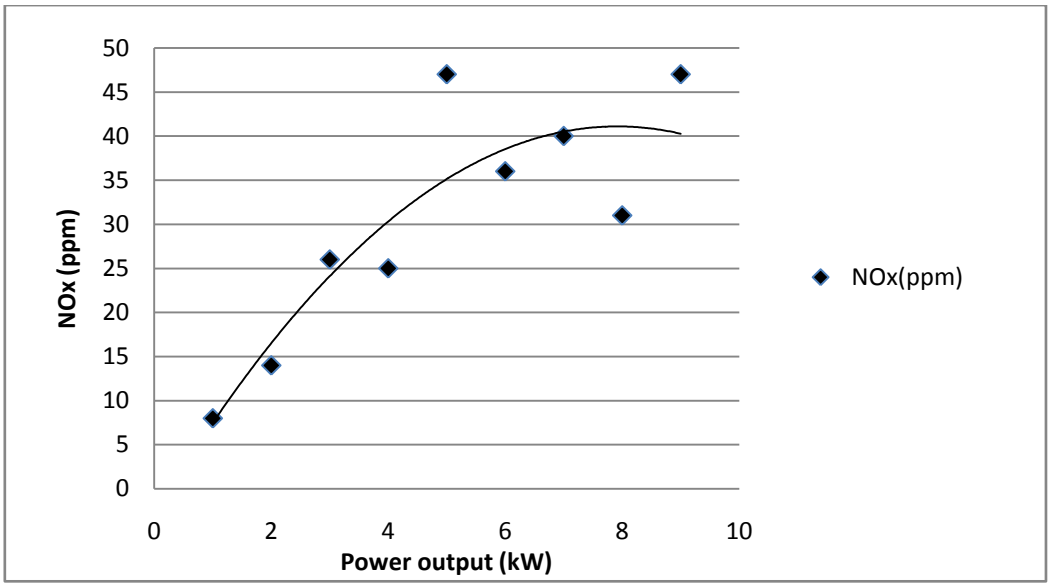

Fig. 3.20 Effect of power output on oxides of nitrogen (NOx) emissions

For each kW power output, the exhaust emissions for carbon monoxide, hydrocarbons, carbon dioxide and NO_x were observed to average 0.465 %, 5.82 ppm, 2.028 % and 6.654 ppm, respectively (refer Table 3.18).

Table 3.18 Measured engine emission with electric load, 240 V

Sr.No	Power(kW)	CO (%)	HC(ppm)	CO_2 (%)	NO_x(ppm)
1	1.0	1.31	21	4.10	8
2	2.0	1.24	34	4.7	14
3	3.0	1.99	44	10.9	26
4	4.0	1.25	15	5.80	25
5	5.0	1.24	43	11.5	47
6	6.0	1.00	20	7.3	36
7	7.0	2.21	14	8.3	40
8	8.0	1.77	6	8.4	31
9	9	2.50	3	8.9	47
Pollutants/kW		0.46	5.82	2.028	6.68

(b) Water pollutants

A biomass gasification plant requires water to be sprayed over hot gas for cooling it; water is re-circulated in a closed loop through water-pumping system. The prolonged exposure of re-circulated water results in contamination of tar, particulates and other hazardous components, which deteriorate the environment seriously. It is necessary to measure the intensity of various water polluting agents by using different equipment. Herein, the water pollution was measured in the laboratory and compared with CPCB standards. The level of components was observed to be on higher side of limits given by CPCB.

Table 3.19 gives the substance/characteristics, equipment description, and amount in affluent before treatment along with CPCB norms.

Table 3.19 Comparing polluting agents/effluents with CPCB norms

Polluting agents/ Effluent	**Equipment description**	**CPCB norms (mg/l)**	**Effluent (mg/l)**
pH value	HACH (USA) HQ 40 d 18	5.5-9.0	7.37
TDS	HACH (USA) HQ 40 d 18	2100	6540
BOD-3 days, 27°C	LOVI BOND Oxidirect	30	55
Free ammonia	Kjeldahl's Digestion unit & SMART 2 Colorimeter La Motte (USA)	5	230
Cyanides as CN	Do	0.2	4.0
Dissolved Phosphates as PO_4	Do	5.0	7.0
Phenols as C_6H_5OH	Do	1.0	3.52

Among the polluting agents (as given in Table 3.19), the pH value of re-circulated water was found to be within the limit. Other agents' viz. TDS, BOD, Cyanides, dissolved phosphates and phenols, are observed to be on higher side, while "free

ammonia" is observed to be highly concentrated among the all pollutants as compared to CPCB norms.

3.5 Conclusions

This chapter presents the characterization of the MSW/RDF feedstock obtained from a typical landfill site in Delhi, and residual ash including SEM images, ash deformation and fusion temperature. The results of characterization and experimental results on a downdraft biomass gasifier coupled with gas-engine operational in single fuel mode with emphasis on exhaust emissions from gas-engine and pollutants in re-circulated water for cooling of hot gas have been highlighted to evaluate the impact of such decentralized power production system on atmosphere.

Some of the salient conclusions from the above chapter are given below

1. Since the MSW compositions vary widely from one location to another and from one season another, thus experiments and tests to characterize MSW/RDF and residual ash need to be performed very carefully. Sampling is identified as the simplest tool for physical characterization of RDF/MSW and is used in this work. The moisture content of MSW is found to vary from 36% to 58.6% and bulk density of MSW is found to vary from 593.80 kg/m^3 to 899.72 kg/m^3.The TG and DG thermograms of RDF sample in reactive (air) environment for mass loss and mass loss rate for conditions prevailing in gasifier have been identified. Proximate and Ultimate analysis of MSW/RDF reveal that RDF can be seen as feedstock for conventional gasifier systems. The pH value, potassium and sulphur content were also obtained. The results of ash composition, the images from EDS analysis of residual ash were presented and discussed. Moreover, the results of tests for ash deformation and fusion temperature of residual ash from RDF sample are analyzed. Proximate and Ultimate analysis of MSW/RDF and analysis of residual ash reveal that RDF can be seen as feedstock for conventional gasifier systems.

2. The downdraft biomass gasifier coupled with gas-engine in single fuel mode was operated successfully for production of electric power using a mixture of RDF briquetes and woody chips in proportion of 1:1. On average basis, for each kW power output, the exhaust emissions for carbon monoxide, hydrocarbons, carbon dioxide and NO_x were observed to be 0.465 %, 5.82 ppm, 2.028 % and 6.654 ppm, respectively. Among the polluting agents, the pH value of re-circulated water was found to be within the CPCB prescribed limit. Other agents' viz. TDS, BOD, Cyanides, dissolved phosphates and phenols, are observed to on the higher side, while "free ammonia" is observed to deviate the most among the all pollutants, as compared to CPCB norms.

The tests and measurements for characterization of MSW/RDF and residual ash reveal that utilization of MSW in pure form is very difficult (if not possible) in conventional fixed bed gasification systems as it poses operational difficulty. Thus, the raw MSW can be upgraded to RDF by sorting for inert and recyclables. The results also reveal that a mixture of RDF in briquettes form and wood chips in suitable proportion can be utilized for thermochemical processing in fixed bed gasification systems.

Chapter 4

MODELING SYNGAS COMPOSITION FROM MSW AND EMISSIONS FROM LANDFILLS

4.1 Introduction

This chapter deals with theoretical study for utilization of MSW in conventional gasification system (i.e., downdraft gasifier). Herein, modeling was carried out to predict gas composition from conventional downdraft biomass gasifier. The emissions from typical landfill site have been modeled. An equilibrium model was developed and commercial CFD software transformed to predict the final syngas composition from conventional gasification system utilizing the mixture of RDF (obtained from major landfill site in Delhi) and wood chips. Predictions of syngas composition using equilibrium modeling and CFD software have been compared with experimental data for validation.

The landfill emissions from the three major landfill sites in Delhi have been modeled by using LandGEM software. Saving of equivalent CO_2 emissions have been modeled for conversion of MSW to electric power via thermochemical conversion route.

4.2 Modeling: Syngas composition

In order to assess the thermal potential of MSW in conventional gasifier systems, it may be important to have good understanding of the complex thermo-chemistry of a downdraft gasifier through modeling and simulation tools and estimation of CH_4 emissions from the landfills in order to identify the impact on atmosphere. Usually the fixed bed gasification systems are designed for pre-processed feedstock (i.e., sun dried particles of desired size). If the objective is to utilize the MSW (i.e., less heating value and high ash content as compared to conventional biomass feedstock), the reaction temperatures get suppressed. It posses not only operational difficulties during gasification of MSW feedstock but also increases the formation of toxic components (e.g., dioxins and furans). Therefore, MSW needs to be converted into RDF by sorting for non-combustible components. On the other hand, the utilization of pure RDF in gasification system leads to high ash content with low ash melting temperature and other operational difficulties. Therefore, for utilization of RDF in conventional gasifier same amount of biomass needs to be added to the RDF feedstock in order to resolve these issues.

In the downdraft gasifier, the thermochemical conversion of feedstock takes place progressively under controlled supply of oxidant. Here, the chemical energy of biomass feedstock is utilized to sustain the partial combustion and heat dissipation to the surroundings and aids to formation of combustibles and diluents. For the present work, the whole process of drying, pyrolysis and oxidation has been described before. Furthermore, as volatiles deplete and oxidation process starts receding (due to scarcity of oxygen), the flames lose intensity leading to char reduction reactions with glowing surface. The reduction zone is a sensitive region in a downdraft gasifier, which plays a lead role in thermochemical conversion process, thus, the performance of the reactor. The reactions in the reduction have been modeled in the reduction zone.

4.2.1 Pyro-oxidation zone

The overall process of drying, pyrolysis and oxidation of these pyrolysis products can be described in the pyro-oxidation zone by a single equation as

$$\left[\left(C_6H_{HB}O_{OB}+\dot{w}_B H_2O\right)+\xi\left(C_6H_{HR}O_{OR}+\dot{w}_R H_2O\right)\right]+\dot{y}O_2+3.76\,\dot{y}N_2=$$
$$\dot{n}_{CO}CO+\dot{n}_{CO_2}CO_2+\dot{n}_{H_2}H_2+\dot{n}_{H_2O}H_2O+\dot{n}_{CH_4}CH_4+\dot{n}_C C(char)+\dot{n}_{N_2}N_2 \qquad (4.1)$$

Here, $C_6H_{HB}O_{OB}$ and $C_6H_{HR}O_{OR}$ are the chemical formulas of dry biomass and RDF respectively. $\dot{w}_B$, $\dot{w}_R$, $\dot{y}$, and $\dot{n}_k$ denote the molar flow rates of water vapour in biomass and RDF respectively, and oxygen in the atmospheric air and molar flow rates of the products, respectively. ξ is molar ratio of biomass and RDF feedstock. The subscripts HB, OB, HR and OR can be obtained from ultimate analysis of biomass and RDF respectively, while char yield can be obtained from proximate analysis

For formulation of oxidation of pyrolysis products in pyro-oxidation zone following assumptions have been made:

1. Drying process is assumed to be instantaneous.
2. Char is considered as pure carbon (Shafizadeh 1982).
3. Only volatiles evolved during pyrolysis process get ignited in the pyro-oxidation zone: since the volatiles get ignited homogeneously, thus much faster than the char oxidation.
4. Methane components in pyro-oxidation zone products neglected, since the average temperature to just beneath the air tuyers is ~1228 K. At such elevated temperatures, the presence of methane component in the product gas can be neglected.
5. Water gas shift equilibrium prevails during rich combustion is (Turns 2000).
6. A plug flow assumption is used when products behave ideally

4.2.2 Reduction Zone

For modeling reduction zone, an equilibrium and kinetic modeling was developed to predict steady state performance of downdraft gasifier in terms of syngas

composition. A 2-dimensional numerical model for a 10 kWe downdraft gasifier was also built employing a CFD softwaere Fluent 6.2 to predict temperature and flow fields in reduction zone. Above modeling approaches were used to predict the sygas composition, temperature profile using initial condition of pyro-oxidation zone (section 4.2.1).

In this analysis, a plug flow assumption is used to model reduction reactions in the reduction zone to predict the gaseous species viz., CO, CO_2, H_2, H_2O, CH_4, N_2 and un-reacted char. Although N_2 is considered to be inert, yet it dilutes the final energy density of gas. In this zone char is consumed gradually in complete absence of oxygen due to char-gas reactions and gas-gas reactions as described by following chemical reactions:

R-1: $C + CO_2 \xleftrightarrow{K_{eq,1}} 2CO$

R-2: $C + H_2O \xleftrightarrow{K_{eq,2}} CO + H_2$

R-3: $C + 2H_2 \xleftrightarrow{K_{eq,3}} CH_4$

R-4: $CH_4 + H_2O \xleftrightarrow{K_{eq,4}} CO + 3H_2$

Using equivalence ratio, biomass composition as input; the gaseous products and solid char (non-equilibrium product) can be obtained using shift equilibrium and atomic balances.

(a) Chemical Equilibrium

Here equilibrium modeling approach of Sharma (2008a, b) has been adopted to model the homogeneous and heterogeneous equilibria of reduction reaction R-1 to R-4. Using the arguments of the natural logarithm and statement of chemical equilibrium at constant temperature and atmospheric pressure (Turns 2000), a relationship between the equilibrium mole fractions (χ_{eq}) and equilibrium constant (K_{eq}) have been established as given by Eqs. (4.2)- (4.5)

R I: $$\chi_{eq,CO}^{2}\left(p/p_0\right)-\chi_{eq,CO_2}K_{eq,1}=0 \tag{4.2}$$

R II: $$\chi_{eq,CO}\chi_{eq,H_2}\left(p/p_0\right)-\chi_{eq,H_2O}K_{eq,2}=0 \tag{4.3}$$

R III: $$\chi_{eq,CH_4}-\chi_{eq,H_2}^{2}K_{eq,3}\left(p/p_0\right)=0 \tag{4.4}$$

R IV: $$\chi_{eq,H_2}^{3}\chi_{eq,CO}-\chi_{eq,H_2O}\chi_{eq,CH_4}K_{eq,4}\left(p/p_0\right)^{2}=0 \tag{4.5}$$

Here superscript 0 represents to atmospheric pressure. $K_{eq,j}$ is the equilibrium constant for reaction j. For each reaction the equilibrium constant can be obtained using Gibbs function change as

$$K_{eq,j}=\exp\left(-\Delta G_j^0(T)/\overline{R}T\right) \tag{4.6}$$

Here T, $\overline{R}$, and $\Delta G_j^0(T)$ are the reaction temperature, universal gas constant and Gibbs function change, the later can be evaluated using thermodynamic data available in Sharma (2008b).

Using Gibbs-Dalton's law, we get

$$\chi_{eq,CO}+\chi_{eq,CO_2}+\chi_{eq,H_2}+\chi_{eq,H_2O}+\chi_{eq,CH_4}+\chi_{eq,N_2}=1 \tag{4.7}$$

The chemical equilibrium equations for boudouard reaction, water-gas reaction, methanation and steam reforming reaction {Eqs. (4.2)-(4.6)}; Eq. (4.7) and the elemental balances for C, H, O and N, are solved for $\chi_{eq,k}$ using Newton's method of convergence (Turns 2000) for known values of initial temperature and inlet product specifications.

In the reduction zone, solid substrate *char* gets converted into gaseous products due to the thermo-chemical conversion process. Thus, conservation of char $\Delta \dot{m}_{char}$ in terms of the inflow and outflow rates in each control volume (CV) can be described as

$$\dot{m}_{char,I-1} - \dot{m}_{char,I} = \dot{m}_{gas,I} - \dot{m}_{gas,I-1} = \Delta \dot{m}_{char} \tag{4.8}$$

It should be noted that the intrinsic mass balance of each species in each control volume is of transient nature, yet, the local mass balance between the production of gases and consumption of char still holds a steady state condition (the net flow rate of char and gases at the inflow and outflow of the control volume is invariant with respect to time).

Energy equation accounts for the heat inflows and outflows in the CV due to fluid and fuel flows, conduction and radiation heat transfer between adjacent CV and the endothermic heat absorbed rate in a CV as shown in Fig. 4.1. Thus, the energy balance can be written as

$$\sum_{react} (\dot{n}\bar{h})_{I-1} + \dot{Q}_{diff,I-1} - \dot{Q}_{loss,I} - \dot{Q}_{reac} = \sum_{prod} (\dot{n}\bar{h})_{I} + \dot{Q}_{diff,I} \tag{4.9}$$

The subscripts *react* and *prod* denote the reactants and combustion products. Axial heat transports ($= -k_{eff} A.\nabla T$) at the boundaries of CV has been modeled using effective thermal conductivity (k_{eff}) model of Sharma (2005) supplying the inputs in terms of bed temperature, particle size and bed porosity. In the present work, bed

porosity and char emissivity are fixed at 0.4 and 0.75, respectively. $\bar{h}_I$ is sensible enthalpy change (kJ/kmol) with respect to ambient, it comprises of char and gaseous products at various stage of combustion.

$$\bar{h}_I = \int_{T_A}^{T} \bar{c}_{p_i} \, dT \tag{4.9a}$$

Heat loss through the wall, $\dot{Q}_{loss}$, is modeled using thermal resistance R as

$$\dot{Q}_{loss,I} = \frac{T_I - T_A}{R_I} \tag{4.9b}$$

Here $\dot{Q}_{loss}$ is heat loss rate from Ith CV to the surrounding, which has been obtained using resistance network. $\dot{Q}_{reac}$ denotes the endothermic heat absorption rate, which can be computed using enthalpy of formation of the reactants and products as given by Turns (2000).

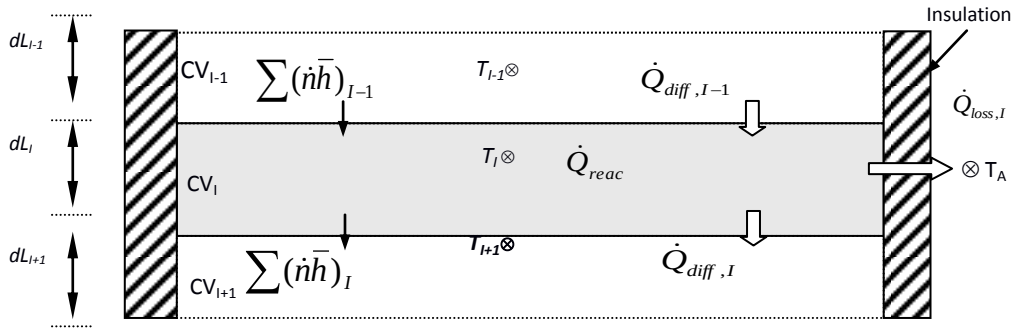

Fig. 4.1 Sketch of a representative control volume for energy interaction

(b) Kinetic modeling

For development of kinetic rate model, the reaction rates of global reactions R I-R IV determined by the departure of the reactant concentrations from their equilibrium values (Wang and Kinoshita 1993; Giltrap et al. 2003) have been employed. These reaction rates are allowed to proceed until such time that the concentrations of the reactants approach their equilibrium values, thus, the reaction rates of each reaction can be written as

R I: $$r_1 = C_{RF} A_1 e^{-E_1/\bar{R}T} \left(\chi_{CO_2} - \chi_{CO}^2 / K_{eq,1}\right) \quad (4.10a)$$

R II: $$r_2 = C_{RF} A_2 e^{-E_2/\bar{R}T} \left(\chi_{HO_2} - \chi_{CO}\chi_{H_2} / K_{eq,2}\right) \quad (4.10b)$$

R III: $$r_3 = C_{RF} A_3 e^{-E_3/\bar{R}T} \left(\chi_{H_2}^2 - \chi_{CH_4} / K_{eq,3}\right) \quad (4.10c)$$

R IV: $$r_4 = C_{RF} A_4 e^{-E_4/\bar{R}T} \left(\chi_{H_2}^2 \chi_{CO} - \chi_{H_2O}\chi_{CH_4} / K_{eq,4}\right) \quad (4.10d)$$

Here, the pre-exponential factors A_j and activation energies E_j for j^{th} reaction are taken from Wang and Kinoshita (1993). C_{RF} is the char reactivity factor, which represents the reactivity of char (or number of active sites on the char surface) and is a key parameter in simulation of fixed bed gasification. The reduction reactions are endothermic in nature, decreasing the reaction temperatures as char burn-off process proceeds leading to shrinkage in char particle as it moves downwards. As char size decreases and char porosity increases, the gas would encounter more active sites. The higher C_{RF}, the process becomes more fast. Therefore, the C_{RF} may be increased along the length of the reduction zone, although the qualitative increase in C_{RF} depends upon the type of biomass and its physical characteristics (Babu and Sheth 2006). In

the present work, therefore, the char reactivity factor has been assumed to have linear relationship with distance covered (z, in mm) by the char particle (as supplied by Babu and Sheth on special request), as

$$C_{RF} = 4.0012\,(10\,z) - 3.0012 \tag{4.11}$$

The net rate of production of the various species thus can be evaluated in terms of the above reaction rates: For example, $\mathrm{Rt_{CO}} = 2\mathrm{r_1} + \mathrm{r_2} + \mathrm{r_4}; \mathrm{Rt_{H2}} = \mathrm{r_2} - 2\mathrm{r_3} + 3\mathrm{r_4}$ etc. These relations describing the net production rate of each species can be used to compute outflow species concentration for known inflow concentration of each species and volume of each CV as:

$$\dot{n}_{k,I} = \dot{n}_{k,I-1} + V_{CV,I} Rt_{k,I} \tag{4.12}$$

where $\dot{n}_{k,I}$ stands for the molar flow rate of the species k. $\mathrm{V_{CV,I}}$ represents volume of $\mathrm{I^{th}}$ control volume and $\mathrm{Rt_k}$ stands for its net production rate of species k in the control volume. Subscripts in and out signify the flow rates at the inflow plane and outflow plane of the control volume, respectively.

Thus, outflow species concentrations can be evaluated from Eq. (4.12). Once outflow and inflow species concentrations are known, this gives the char conversion in each CV in terms of residence time and temperature.

(c) CFD modeling

Due to increased computer efficacy vis-à-vis advanced numerical techniques, the numerical simulation tools such as CFD become an effective means of quantifying the physical and chemical process in gasifiers but at the expense of simulation time. In downdraft gasification systems, the reduction zone is a sensitive region since char gets consumed gradually at glowing surface in complete absence of oxidant. The reaction rates are slow and thus it plays a key role in determining the quantity of the final gas or the performance of the reactor. In this work, therefore, CFD commercial

software namely FLUENT 6.2® in addition to thermodynamic modeling (as described in section 4.2.4) has been employed to understand the gasification mechanism. A CFD model mainly consists of three main parts. The first part is the physical models which are a set of conservation equations of mass, momentum, energy, state equation, turbulent equations, chemical reaction and source term equations. The second part is a series of solution approaches for solving these physical models and the third part is the pre-processor of discretization of computational domain and the postprocessor of visualization of numerical results.

The Fluent solves the fundamental conservation equations for microscopic regions (Pallares et al. 2007). It solves the Navier-Stokes equations using a finite volume method on a grid, which is generated directly integrated in Fluent (Kaer et al. 2006). In case of a chemically reacting flow, the system at each point can be completely described by specifying temperature, pressure, density and the velocity of the flow as well as the concentration of each species. The latter is computed from corresponding chemical species conservation equations. Boundary conditions and selecting the right sub-model have critical importance in the model of a system. Discussions on the chosen options to address major problems in achieving heat transfer, turbulence and species evaluation, discrete phase, and radiation leading to ways to set up an adequate gasifier model are emphasized. The various sub-models and solution methods are described briefly as:

Physical models

Physical models are also required for the simulation of the reduction zone of gasifier. These models take into consideration the effect of turbulence, thermal radiation and the interaction of the gas phase with the char phase.

Governing equations

The basic governing equations for obtaining the flow field characteristics of the reduction zone of the Gasifier are given as (Marklund et al. 2007). The general form of the mass conservation equation can be written as

$$\frac{\partial \rho}{\partial t} + \nabla.(\rho \vec{v}) = S_m \tag{4.13}$$

Where S_m is the mass added to the continuous phase from the dispersed second phase (e.g., due to vaporization of liquid droplets.

The momentum conservation equation can be written as (Piquet 1999):

$$\frac{\partial}{\partial t}(\rho \vec{v}) + \nabla.(\rho \vec{v}\vec{v}) = -\nabla p + \nabla.(\bar{\tau}) + \rho \vec{g} + \vec{F} \tag{4.14}$$

where p is the static pressure, $\rho \vec{g}$ and $\vec{F}$ are the gravitational body force and external body forces that arises from interaction with the dispersed phase (Ansys Fluent 2009). The $\bar{\tau}$ is the stress tensor, which can be defined as

$$\bar{\tau} = \mu \left[(\nabla \vec{v} + \nabla \vec{v}^T) - \frac{2}{3}(\nabla.\vec{v} I) \right] \tag{4.15}$$

Where, I is the unity matrix and $\vec{v}^T$ is the transpose of $\vec{v}$.

The equation of conservation of energy can be presented in the following general form

$$\frac{\partial}{\partial t}(\rho \mathrm{E}) + \nabla.(\vec{v}(\rho \mathrm{E} + p)) = \nabla.(k_{eff} \nabla T - \sum_{j=1}^{N} h_j \vec{J}_j + (\bar{\tau}.\vec{v}) + S_h \tag{4.16}$$

in Eq. (4.16), $\mathrm{E} = h - p/\rho + v^2/2$, k_{eff} is the effective thermal conductivity. The first terms of the right hand side represent heat flux due to conduction, second term denote the species diffusion, viscous dissipation due to normal shear stresses is represent the third term, while the fourth one designates to the heat source/sink due to energetic of chemical reactions (Ansys Fluent 2009).

The enthalpy h is defined as

$$h = \sum_{j=1}^{N} Y_j h_{j,} \tag{4.17}$$

Where Y_j and $h_j \left(= \int_{T_{ref}}^{T} C_{p,j} dT \right)$ are the mass fraction and enthalpy of the species j respectively.

For no premixed combustion, Lewis number $Le \left(= \frac{\lambda}{\rho c_p D_{i,m}} \right)$ is assumed unity, thus the total enthalpy $H \left(= \sum Y_j H_j \right)$ is related as

$$\frac{\partial}{\partial t}(\rho H) + \nabla.(\rho \vec{v} H) = \nabla.(\frac{\lambda_t}{c_p} \nabla H) + S_H \tag{4.18}$$

$$H_j = \int_{T_{ref}}^{T} c_{p,j} dT + h_j^0 (T_{ref})$$

(4.18a)

where $h_j^0 (T_{ref})$ is the enthalpy of formation of species j at the reference temperature.

The species mass conservation equation for each chemical species has been written in terms of species mass fraction (Y_i) as

$$\frac{\partial}{\partial t}(\rho Y_i) + \nabla.(\rho \vec{v} Y_i) + \nabla.\vec{J}_i = R_i + S_i \tag{4.19}$$

where R_i is the rate of production of i[th] species due to chemical reactions and S_i is any other source term. The diffusion flux $\vec{J}_i$ of the species i is given by

$$\vec{J}_i = -\left(\rho D_{i,m} + \frac{\mu_t}{Sc_t} \right) \nabla Y_i - D_{T,i} \frac{\nabla T}{T} \tag{4.20}$$

The diffusion flux term consists of the regular mass diffusion term according to the Fick's law and a thermal diffusion term according to the Soret effect (Warnatz 2006). Sc_t and μ_t are the turbulent Schmidt number and viscosity, respectively. In turbulent flow it is not generally required to specify detailed laminar diffusion properties as the turbulent properties overwhelm the laminar ones (Ansys Fluent 2009). Here $D_{T,i}$ is the coefficient of thermal diffusion, which is only important for light species and low temperature (Warnatz 2006).

When the system consists of N species, the Eq. (4.19) needs to be solved for N−1 species as according to the definition of Y_i the sum of mass fractions of all species is unity. Therefore for the last species the mass fraction is calculated as one minus the sum of N−1 solved mass fractions (Ansys Fluent 2009).

Full numerical solution of Navier-Stokes equation is a very difficult task for most engineering applications. In such flow problems with turbulent nature, the information of interest is limited usually to determine the mean values of quantities of interest, some measures for the extend of fluctuation and some measure to correlate these various quantities. The idea of averaging consists in neglecting the whole set of flow details and consider that the flow can be described as the superposition of the mean field and a fluctuating field defined as the difference between the instantaneous and the mean field (Piquet 1999).

Reynolds averaged equations for conservation of mass and momentums i.e. Eqs. (4.13)- (4.14) are as follows:

$$\frac{\partial \rho}{\partial t} + \nabla.(\rho \bar{\vec{v}}) = \bar{S}_{m,} \tag{4.21}$$

$$\frac{\partial}{\partial t}(\rho \bar{\vec{v}}) + \nabla.\left(\bar{\rho}\vec{v}''\vec{v}''\right) = -\nabla \bar{p} + \nabla.(\bar{\tau}) - \nabla.(\rho \overline{\vec{v}'\vec{v}'}) + \rho \vec{g} + \bar{\vec{F}}. \tag{4.22}$$

Eq. (4.22) is similar to Eq. (4.14) except for the third term on the right hand side $\nabla.\left(\rho \overline{\vec{v}'\vec{v}'}\right)$ and $\nabla.\left(\bar{\rho}\vec{v}''\vec{v}''\right)$ on the left hand side of Eq. (4.22) is due to the fluctuation in

turbulent flows. These unknown correlation terms need to be modeled in order to close the system of equations.

Turbulence model

Hinze (1975) defined a turbulent fluid motion as an irregular condition of flow with random spatio temporal variation of various quantities so that statistically distinct average values can be discerned. Turbulence causes an enhancement in mixing and accounts for the flow regime in most of the combustion applications. The two equations models for turbulence (viz., k-ε, k-ω) are very common. In this work, the k-ε model defines the turbulent viscosity as a function of turbulent kinetic energy k and its dissipation rate ε is employed.

The empirical values for k and ε, Prandtl numbers (σ_k and σ_ε) as well as the constants $C_{1\varepsilon}$ and $C_{2\varepsilon}$ are listed in Table 4.1.

Table 4.1: Constants for k-ε models (Ansys Fluent 2009; Shih et al. 1995)

	$C_{1\varepsilon}$	$C_{2\varepsilon}$	C_1	C_2	σ_k	σ_ε	$C\mu$
Standard $k-\varepsilon$	1.44	1.92	-	-	1.0	1.3	0.09

Radiation heat transfer

Radiation along a certain path is enhanced by emission and by scattering from other directions and is attenuated by absorption and scattering. Thus, following Siegel and Howell (1992), radiative transfer equation can be presented as

$$\frac{dI(\vec{r},\vec{s})}{ds} = -(a+\sigma_s)I(\vec{r},\vec{s}) + a\frac{\sigma T^4}{\pi} + \frac{\sigma_s}{4\pi}\int_0^{4x} I(\vec{r},\vec{s})\phi(\vec{s},\vec{s}')d\Omega' \qquad (4.23)$$

In Eq. (4.23), a and σ_s are the absorption and scattering coefficients. The sum $a+\sigma_s$ is extinction coefficient, which is usually known as optical thickness or opacity of the medium. Furthermore, I, ϕ and Ω' are the radiation intensity, phase function and solid angle, respectively. The phase function has the physical interpretation of being the scattered intensity in a direction, divided by the intensity that would be scattered in that direction if the scattering were isotropic (Siegel and Howell 1992). For present work, isotropic scattering ($\phi = 1$) has been used.

P-l Model is simplest of the more general P-N radiation model, which is based on the expansion of the radiation intensity, I, into an orthogonal series of spherical harmonics. The method of spherical harmonics provides a means to obtain an approximate solution of arbitrary high order (i.e. accuracy), by transforming the radiative transfer equation into a set of simultaneous partial differential equations. Using only four terms in the series solution of the respective differential equation, the following relation is obtained for the radiation flux:

$$q_r = -\frac{1}{3(\alpha+\sigma_s)}\nabla G \qquad (4.24)$$

where G is the incident radiation. The problem is then much simplified since it is only necessary to find a solution for G rather than determine the direction dependent intensity (Habibi et al. 2007). Then the following expression for q_r can be directly

substituted into the energy equation to account for heat sources (or sinks) due to radiation as follows:

$$-\nabla q_r = aG - 4a\sigma T^4 \tag{4.25}$$

Radiation in Reactive Flow: There are different methods for specifying absorption-emittance of the radiating gases (Siegel and Howell 1992; Ludwig et al. 1973) for more detail about the available methods. One acceptable compromise between the very simple method of Gray Gases and complete models, taking into account the particular absorption bands, is the so called Weighted Sum of Gray Gases Model (WSGGM). In this model the gas is assumed to behave like a mixture of gray gases and a transparent medium to account for the windows between the absorption bands (Siegel and Howell 1992). In this model the total emissivity over the distance is calculated as

$$\in = \sum_{i=0}^{I} a_{\in,i}(1 - e^{-k_i ps}) \tag{4.26}$$

The weighting factor $a_{\in,i}$ depends on temperature and is defined in (Smith et al. 1982) as

$$a_{\in,i} = \sum_{j=1}^{J} b_{\in,i,j} T^{j-1} \tag{4.27}$$

where $b_{\in,i,j}$ are the emissivity gas temperature polynomial coefficients, which together with k_i , are determined by curve fitting of the experimental values of emittance of CO_2, H_2O and a mixture of these two gases defined in reference (Siegel and Howell 1992; Ludwig et al. 1973). Good results are obtained with a substantial reduction in computation time.

Discrete phase model

The dispersed phase model uses the Navier-Stokes equations to describe a continuous fluid phase, and a Lagrangian particle tracking method to describe a dispersed phase consisting of particles, droplets, or bubbles (Gronli 1996). Heat, mass, and momentum exchange is permitted between the dispersed and fluid phases. Thus gas bubbles can rise in a liquid, sand particles can settle, and water droplets can evaporate or boil, releasing steam to a background of warm gas (Maughan et al 1994). The model is widely used for coal and liquid fuel combustion and bubble columns in stirred tanks (Christensen 1995). It is best when the dispersed phase does not exceed 10% by volume of the mixture in any region (Gil et al. 1997).

In the Lagrangian approach, the particles are treated as a discrete phase made of spherical particles dispersed in the continuous phase. The particle volume loading is usually assumed negligible, so that particles have no feedback effect on the carrier gas and particle-particle interactions are neglected (Brunner et al. 2004). In the Lagrangian framework, the controlling phenomena for particle dispersion in the field are assessed using a rigorous treatment of the forces acting on the particle. In general, the detailed flow field is computed first, then a representatively large number of particles are injected into the field, and their trajectories determined by following individual particles until they are removed from the gas stream or leave the computational domain (Neilson 1998). Particle motion is extracted from the time integration of Newton's second law, in which all the relevant forces can be incorporated (i.e., drag, gravity, lift, thermophoretic force). The Lagrangian approach is computationally intensive, because it entails tracking a large number of particles until stationary statistics are achieved (Bentzen and Henriksen 2000). On the other hand, the results of Lagrangian particle tracking are physically easier to interpret. Therefore, in the following investigation, the Lagrangian methodology was used, along with the assumption that the dispersed phase was dilute enough not to affect the continuous flow field.

Particle motion theory

Newton's second law of motion is the governing equation of motion of the particles in the DPM. According to this law, the sum of the forces acting on a particle is responsible for its acceleration.

The drag force is often dominating the motion of the particle (Chrigui 2005). The drag coefficient C_D is used to model the dependency between particle and flow condition. The spherical drag law is considered in this study.

In order to take into account the effect of turbulence on the dispersion of the particles, the stochastic tracking model has been used, which employs the instantaneous gas velocity, $u = \bar{u} + u'(t)$ along the particle path during the calculations. A stochastic method (random walk model) is used to determine the instantaneous gas velocity. In the discrete random walk (DRW) model, also known as eddy lifetime model, the fluctuating velocity components are discrete piecewise constant functions of time. Their random value is kept constant over an interval of time as given by the characteristic lifetime of eddies (Ansys Fluent 2009).

Gaseous turbulent combustion models

The reaction rate of a gaseous reaction process is determined by mixing the reacting species, and by the reaction kinetics, which is usually strongly depends on the reaction temperature in a reduction zone (Kallio an Reeks 1989). Actually, the combustion process, even only for simple fuel combustion, concerns numerous intermediate reactions that are, in practice, impossible to calculate in detail (Kaer and Rosendahl 2003). Therefore, some simplifications and assumptions have to be done to deal with combustion reaction problems. In order to perform a CFD simulation of a reactive flow, chemistry models should be used together with other fluid mechanical sub-models.

Chemical reaction mechanism

A chemical reaction with N chemical species can be described by:

$$\sum_{i=1}^{N} v_i' A_i \xrightarrow{k_f} \sum_{i=1}^{N} v_i'' A_i \tag{4.28}$$

where v_i' and v_i'' are the stoichiometric coefficients for reactants and products, A_i denotes the chemical species i and k_f is the rate coefficient. The reaction rate of creation/destruction of species i can be written as

$$\frac{dc_i}{dt} = (v_i'' - v_i')(k_f \prod_{i=1}^{N} c_i^{n_i, f}) \tag{4.29}$$

$$\frac{dc_i}{dt} = -(v_i'' - v_i')\left(k_r \prod_{i=1}^{N} c_i^{n_i, r} \right) \tag{4.30}$$

Here c_i is concentration of i^{th} species and superscript n_i is the reaction order. The superscript f and r designate to forward and reverse reaction direction for respective reaction.

As chemical equilibrium established, the forward and reverse reactions becomes equal, thus the equilibrium constant K_c can be related as

$$K_c = \frac{k_f}{k_r} = \prod_{i=1}^{N} c_i^{(v_i'' - v_i')} \tag{4.31}$$

The equilibrium constant for j^{th} reaction can be computed using change in Gibbs free energy, thus

$$K_{c,j} = \exp\left(\frac{\Delta S_j^0}{R} - \frac{\Delta H_j^0}{RT} \right) \left(\frac{p_0}{RT} \right)^{\left(\sum_{i=1}^{N} v_{i,j}'' - v_{i,j}' \right)} \tag{4.32}$$

where p_0 is atmospheric pressure, R is the universal gas constant. The values of ΔS_j^0 and ΔH_j^0 being the entropy and enthalpy change of reaction at standard conditions, respectively, are calculated from thermodynamic databases (Burcat 1984; Kee et al. 1987). The reverse reaction rate coefficient k_r can then be determined from k_f and the equilibrium constant calculated from Eq. (4.32).

The reaction rate coefficient k depends strongly on temperature in a nonlinear manner (Warnatz 2006). Arrhenius gave an empirical expression for the form of this dependence (Arrhenius 1889)

$$k = A'.e^{\left(-\frac{E_a'}{RT}\right)} \tag{4.33}$$

The pre-exponential factor A' in the above equation can be a function of temperature as well (Warnatz 2006). Therefore, the following expression is used to calculate the rate coefficient:

$$k = AT^b e^{\left(-\frac{E_a}{RT}\right)} \tag{4.34}$$

in Eq. (4.34), the A and b is the pre-exponential factor and temperature exponent, respectively. The activation energy E_a corresponds to an energy barrier to be overcome during the reaction. Its maximum value corresponds to the bond energies in the molecule, but can be much smaller if new bonds are formed simultaneously as the old bonds break (Warnatz 2006). Under certain conditions for some dissociation/recombination reactions, the reaction rates depend strongly on pressure as well as temperature. The pressure dependence of these so called fall-off reactions is described by two limiting situations; high pressure and low pressure limits. For both low pressure limit (k_0) and high pressure limit (k_∞), the rate coefficients are in the form of Eq. (4.34). The rate coefficients for these two limits are then blended to produce a smooth pressure dependence rate expression (Gilbert et

al. 1983). In this method the scaled rate coefficient k is expressed as the product of the Lindemann-Hinshelwood formula (Atkins and Paula 2006) and a factor F:

$$\frac{k}{k_\infty} = \left(\frac{p_r}{1+p_r}\right) F \tag{4.35}$$

where p_r is defined as

$$p_r = \frac{k_0[M]}{k_\infty} \tag{4.36}$$

Here [M] is the concentration of the collision partner. F is Lorentzian broadening factor which is used to reduce the systematic errors associated with the Lindemann-Hinshelwood formula in the pressure fall-off range (Zhang and Law 2009) and is given by

$$\log F = \log F_{cent} \left\{ 1 + \left(\frac{\log p_r + c}{n - d(\log p_r + c)} \right)^2 \right\}^{-1} \tag{4.37}$$

in Eq. (4.37), the values of c, n and d are $-0.4 - 0.67 \log F_{cent}$, $0.75 - 1.27 \log F_{cent}$ and 0.14, respectively. F_{cent} describing the center of the fall-off range as a function of temperature

$$F_{cent} = (1-a)\exp\left(-\frac{T}{T^{***}}\right) + a\exp\left(-\frac{T}{T^{*}}\right) + \exp\left(-\frac{T^{**}}{T}\right) \tag{4.38}$$

in Eq. (4.38), T^{***}, T^{*} and T^{**} and well as the Arrhenius parameters for the low and high pressure limits are specified for each pressure dependent reaction.

Eddy dissipation concept

The EDC model (Magnussen 1981) can consider detailed chemical reaction mechanisms in turbulent reactive flow simulations. It is an extension of the Eddy Dissipation Model (Magnussen and Hjertager 1996). The basic idea behind EDC is that the reactions occur in regions where the dissipation of turbulence energy takes place. These regions occupy a small fraction of the flow. The small turbulent structures (the so called fine structures) have a characteristic dimensions in the Kolmogorov length scale order in one and two dimensions (Magnussen and Gran 1996).

The ordinary differential equation system governing the combustion process is normally stiff and its numerical solution is computationally costly and often unstable (Warnatz et al. 2006). Therefore, simulating detailed chemical reaction schemes using the EDC model needs more computational resources than equilibrium chemistry or the flamelet model. Efficient numerical procedures are hence required to decrease the computational resources required to treat the detailed chemistry using EDC. In this thesis, the EDC model is used in conjunction with ISAT procedure.

Porous media model

The porous media assumption can be justified for fixed bed gasification (Milligan 1994). The arrangement of biomass particles in the fixed bed forms void spaces. The devolatilization volatiles and gases passes through the voids. The particles move downward during thermochemical conversion process (i.e. devolatilization, oxidation and reduction process) due to shrinkage of particles. In this process to mesh all associated geometry with a complex unstructured or body fitted system was out of both computational power and CFD algorithms a level [Kaer et al. 2006]. At high flow velocities, the modification of this law corrects for inertial losses in the porous medium by the Darcy-Forchemier equation [Sharma 2007]

$$\frac{\partial p}{\partial x} = -\frac{\mu}{\alpha} v + \rho C_F v^2 \tag{4.39}$$

Fluid flow, heat transfer and mass transport are described in the sub-domain by the laws of conservation of mass, momentum and energy in the terms of macroscopic variables and are provided by the volume averaged Navier-Stocks equations in a version of Darcy's law.

Discretization

Several methods have been developed over the years to solve the Navier-Stokes equations numerically, including the finite difference, finite element, spectral element, and finite volume methods (Kaer et al. 2006). In this gasifier simulations work, the finite volume method is employed. The brief description is given here

For control volume V, the differential equation for transport of the scalar quantity ϕ can be written in integral form as

$$\int_V \frac{\partial \rho \phi}{\partial t} dV + \oint \rho \phi \vec{v}.d\vec{A} = \oint \Gamma_\phi \nabla_\phi .d\vec{A} + \iint_V S_\phi dV \tag{4.40}$$

Where Γ_ϕ is the diffusion coefficient, S_ϕ indicates the source of ϕ per unit volume. Discretization and integration of the above equation on the control volume results in the following equation:

$$\frac{\partial \rho \phi}{\partial t} V + \sum_f^{N,faces} \rho_f \vec{v}_f \phi_f .A_f = \sum_f^{N,faces} \Gamma_\phi \nabla \phi_f .\vec{A}_f + S_\phi V \tag{4.41}$$

where N, faces is the number of faces enclosing the cell and ϕ_f is the amount of ϕ convected through the face. For the steady state case considered in this study, $\frac{\partial \rho \phi}{\partial t} V = 0$ and no temporal discretization is required. Eq. 4.41 can then be written in the form

$$\sum_f J_f \phi_f = \sum_f D_f + S_\phi V \tag{4.42}$$

where J_f the mass flow is rate and D_f shows the transport due to the diffusion through the face f. The mass flow rate is defined from the solution of continuity and momentum equations.

The face value of the scalar ϕ is calculated using a first-order upwind scheme indicating that the face value ϕ_f is equal to the cell value of the scalar of the upstream cell. Hence,

$$\phi_f = \phi_{upwind} \tag{4.43}$$

One needs to determine the gradient $\nabla\phi$ of the scalar ϕ not only to calculate velocity derivatives, but also the secondary diffusion terms. Calculation of the gradients is based on the divergence theorem stating that the gradient of ϕ at the cell center is defined as

$$(\nabla\phi)_0 = \frac{1}{V}\sum_f \bar{\phi}_f \vec{A}_f \tag{4.44}$$

where the summation is over all the faces of the cell and the face value of ϕ is obtained by arithmetic averaging at the neighboring cell

$$\bar{\phi}_f = \frac{\phi_0 + \phi_1}{2} \tag{4.45}$$

The discretization procedure yields a linearized form of the Eq. (4.46) for ϕ at the cell center in the form

$$a_p\phi_p = \sum_{nb} a_{nb}\phi_{nb} + b_p \tag{4.46}$$

where the subscript *nb* indicates the neighbor cells and *a* is the linearized coefficient for ϕ. Here the summation is over all the neighbor *nb* of cell *p*.

Likewise, the equations can be written for all the cells in the domain. The system of equations is solved using a Gauss-Seidel linear equation solver in conjunction with an algebraic multi grid (AMG) method (Wesseling 2000; Hutchinson and Raithby 1986; Hackbusch 1985).

By setting ϕ = u, one can obtain the discretized equation for momentum in the same manner as discussed above. The equation has the form

$$a_p u = \sum_{nb} a_{nb} u_{nb} + \sum p_f A.\hat{i} + S \tag{4.47}$$

and the discrete continuity equation is written as

$$\sum_{f}^{N_{faces}} J_f A_f = 0 \tag{4.48}$$

Both velocity and pressure components are stored at cell centers. Computing J_f averaging the cell velocities causes checker boarding (Mathur and Murthy 1997). This can be avoided by using a scheme similar to that proposed in literature (Patankar 1980; Rhie and Chow 1983). A momentum-weighted averaging is used with weighting factors based on the a_p coefficient from Eq. (4.48). The mass flow rate can then be written as

$$J_f = \rho_f \frac{a_{p,0} v_{n,0} + a_{p,1} v_{n,1}}{a_{p,0} + a_{p,1}} + d_f \left[(p_0 + (\nabla p)_0 . \vec{r}_0) - (p_1 + (\nabla p)_1 . \vec{r}_1) \right] = \hat{J}_f + d_f (p_0 - p_1) \tag{4.49}$$

where $p_0, p_1, v_{n,0}$ and $v_{n,1}$ are the pressure and normal velocity, respectively, of the cells at both sides of each face. The term d_f is a function of $\overline{a}_p$, the average of the momentum equation coefficients for the cells on either side of the face.

Discretization scheme

Since all of the problem variables are stored at the cell centre, the face values (the derivatives, for example) need to be expressed in terms of cell centre values (Patankar 1980). To do this, consider a steady-state conservation equation in one dimension without any source terms:

$$\frac{d(\rho U\phi)}{dx} = \frac{d}{dx}\left(\Gamma \frac{\partial \phi}{\partial x}\right) \tag{4.50}$$

This Eq. can be solved exactly. On a linear domain of x can be extended from 0-L, corresponding to the locations of two adjacent cell nodes, with $\phi_0 = 0$ at x = 0 and $\phi = \phi_L$ at x = L, the solution for ϕ at any intermediate location (such as the face) has the form (Patankar 1980)

$$\phi = \phi + (\phi_L - \phi_0)\frac{\exp\left(P_e \frac{x}{L} - 1\right)}{\exp(P_e - 1)} \tag{4.51}$$

P_e is the Peclet number, Ma et al. (2007) defined it as

$$P_e = \frac{\rho UL}{\Gamma} \tag{4.52}$$

Depending on the value of the Peclet number, different limiting behaviour exists for the variation of ϕ between x = 0 and x = L (Sharma 2007). These limiting cases are discussed below, along with some more rigorous discretization, or differencing schemes that are popular today.

Discretization of the domain

To break the domain into a set of discrete sub-domains, computational cells, or control volumes, a grid is used (Willcox 1998). Also called a mesh, the grid can contain elements of many shapes and sizes. In 2-D domains, for example, the elements are usually either quadrilaterals or triangles. A series of line segments (2-D) or planar faces (3-D) connecting the boundaries of the domain are used to generate the elements. Structured grids are always quadrilateral (2-D) or hexahedral (3-D). In general, the density of cells in a computational grid needs to be fine enough to capture the flow details, but not so fine that the overall number of cells in the domain is excessively large, since problems described by large numbers of cells require more time to solve (Xiu et al. 2008). Non-uniform grids of any topology can be used to focus the grid density in regions where it is needed and allow for expansion in other regions (Luo et al. 2005). In laminar flows, the grid near boundaries should be refined to allow the solution to capture the boundary layer flow detail.

Solution methods

The result of the discretization process is a finite set of coupled algebraic equations that need to be solved simultaneously in every cell in the solution domain. Two methods are commonly used, namely the segregated and the coupled approach (Higman and Burgt 2003). A segregated solution approach is one where one variable at a time is solved throughout the entire domain (Schlichting and Gersten 2000). Thus the x-component of the velocity is solved on the entire domain, and then the y-component is solved, and so on. An iteration of the solution is complete only after each variable has been solved in this manner. A coupled solution approach, on the other hand, is one where all variables, or at least, momentum and continuity, are solved simultaneously in a single cell before the solver moves to the next cell, where the process is repeated (Kallio and Reeks 1989). The segregated solution approach is popular for incompressible flows with complex physics, typical of those found in mixing applications. For this reason, the segregated approach will be implemented to solve the algebraic equations.

Residuals

The total residual is the sum over all cells in the computational domain of the residuals in each cell and is given by (Di Blasi 2008)

$$\sum_{pcell} Rp = R \tag{4.53}$$

Since the total residual, R, defined in this manner, depends on the magnitude of the variable being solved, it is customary to either normalize or scale the total residual to gauge its changing value during the solution process (Di Blasi 2008). While normalization and scaling can be done in a number of ways, it is the change in the normalized or scaled residuals that is important in evaluating the rate and level of convergence of the solution (Kaer and Rosendahl 2003).

Convergence criteria

The convergence criteria are preset conditions usually normalized or scaled for the residuals that determine when an iterative solution is converged. One convergence criterion might be that the total normalized residual for the pressure equation drop below 1×10^{-3}(Ma et al 2007). Another might be that the total scaled residual for a species equation drop below 1×10^{-6} (Kaer and Rosendahl 2003). Alternatively, it could be that the sum of all normalized residuals drop below 1×10^{-4} (Ma et al 2007). For any set of convergence criteria, the assumption is that the solution is no longer changing when the condition is reached, and that there is an overall mass balance throughout the domain. When additional scalars are being solved (for example, heat and species); there should be overall balances in these scalars as well.

Under relaxation

The solution of a single differential equation, solved iteratively, uses information from the previous iteration. If Φ_n is the value of the variable from the previous iteration and Φ_{n+1} is the new value, then some small difference or change in the variable brings the variable from the old value to the new one (Kallio and Reeks 1989). Rather than using the full computed change in the variable, $\Delta\Phi$ it is often necessary to use a fraction of the computed change when several coupled equations are involved (Xiu et al. 2008). This process is called under relaxation, and under relaxation factors, f, typically range from 0.1 to 1.0 (depending on laminar flow or

turbulent reacting flow), the variable being solved (pressure or momentum), the solution method being used, and the state of the solution (during the first few iterations or near convergence) (Kaer et al. 2006). Under relaxation makes the convergence process stable, but slower. Guidelines exist for the optimum choices for under relaxation factors for a variety of conditions. As the solution converges, the under relaxation factors should be gradually raised to ensure convergence that is both rapid and stable at all times. For gasifier simulation, it was found that relaxation factors around 0.3 were necessary to obtain a stable solution, of which the under relaxation of the pressure equation was the most critical.

4.3 Modeling : emissions from landfills

Air pollutants emitted from landfills contribute to the emission in the atmosphere of greenhouse gases and cause serious problems to human health. In particular the disposal of waste in landfills generates methane, which has very high global warming potential. Effective mitigation of greenhouse gas emissions is an important aspect and could provide environmental benefits in terms of sustainable development and mitigation of adverse impacts on human health. Landfills account for about 10-19% of annual global methane emissions (Kumar et al. 2004; EPA-USA 2006). In India, landfilling is the primary waste disposal strategy (Sharholy et al. 2007) and it is among the nation's largest emitters of methane. The greenhouse gases emissions related to landfilling are mainly due to presence of methane and carbon dioxide in the biogas produced via anaerobic route (Jha et al. 2007). Non-methane organic compounds (NMOCs) usually make up less than 1% of landfill gas. Mindaugas (2011) has reported that methane has more than 20 times more global warming potential than carbon dioxide (Mindaugas 2011). Thus methane gas is regarded as one of the most important greenhouse gases.

In landfills, the organic materials decompose under anaerobic conditions to produce LFG. Usually, landfill gas is composed of approximately equal parts of methane and carbon dioxide. Landfill gas also includes a smaller amount of oxygen, nitrogen, water vapor, traces of volatile organic compounds (VOCs) and hazardous air pollutants (HAPs) as well. Although, both methane and carbon dioxide are among potential greenhouse gases, nevertheless, Intergovernmental Panel on Climate change (IPCC) excludes the landfill carbon dioxide emissions from the domain of greenhouse gases. Since, carbon dioxide in landfill gas is "biogenic" and thus, is a part of the natural carbon cycle (Jha et al. 2007). The volume and rate of methane emission from a landfill is a function of size, type, age, moisture content, temperature, pH value and site location of waste. Even after closer of landfill, the emissions of methane gas continue for many years with decreasing trend (as the organic components deplete continuously with time).

There is considerable interest in quantifying the methane emissions from landfills (Mackie 2009). This section focuses on the modeling of landfill emissions from the major landfill site in Delhi (i.e. Ghazipur, Okhla and Bhalswa). A suitable model for assessment of landfill gas emission has been chosen from literature (Chalvatzaki 2010). Saving of equivalent CO_2 emissions have been modeled for conversion of MSW to electric power via thermochemical conversion route. (Waste Management Siam Ltd. 2009).

4.3.1 Landfill characteristics

The amount and methane production rate for landfill over the time depends on following five key characteristics factors (IEA 2008) as summarized below:

The most significant factor driving landfill methane generation is the quantity of organic materials such as paper, food and yard wastes, availability and sustainability of methane-producing microorganisms. The methane production capacity of a landfill is directly proportional to its quantity of organic waste.

Methane generating bacteria needs nitrogen, phosphorus, sulfur, potassium, sodium, and calcium for cell growth.

The bacteria also need water for cell growth and metabolic reactions. Landfills receive water from incoming waste, surface water infiltration, groundwater infiltration, water produced by decomposition, and materials such as sludge. Another source of water is precipitation. In general, methane generation occurs at slower rate in arid climates in contrast to non-arid climates.

Warm temperatures in a landfill speed up the growth of methane producing bacteria, which in turn depends on depends on number of layers covering the landfill and its depth, and ambient conditions.

Methane is produced in a neutral environment with pH value around 7. The pH value of most landfills lies between 6.8 and 7.2. Whenever, the pH value of landfill reaches above 8.0, the methane production may be negligible.

4.3.2 Modeling

Softwares for computation of emissions from landfills exist. Most of these softwares are based either on first-order decay model or multi-phase model. Landfill gas emissions are site-specific and depend on both controllable and uncontrollable factors. It is, therefore, difficult to ensure accurate prediction of landfill gas emission rate. One of the approaches (that used to predict gas generation from a municipal solid waste landfill) includes a simplified model that is consistent with fundamental principles. Several other approaches for landfill consider the site-specific gas generation rate. The LandGEM model is based on such approach, which was developed by the US Environmental Protection Agency for estimating the landfill gas emissions. It can also be used to determine regulatory applicability to Clean Air Act (CAA) requirements. The CAA regulations also allow the use of results from models other than LandGEM. There are other landfill gas emission models, which work very well and are frequently used for industrial applications. In this work, however, the emissions (methane) are computed using LandGEM (Version 3.02) model.

(a) LandGEM model

In the present work, LandGEM model is employed, which provides an interesting automated estimation tool for quantifying air emissions from municipal solid waste (MSW) landfills. It is based on methane mass-balance (LandGEM Version 3.02 User's Guide) as written below

$$\text{Emissions} = \text{generation} - \text{recovery} - \text{oxidation} \tag{4.54}$$

where methane generation can be written in terms of landfill gas and methane content as

Methane generation = Landfill gas generation × methane content (4.55)

The software enables the user to estimate emissions over time using the following:

1. Landfill design capacity
2. Amount of waste in place or the annual acceptance rate.
3. Methane generation rate (k), and potential methane generation capacity (L_o)
4. Concentration of non-methane organic compounds (NMOCs).
5. Years the landfill has been accepting waste.
6. Whether the landfill has been used for disposal of hazardous waste.

First order decomposition rate equation

LandGEM model uses the following first-order decomposition rate equation to estimate annual emissions over a prescribed time period.

$$Q_{CH4} = \sum_{i=1}^{n} \sum_{j=0.1}^{1} kL_0 \left(\frac{M_i}{10} \right) e^{-kt_{i,j}} \quad (4.56)$$

where:

Q_{CH_4} = annual methane generation in the year of the calculation (m^3/year)

i = 1 year time increment

n = year of the calculation - initial year of waste acceptance

j = 0.1 year time increment

k = methane generation rate (year-1)

L_o = potential methane generation capacity (m^3/Mg)

M_i = mass of waste accepted in the i^{th} year (Mg)

$T_{i,j}$ = age of the j^{th} section of waste mass M_i accepted in the i^{th} year

Determining model parameters

LandGEM relies on several model parameters, which are given below to estimate landfill emissions.

1. Methane generation rate (k),

2. Potential methane generation capacity (L_o),
3. NMOC concentration, and
4. Methane content.

Methane Generation Rate

The methane generation rate is designated by k. It is used to determine the rate of methane generation for the given waste mass. The higher the value of *k*, the faster will be the methane generation rate. The methane generation rate primarily is a function of following four different factors listed below

i. Moisture content of the waste mass,
ii. Availability of the *nutrients for microorganisms* that break down the waste to methane and carbon dioxide,
iii. pH value of the waste mass, and
iv. Temperature of the waste mass

The climate of Delhi is characterized by a dry and gradually increasingly hot season between March and June, a dry and cold winter from October to February a warm, mansoon period from July to September. The average rainfall is 721 mm/year (India Meteorological Department, IMD, 1990-2004). On an average, the minimum and maximum temperature values are observed to be 9.2°C and 31.5°C, respectively, with daily maximum temperatures during the hottest months commonly exceeding 44.2°C.

In this work, the methane generation rate k can be determined using equation (EPA-USA, 2004)

$$k = 3.2 \times 10^{-5}(\text{annual average precipitation}) + 0.01$$

Thus, the methane generation rate k is equal to $3.2 \times 10^{-5} \times 721 + 0.01$ (= 0.03 yr^{-1})

Potential Methane Generation Capacity

The potential methane generation capacity is designated by L_o. It depends on the type and composition of waste placed in particular landfill. The higher the cellulose

content in the MSW; the higher will be L_o. For Delhi landfills, the value of L_o of 64.3 m^3/Tonne (Stege 2006) has been considered as representative of MSW, which is based on available waste composition, moisture & inert contents for waste in Delhi.

Table 4.2 Model input parameters

Parameter	Value	Rationale
L_0 (Ultimate CH_4 generation potential, m^3/ton)	64.3	Based on waste composition, moisture & innert contents for waste in Delhi.
K (CH_4 generation rate constant)	0.03	Based on weather & rainfall condition in Delhi.

Non-methane organic compound concentration

Non-methane organic compound concentration (NMOC) in landfill gas depends on waste type in the landfill and extent of reactions that produce various compounds through the anaerobic decomposition. In LandGEM software, non-methane organic compound concentration is specified in parts per million by volume (ppmv).

The NMOC concentration for the CAA default is 4,000 ppmv as hexane. The NMOC concentration for the inventory default is 600 ppmv where co-disposal of hazardous waste has either not occurred or is unknown and 2,400 ppmv where co-disposal of hazardous waste has occurred.

Methane content

For LandGEM software, landfill gas is considered to have 50 % of methane and 50 % of carbon dioxide, in addition to trace constituents of NMOCs and other air pollutants. When employing LandGEM software for complying with the Clean Air Act (CAA) regulations, the methane content must remain fixed at 50 % by volume (i.e., default value to the model). If the methane content is beyond the range of 40 to 60 %, the application of LandGEM software cannot be recommended, since the first-order

decomposition rate equation used in LandGEM software to determine emissions may not be valid beyond the methane range of 40-60%.

The production of methane as determined using the first-order decomposition rate equation is not affected by the concentration of methane; however, the concentration of methane affects the production of carbon dioxide.

Table 4.3 LFG emission from landfill sites of Delhi (Mg/year)

Year	Case 1: LFG ($\times 10^5$)	Case 2: LFG ($\times 10^5$)
2013	1.596	1.486
2014	1.662	1.442
2015	1.728	1.399
2016	1.794	1.358
2017	1.862	1.318
2018	1.929	1.279
2019	1.997	1.241
2020	2.065	1.204
2021	2.134	1.169
2022	2.071	1.134
2023	2.010	1.101
2024	1.951	1.068
2025	1.893	1.036
2026	1.837	1.006
2027	1.783	0.9761
2028	1.730	0.9473
2029	1.679	0.9193
2030	1.629	0.8921
2031	1.581	0.8657
2032	1.534	0.8401
2033	1.489	0.8153
2034	1.445	0.7912
2035	1.402	0.7678
2036	1.361	0.7451
2037	1.321	0.7231
2038	1.282	0.7018
2039	1.244	0.6810
2040	1.207	0.6609
2041	1.171	0.6414
2042	1.137	0.6224
2043	1.103	0.6040
2044	1.071	0.5862
2045	1.039	0.5688
2046	1.008	0.5520
2047	0.9784	0.5357
2048	0.9495	0.5199
2049	0.9214	0.5045
2050	0.8942	0.4896

Table 4.4 Methane emission from landfill sites of Delhi (Mg/year)

Year	Case 1: Methane ($\times 10^4$)	Case 2: Methane ($\times 10^4$)
2013	4.263	3.968
2014	4.438	3.851
2015	4.615	3.737
2016	4.793	3.627
2017	4.972	3.519
2018	5.153	3.415
2019	5.334	3.315
2020	5.517	3.217
2021	5.701	3.122
2022	5.532	3.029
2023	5.369	2.940
2024	5.210	2.853
2025	5.056	2.769
2026	4.907	2.687
2027	4.762	2.607
2028	4.621	2.530
2029	4.485	2.455
2030	4.352	2.383
2031	4.223	2.312
2032	4.099	2.244
2033	3.977	2.178
2034	3.860	2.113
2035	3.746	2.051
2036	3.635	1.990
2037	3.528	1.932
2038	3.423	1.874
2039	3.322	1.819
2040	3.224	1.765
2041	3.129	1.713
2042	3.036	1.662
2043	2.947	1.613
2044	2.859	1.566
2045	2.775	1.519
2046	2.693	1.474
2047	2.613	1.431
2048	2.536	1.389
2049	2.461	1.348
2050	2.388	1.308

Table 4.5 NMOC emission from landfill sites of Delhi (Mg/year)

Year	Case 1: NMOC ($\times 10^3$)	Case 2: NMOC ($\times 10^3$)

2013	1.832	1.706
2014	1.908	1.655
2015	1.984	1.606
2016	2.060	1.559
2017	2.137	1.513
2018	2.215	1.468
2019	2.293	1.425
2020	2.371	1.383
2021	2.450	1.342
2022	2.378	1.302
2023	2.308	1.264
2024	2.240	1.226
2025	2.173	1.190
2026	2.109	1.155
2027	2.047	1.121
2028	1.986	1.088
2029	1.928	1.055
2030	1.871	1.024
2031	1.815	0.9940
2032	1.762	0.9646
2033	1.710	0.9361
2034	1.659	0.9084
2035	1.610	0.8816
2036	1.562	0.8555
2037	1.516	0.8302
2038	1.471	0.8057
2039	1.428	0.7819
2040	1.386	0.7588
2041	1.345	0.7363
2042	1.305	0.7146
2043	1.267	0.6935
2044	1.229	0.6730
2045	1.193	0.6531
2046	1.158	0.6338
2047	1.123	0.6150
2048	1.090	0.5969
2049	1.058	0.5792
2050	1.027	0.5621

Table 4.6 CO_2 emission from landfill sites of Delhi (Mg/year)

Year	Case 1: CO_2 ($\times 10^4$)	Case 2: CO_2 ($\times 10^4$)
2013	11.70	10.89
2014	12.18	10.57

2015	12.66	10.25
2016	13.15	9.95
2017	13.64	9.65
2018	14.12	9.37
2019	14.64	9.09
2020	15.14	8.82
2021	15.64	8.56
2022	15.18	8.31
2023	14.73	8.06
2024	14.30	7.83
2025	13.87	7.59
2026	13.46	7.37
2027	13.07	7.15
2028	12.68	6.94
2029	12.30	6.73
2030	11.94	6.53
2031	11.59	6.34
2032	11.25	6.15
2033	10.91	5.97
2034	10.59	5.79
2035	10.28	5.62
2036	9.97	5.46
2037	9.69	5.30
2038	9.39	5.14
2039	9.11	4.99
2040	8.84	4.84
2041	8.58	4.70
2042	8.33	4.56
2043	8.08	4.42
2044	7.84	4.29
2045	7.61	4.17
2046	7.38	4.05
2047	7.17	3.92
2048	6.95	3.81
2049	6.75	3.69
2050	6.55	3.59

(b) Emissions trading

The trading of greenhouse gas emissions reduction as a result of any activity has strong environmental concern, in present context. Methane from MSW disposal is one

of the major sources of anthropogenic greenhouse gas emissions. Its reduction may be measured and traded under a number of different emission reduction trading schemes worldwide (IEA 2008).

To qualify for trading of emission reductions, the emission reduction calculation is defined by methodologies relating to the particular trading mechanisms. As part of all methodologies, it must be ensured that normal business practice does not alter the emissions of greenhouse gases.

The amount of emission reductions available in each year from the landfill as a result of direct methane reduction can be estimated using Eq. 4.57.

$$T_{Avail.CO2eq} = X_{CH4} \times 21 \times Q_{Avail} \times \rho_{CH4} \tag{4.57}$$

where:

$T_{Avail.CO2eq}$ is total emission reductions available in tons of carbon dioxide equivalent (tCO_{2e}),

X_{CH4} is volumetric percentage of methane in landfill gas

Q_{Avai} is total quantity of methane gas available, and

ρ_{CH_4} is the density of methane (i.e., 0.0007168 ton/ cubic meter)

Any process which prevents the emission of methane to the atmospheric also quantifies for tradable emission reductions. If the decentralized system is used for electric power production, it should be included, and that power is either exported to the local distribution network or used to displace other electricity used, it is possible to gain additional emission reductions as a result of the displacement of fossil fuel use. To calculate the number of emission reductions available in each year from the export of electricity, the following relation can be used

$$T_{CO2eq} = EF_{grid} \times MWh_{exported} \tag{4.58}$$

where

T_{CO2eq} is total emission reduction in tons of

T_{CO2eq} is total emission reductions in tons of carbon dioxide equivalent ($tCO_{2e)}$,

EF_{grid} is grid emission factor (0.5057 tCO_2/MWh

$MWh_{exported}$ is total number of megawatt hours expected to the grid

Assuming the coal (fossil fuel) is replaced from MW feedstock during production of electric power. The emission factor of coal fired power plants is nearly 1.2 kg/kWh (CEA 2011). It is also possible to gain additional reduction as a result of the replacement of fossil fuel.

4.4 Results and Discussions

4.4.1 Results of Equilibrium modeling

(a) Validation

The above reduction zone model is used to predict the dry gas composition, calorific value of gas, un-reacted char, reaction temperature, thermal efficiency. For general validity, rubber wood (Table 4.7 for chemical composition analysis) with average particle diameter of 3.3 cm with 16 % moisture content has been used to compare the predictions of dry gas composition (using equilibrium and kinetic modeling) against experimental data. Base line values of air fuel ratio and gas flow rate has been fixed at 2.2 and 8.23489 g/s, respectively.

Table 4.7 Proximate and ultimate analysis of feedstock

Feedstock	Ref.	Proximate analysis (%)			Ultimate analysis (%)			
		Volatiles	Fixed carbon	Ash	C	H	N	S
Rubber wood	Jayah et al, 2003	80.1	19.2	0.7	50.6	6.5	-	-
MSW	Exp.	31.89	3.01	25.1	24.22	3.59	0.94	0.09
RDF	Exp.	56.00	8.00	16.0	38.58	6.52	7.28	0.38

With these base values and for typical 30 cm char bed length (as per design specifications for a reduction zone in a typical downdraft gasifier); the simulation results for dry gas composition are performed for dry gas composition based on equilibrium modeling. These results are compared with experimental data of Jayah et al. (2003) as shown in Fig. 2. For hydrogen component, the equilibrium computations over-predict when compared with the experimental values, while kinetic computations show under-prediction. For carbon-monoxide, equilibrium approach predicts better

agreement then kinetic modeling when compared with the experimental data. On the other hand, methane content in final gas has been observed to be negligibly small for both modeling approaches. Under prediction of methane concentration should be looked at as a limitation with equilibrium modeling, while for the kinetic modeling, it is expected, since the methane concentration from the pyro-oxidation sub-module (at the inlet of the reduction zone) is theoretically absent. Predictions based on both equilibrium and kinetic modeling approaches show reasonably good agreement with experiments conducted by Jayah et al. (2003) for a given char bed length of 30 cm in the reduction zone. This comparison reflects that for downdraft gasifiers, the equilibrium modeling approach can be used safely to predict gas composition for general purpose.

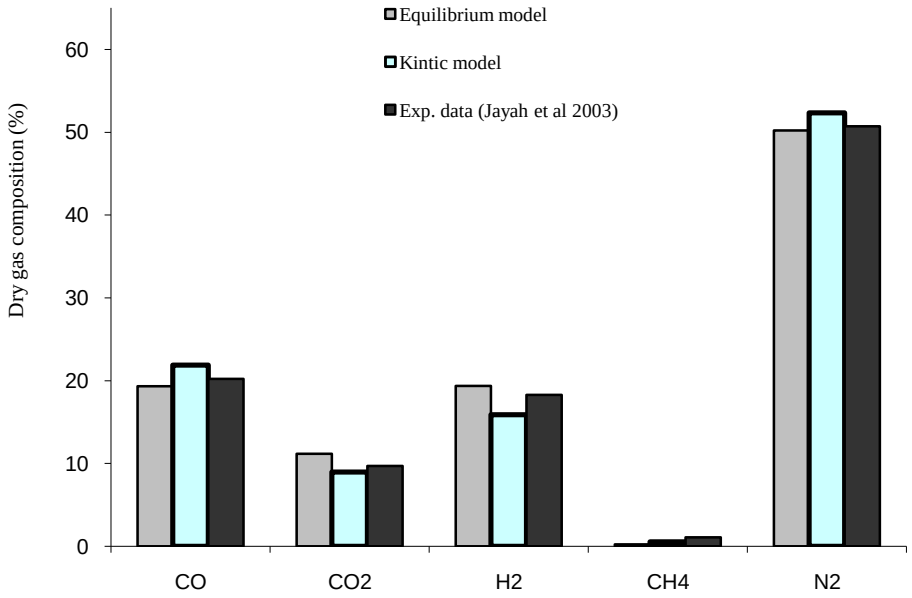

Fig. 4.2 Comparison of predicted dry gas compositions against the experimental data (Jayah et al. 2003), Char bed length = 30 cm.

(b) Parametric studies

The equilibrium model for reduction zone has been used to predict gas composition, calorific value of gas and reaction temperature, using mixture of RDF and rubber

wood in 1:1 proportion. The chemical analysis of RDF and rubber wood is given in Table 4.2. For present study, the effect of variation in moisture content on the gas composition and calorific value of syngas and reaction temperature has been highlighted in figs. 4.3-4.8.

In Fig. 4.3, the effect of variation in moisture content from 0 to 30% (as expected in feedstock) has been investigated. Result show that volumetric percentage of hydrogen component gradually improves, while CO component decreases with increasing moisture content in feedstock. In figs. 4.4 and 4.5, on other hand, both the reaction temperature and calorific value of syngas are found to be decreasing with moisture content.

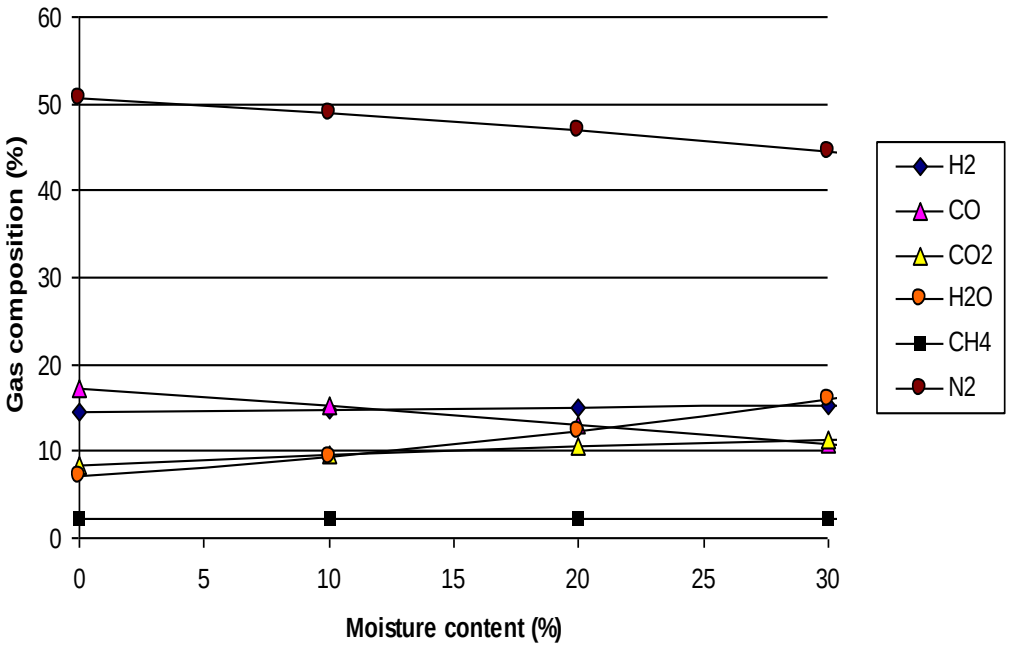

Fig. 4.3 Effect of feedstock moisture content on syngas composition

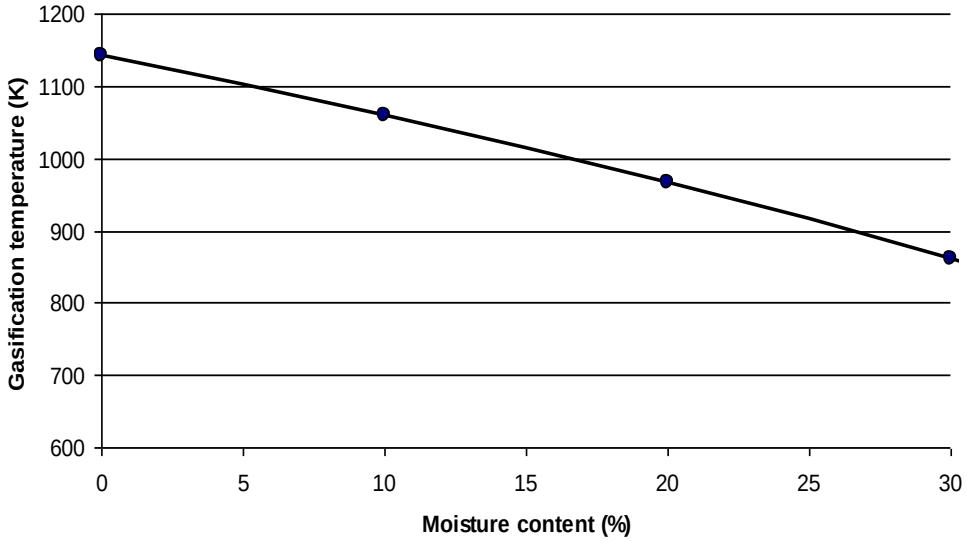

Fig. 4.4 Effect of feedstock moisture content on reaction temperature

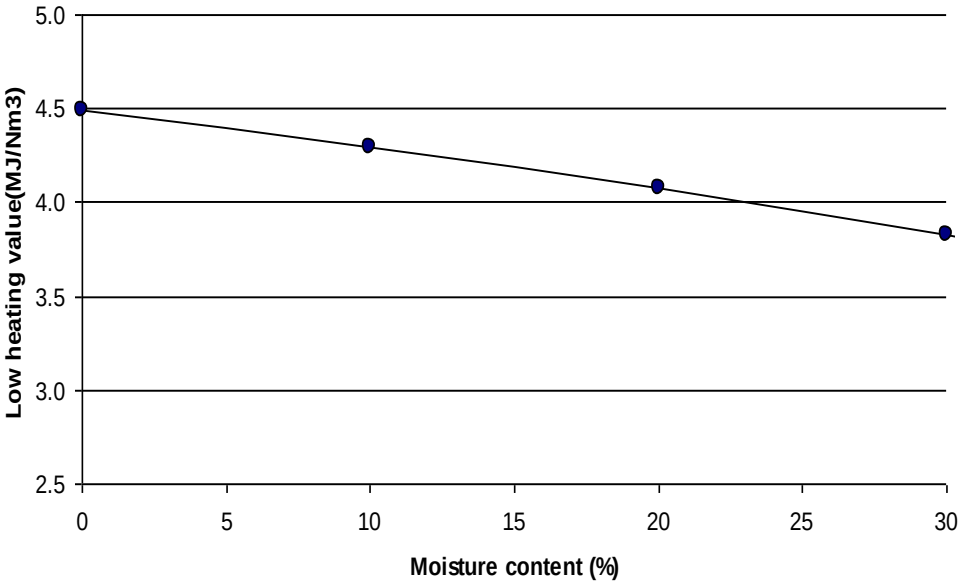

Fig. 4.5 Effect of feedstock moisture content on lower heating

The effect of equivalence ratio (which is defined as ratio of actual air supplied to the stoiciometric air requirement for a given feedstock) on syngas composition, calorific value and reaction temperature is given by figs. 4.6-4.8. It can be observed that the

reaction temperature increases with increasing equivalence ratio, while heating value of syngas decreases due to nitrogen dilution effect of nitrogen.

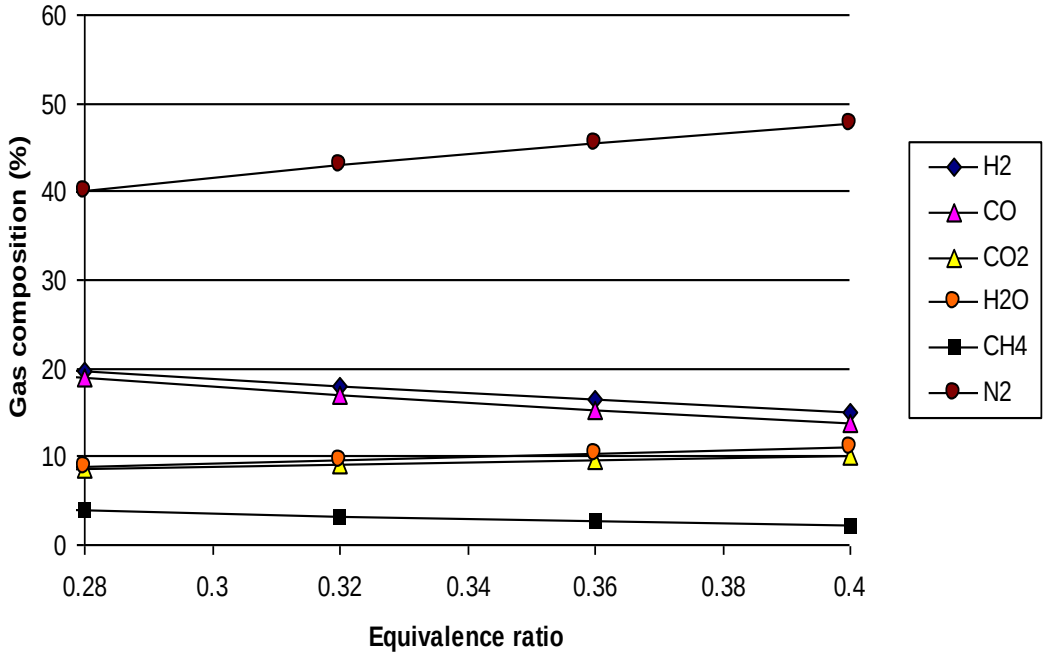

Fig. 4.6 Effect of equivalence ratio on syngas composition

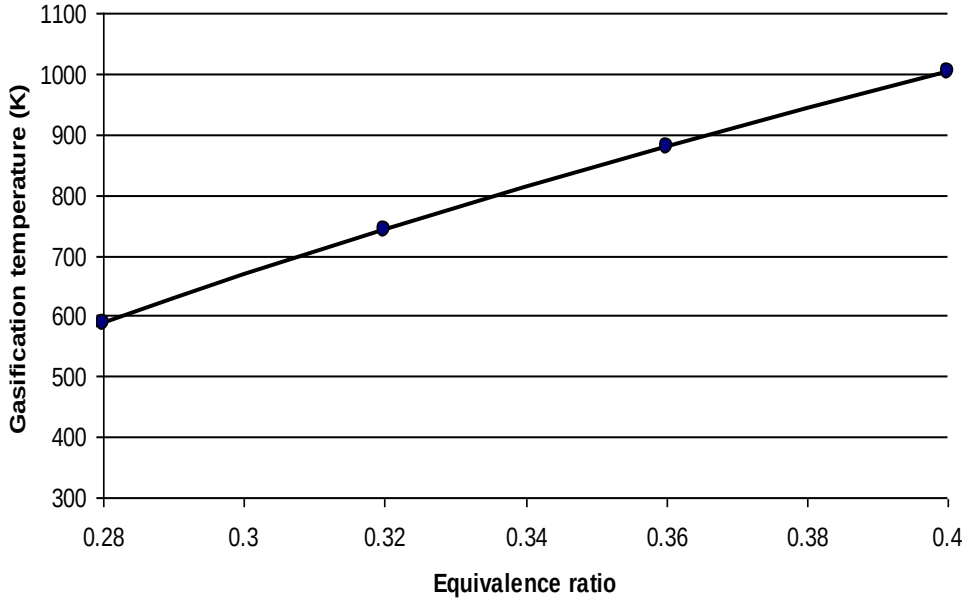

Fig. 4.7 Effect of equivalence ratio on reaction temperature

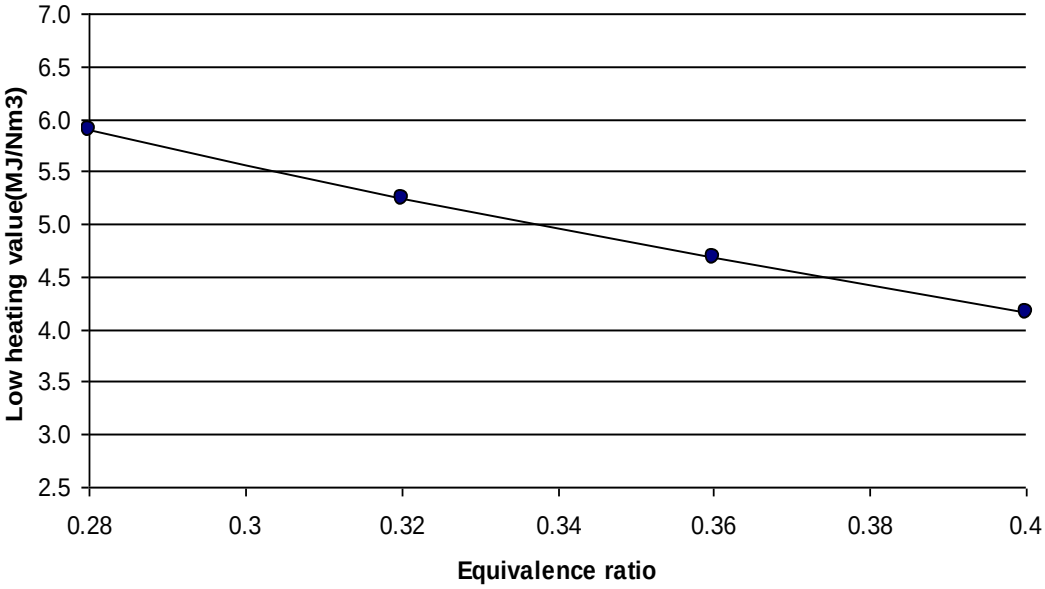

Fig. 4.8 Effect of equivalence ratio on lower heating value

These findings reveal that lower equivalence ratio and moisture content in feedstock should be used. Therefore, optimized equivalence ratio and adequate drying of waste are necessary for effective and efficient gasification of MSW (by proper waste segregation in form of RDF).

4.4.2 Results of CFD modeling

A CFD FLUENT 6.2® software was used to describe the reduction zone of downdraft biomass gasifier. The geometry of 10 kWe downdraft biomass gasifier (NETPRO) and mixture of RDF feedstock is taken as input to predict the concentration contours of syngas major species (viz. CO, H_2 and CH_4), calorific value and temperature contours across the reduction zone. The results of concentration contours of CO, H_2 and CH_4 and temperature are shown in Figs. 4.9-4.14.

The comparison of the CFD model results at the outlet with experimental data is done by calculating the area averaged concentration of species discussed above along with temperature. The area averaged fraction of H_2 is 11.33%, CO is 19.37% and CH_4 is

2.36% which has similarity to what is obtain at the outlet of downdraft gasifier in experiments. The temperature contour is same as what we obtain in actual, which suggests the proper proceedings of reactions inside the reduction zone The CFD model results are satisfactory and have good agreements with the experimental data (Table 4.7).

Table 4.8 Comparing predicted and experimental values of gas composition (% vol)

	CO	H_2	CH_4
Simulated	19.37	11.33	2.36
Exp.	20 ± 3	17 ± 4	2 ± 1

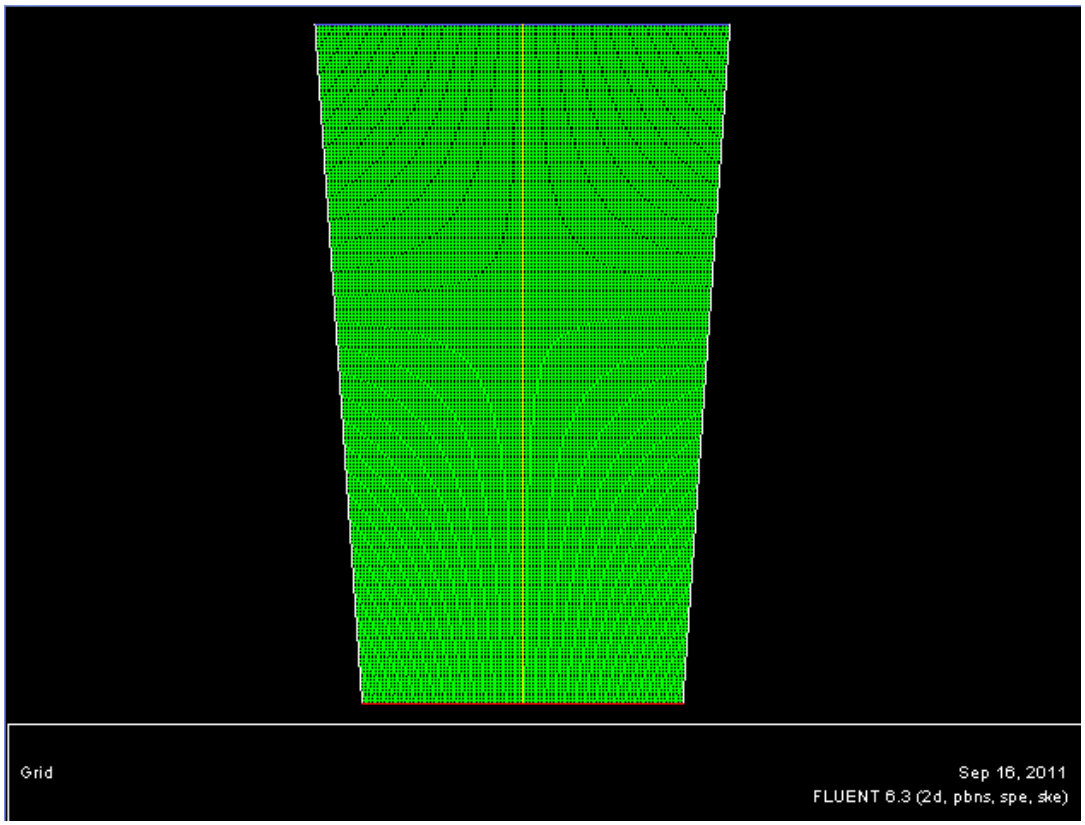

Fig. 4.9 Reduction zone grid

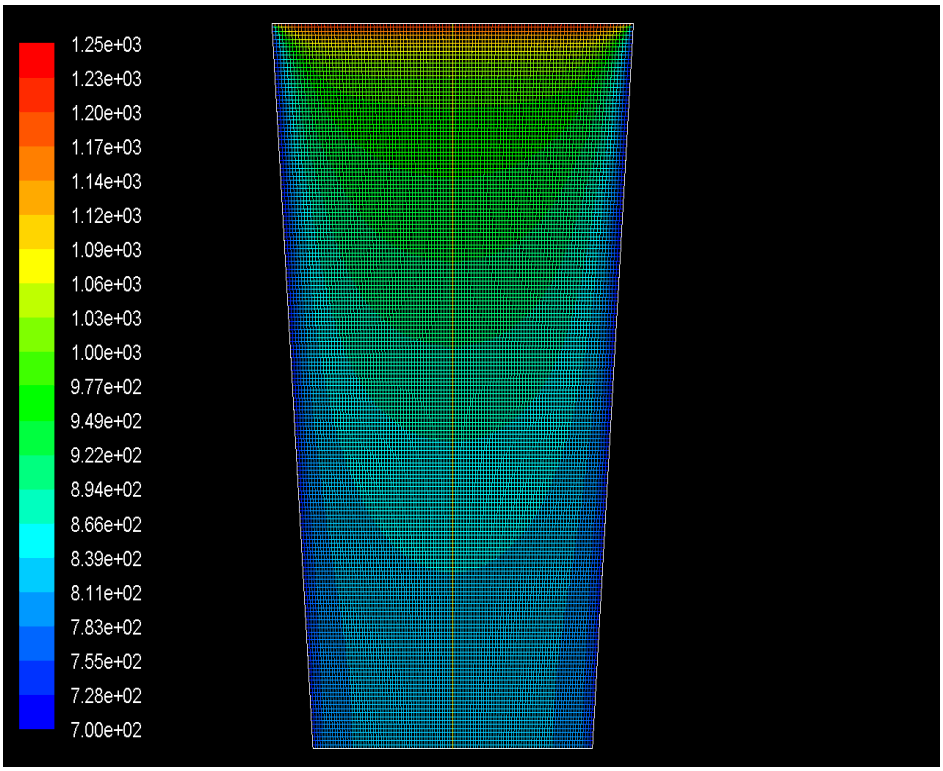

Fig. 4.10 Contours of temperature (K)

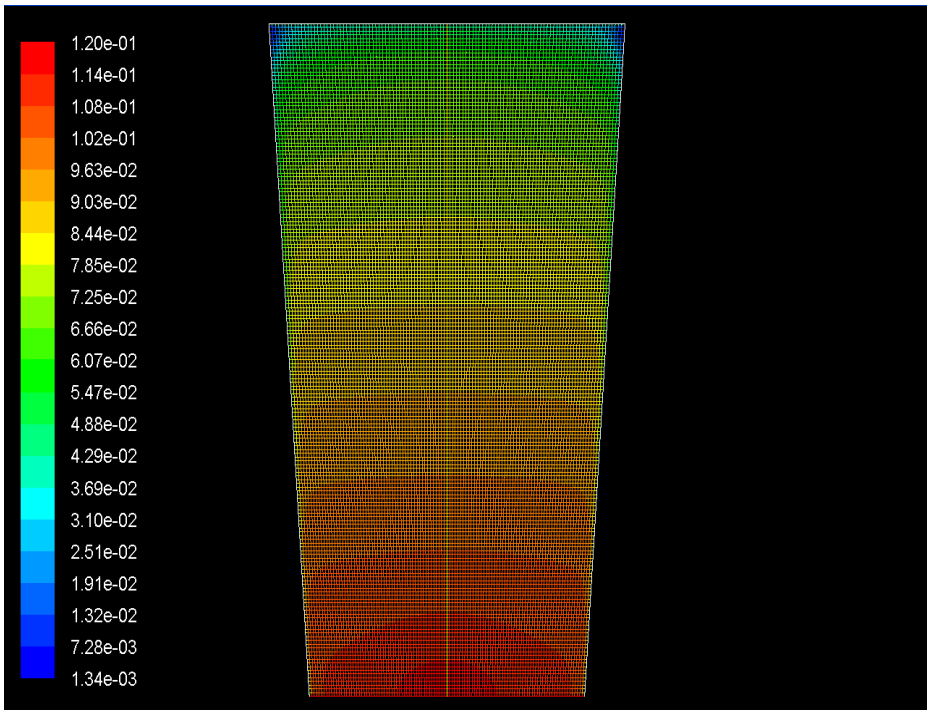

Fig. 4.11 Contours of hydrogen

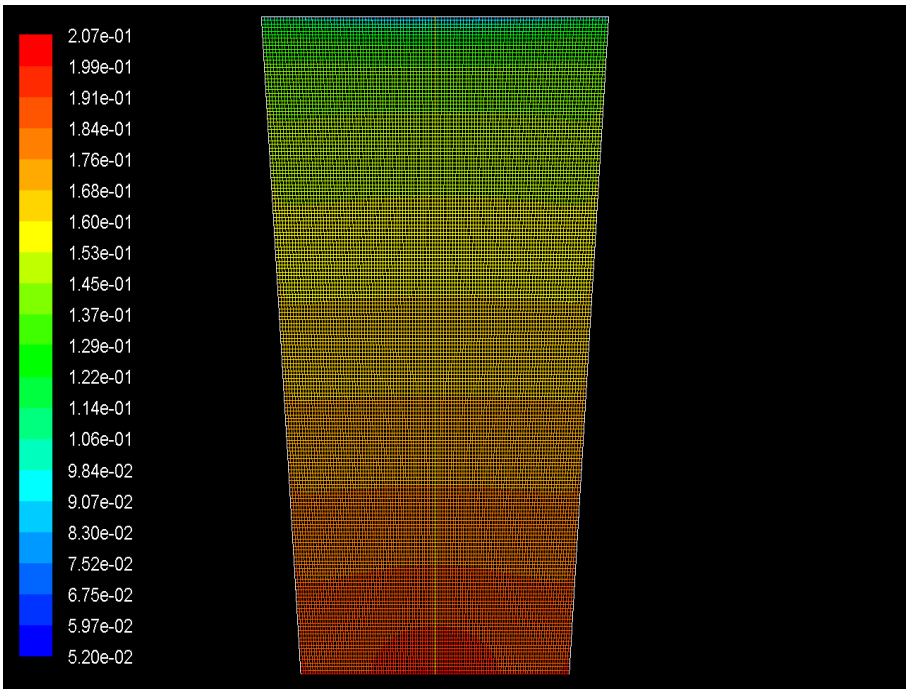

Fig. 4.12 Contours of CO

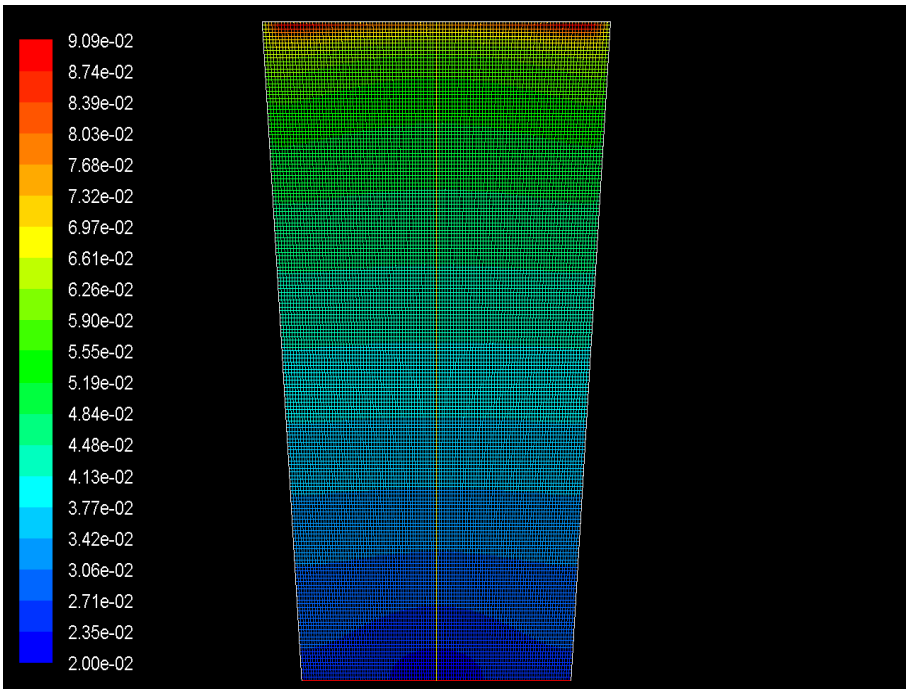

Fig. 4.13 Contours of CH_4

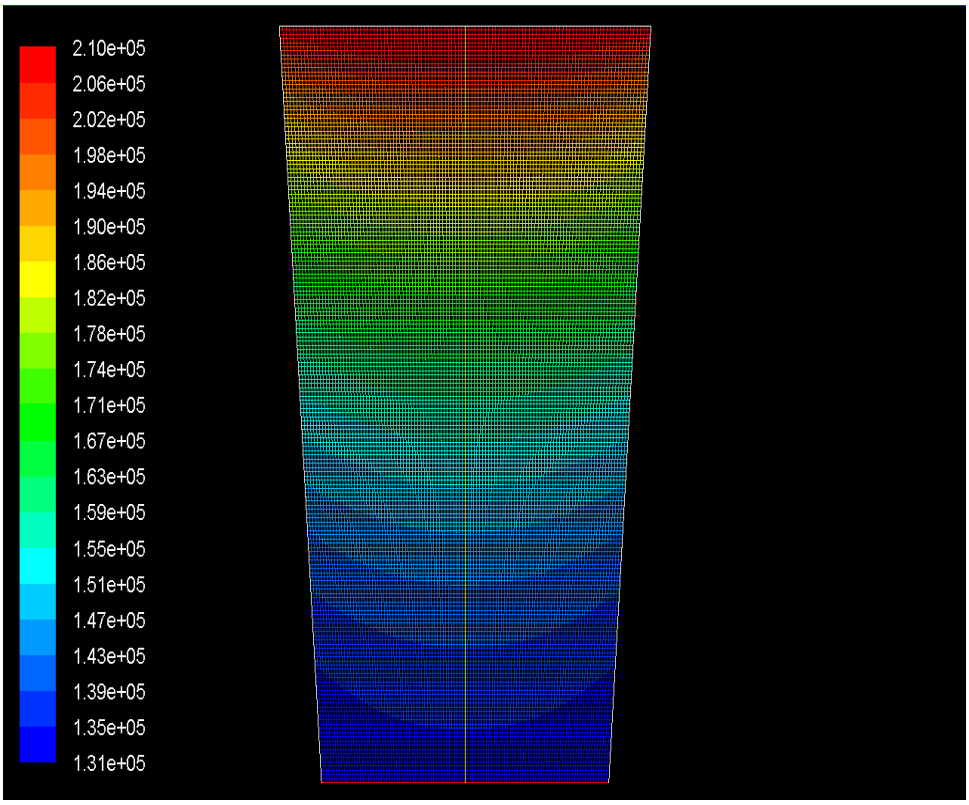

Fig. 4.14 Contours of Incident radiation (W/m^2)

4.5 Emissions modeling from landfill

For present phase of computations LandGEM software is employed. The two possible case scenarios have been considered for comparative analysis of landfill gas emission from three major landfill sites in Delhi. Case-1: when MSW is being dumped at landfill site till year 2020; Case-2: if MSW, instead of getting dumped into landfills is utilized in gasifier-engine systems from 2012 onwards to produce electric power.

For Case-1, a regression analysis of the past MSW data from year 1984 to 2011 as supplied by Table 4.8 was used. The forecast of MSW generation from 2012 to 2020 was made based on these trends as listed in Table 4.8.

A linear relation between MSW dumped at landlill with respect to time (year) has been derived by assuming other variables minorly influencing MSW generation are fixed at a specific value. The linear relationship is given by the following form

$$Y = 51506.882\,X + 839310.658 \tag{4.59}$$

Where, X and Y designated to time (in years) and MSW(Mg/year) respectively.

The forecasting error is 152696.0, while forecasting error was defined as

$$\text{Forecasting error} = \sum \frac{(Ft - At)}{N} \tag{4.59a}$$

The coefficienct of determination (R^2) is found to be 0.806. F value of the regression 104.154 and standardized β coefficient is 0.898. The relationship between MSW and year is significant as $P \leq 0.000$.

Table 4.9 MSW dumped at three landfill sites projected till 2020.

Year	Input Units(*Mg/year)*
1984	753,257
1985	805,985
1986	862,404
1987	922,772
1988	987,366
1989	1,056,482
1990	1,130,436
1991	1,209,566
1992	1,294,236
1993	1,384,832
1994	1,481,771
1995	1,585,495
1996	1,696,480
1997	1,815,233
1998	1,942,300
1999	2,078,260
2000	1,962,067
2001	1,663,456
2002	1,787,371
2003	2,015,788
2004	2,042,242
2005	2,157,024
2006	1,991,885
2007	1,615,569
2008	1,763,165
2009	1,953,409
2010	2,172,138
2011	2,281,503
Year	**Forcasted Units(*Mg/year)***
2012	2,333,010
2013	2,384,517
2014	2,436,024
2015	2,487,531
2016	2,539,038
2017	2,590,545
2018	2,642,052
2019	2,693,558
2020	2,745,065

Case1: The landfill gas emission results of the LandGEM model are given in Fig. 4.15 which shows expected total landfill gas emission along with

its constituents i.e. Methane, Carbon dioxide and NMOC. It is expected that LFG emission will peak in the year 2021 with its peak value $2.134x10^5$Mg/year. The peak rate of generation of Methane, Carbon dioxide and NMOC is $5.701x10^4$, $1.564x10^5$and $2.450x10^3$Mg/year respectively.

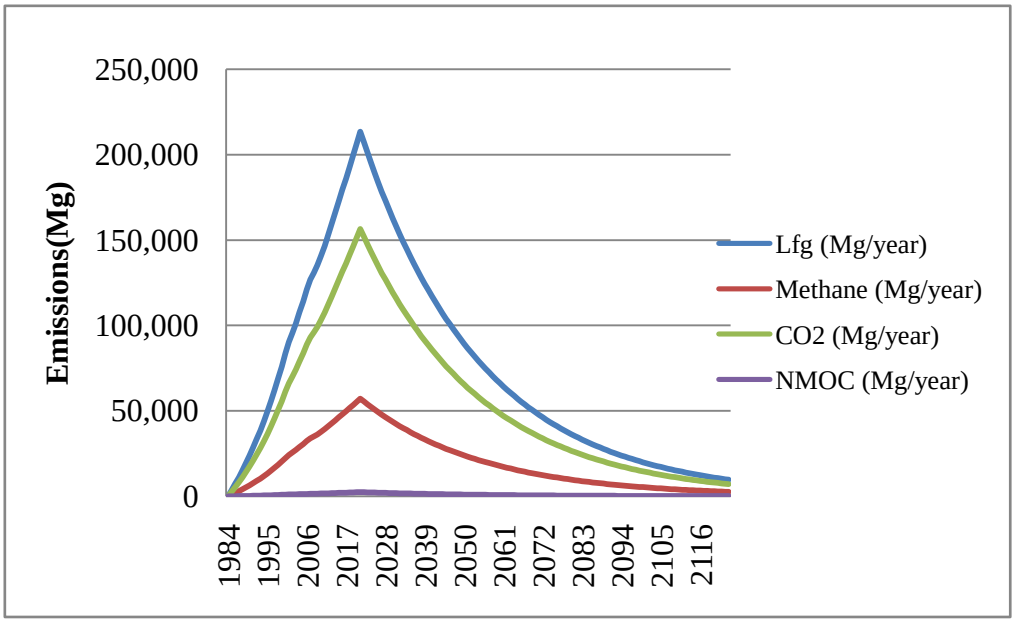

Fig. 4.15 Case-1.

Predicted emissions of CH4, CO2, NMOC and total emissions with respect to time.

Case 2: The results of the mentioned model for this case are given in the following graph (Fig. 4.16).

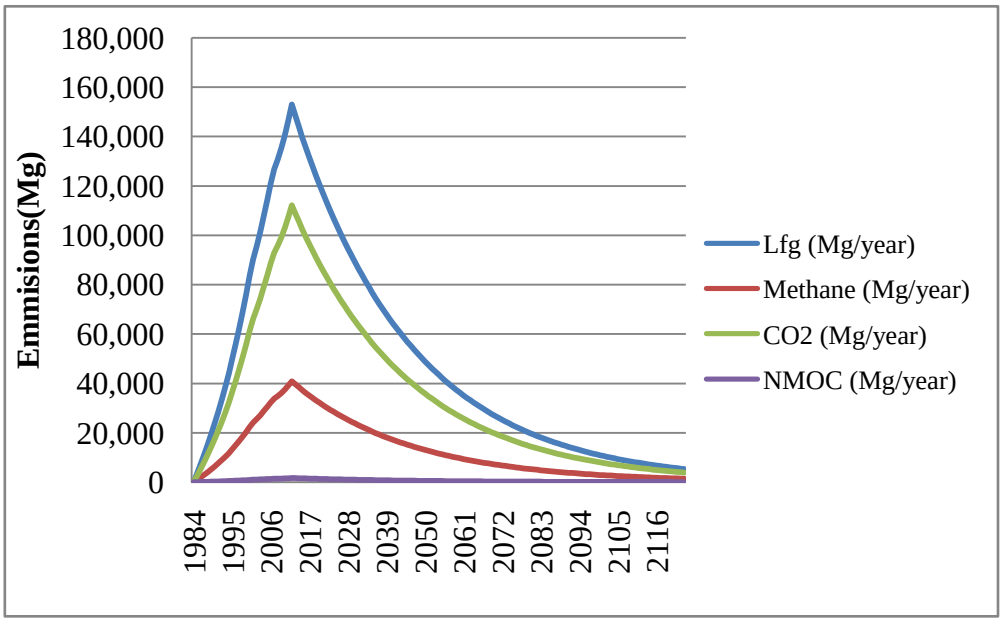

Fig. 4.16 Predicted emissions of CH4, CO2, NMOC and total emissions with respect to time, Case-2.

It is proposed that if case 2 is taken as a policy decision then in that case the methane, Carbon dioxids and NMOC generation would be reduced 368236, 1010354 and 15828Mg. respectively in next 20 years. The results of the estimated emissions for both the cases are given in the following graphs (Fig. 4.17, 4.18 and 4.19) and reduction of these pollutants is given in Table 4.9.

Table 4.10 Saving of Emissions (Mg/Year) for case 2.

Year	Methane	CO_2	NMOC

	Emission (Mg/Year)	Emission (Mg/Year)	Emission (Mg/Year)
2013	2,948	8,090	127
2014	5,875	16,119	253
2015	8,780	24,090	377
2016	11,664	32,004	501
2017	14,528	39,862	624
2018	17,373	47,667	747
2019	20,198	55,419	868
2020	23,005	63,122	989
2021	25,795	70,775	1,109
2022	25,032	68,683	1,076
2023	24,293	66,653	1,044
2024	23,575	64,683	1,013
2025	22,878	62,772	983
2026	22,202	60,916	954
2027	21,546	59,116	926
2028	20,909	57,369	899
2029	20,291	55,673	872
2030	19,691	54,028	846
2031	19,109	52,431	821
2032	18,544	50,882	797

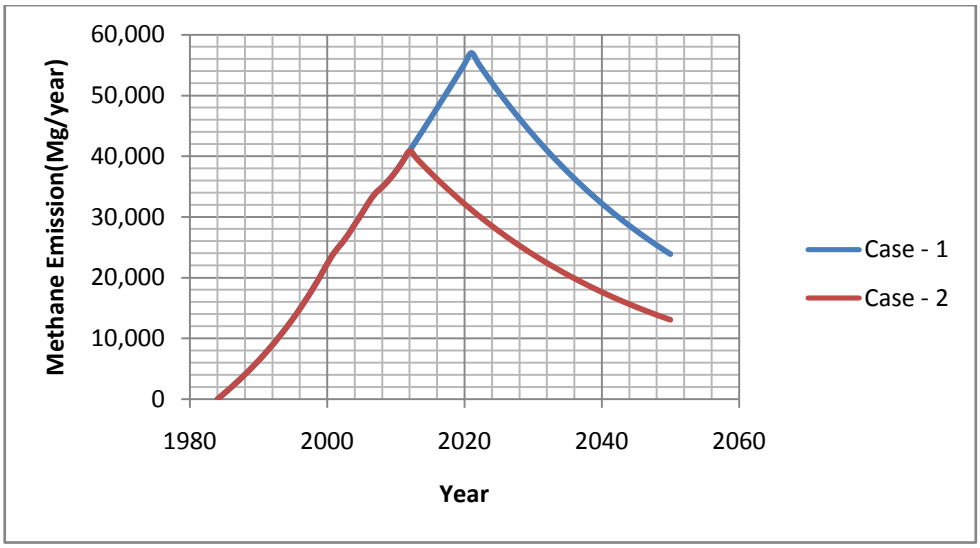

Fig. 4.17 Methane emission for case 1 and 2.

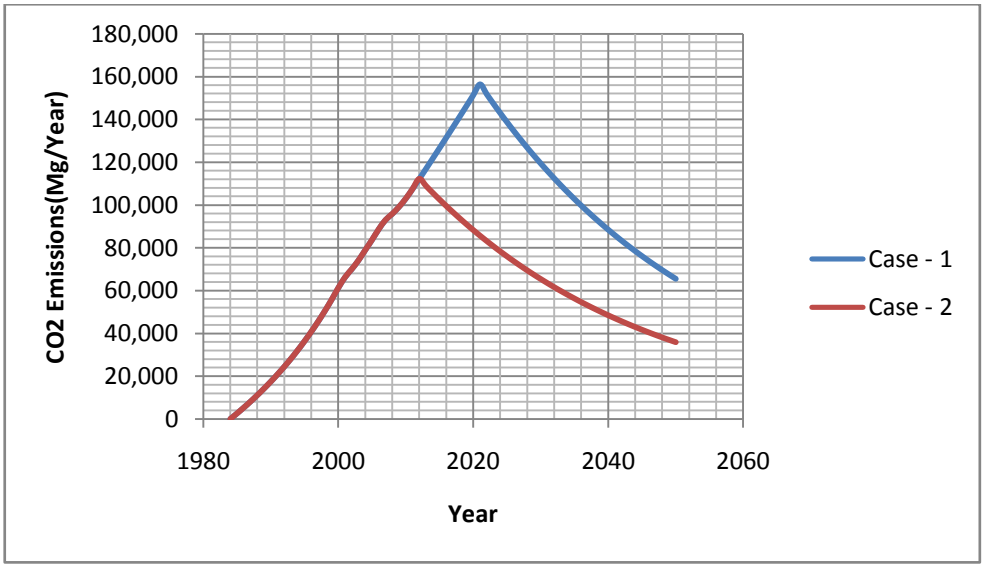

Fig. 4.18 CO_2 emission for case 1 and 2.

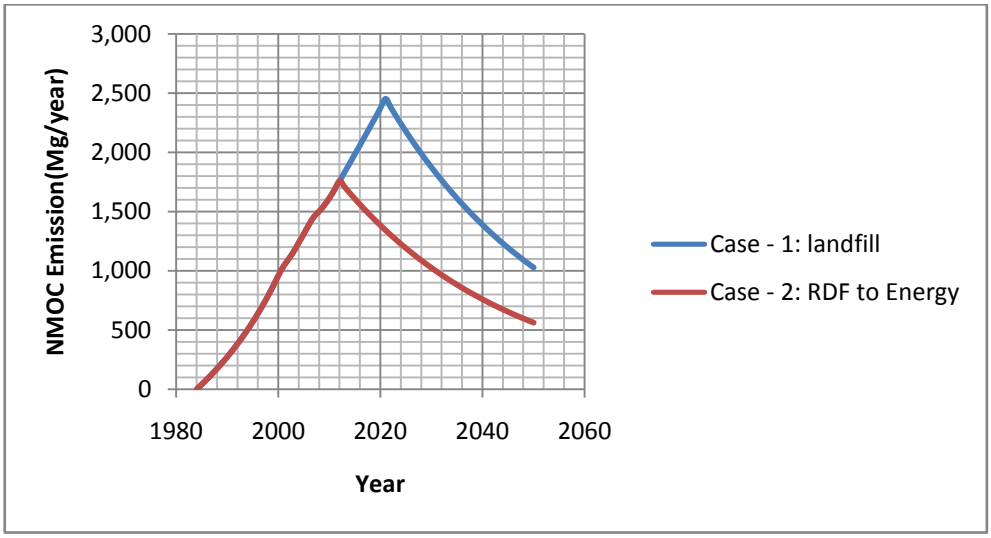

Fig. 4.19 NMOC emission for case 1 and 2.

The estimation of emission reduction in terms of equivalent carbon dioxide was calculated for each year due to conversion of MSW into RDF, which reduces methane generation at the landfills. Emission reduction due to electricity generated from the RDF was calculated and added to the emission reduction due to reduction in Methane. It gave overall reduction of emission for the case 2 scenario. The saving of methane and overall saving of emission is shown in Fig. 4.20 and 4.21 and saving/reduction for the next 20 years would be 19296162 Mg. as shown in Table 4.10.

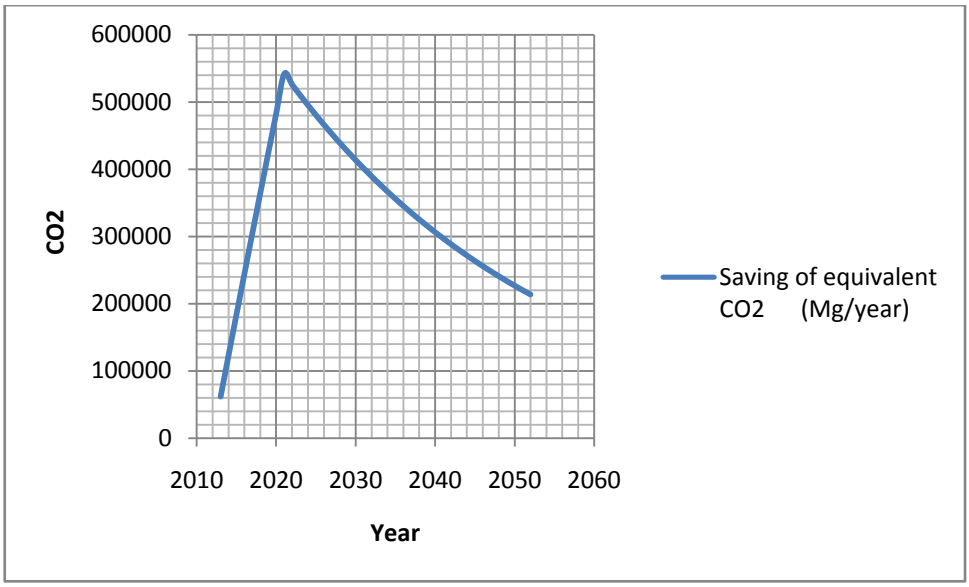

Fig. 4.20 saving of methane (equivalent co_2)

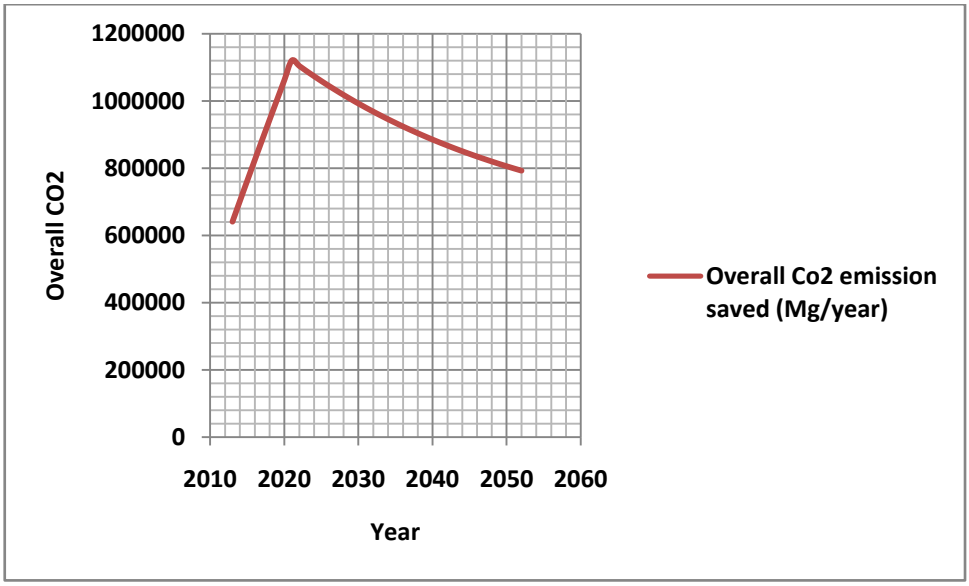

Fig. 4.21 overall co_2 emmission saved

Table 4.11 Saving of equivalent CO_2 emissions (Mg/Year) for case 2.

Year	Saving of equivalent CO_2 (Mg/year)due to reduction of methane emission	Overall CO_2 emission saved (Mg/year). *
2013	61917.4065	640077.4065
2014	123371.8546	701531.8546
2015	184377.0268	762537.0268
2016	244946.2012	823106.2012
2017	305092.2635	883252.2635
2018	364827.7185	942987.7185
2019	424164.7016	1002324.702
2020	483114.9893	1061274.989
2021	541690.0102	1119850.01
2022	525680.651	1103840.651
2023	510144.4398	1088304.44
2024	495067.3931	1073227.393
2025	480435.9404	1058595.94
2026	466236.9125	1044396.913
2027	452457.5294	1030617.529
2028	439085.3885	1017245.388
2029	426108.4541	1004268.454
2030	413515.0461	991675.0461
2031	401293.8295	979453.8295
2032	389433.8045	967593.8045

**It includes emission saved in replacing coal for producing electricity*

4.6 Conclusions

In this chapter, the computational efforts for predicting syngas composition and LFG emissions have been described in details. An equilibrium and kinetic modeling was developed to predict steady state performance of downdraft gasifier in terms of syngas

composition. Moreover, a 2-dimensional numerical model for a 10 kWe downdraft gasifier was also built by employing a CFD code "Fluent 6.2" followed by Gambit 2.4 (for geometrical treatment). It was used to predict temperature and flow fields in reduction zone. Prediction for higher moisture content of wood and larger particle sizes may deviate from reality since the model does not account for or the effect of particle size on pyrolysis, oxidation and reduction processes. The Syngas composition at the exit of reduction zone was experimentally verified. A parametric study of the effect of gasifier operating parameters has been carried out. The predicted calorific value of gas compare reasonably well with experimental data.

The computations are performed by using commercially available software LandGEM to predict landfill gas (LFG) emissions for three major landfill sites in Delhi. The policy options proposed in waste management policy were analysed under two expected scenarios- (i) when MSW is being dumped at landfill site till 2020 and (ii) if MSW, instead of getting dumped into landfills is utilized in gasifier-engine systems from 2012 onwards to produce electricity. Forecasting based on baseline scenario revealed that Delhi will produce 2.134×10^5 Mg/year methane emission by the year 2021. The treatment capacity enhancement by introducing WTE, for producing 55MW electricity from RDF would reduce methane emission by 368236 Mg in next 20 years.

The production of electricity by using WTE technology is expected to reduce the dependence on conventional fossil fuels.

Chapter 5

CONCLUSIONS AND FUTURE WORK

6.1 Conclusions

This chapter describes the major and significant contributions based on characterization of MSW feedstock, analysis and tests, and experimental observations on utilization of MSW in gasifier-engine system and its environmental impact. Computational efforts for modeling of syngas composition and LFG emissions are also employed keeping in view the objectives of the present study. Some of the salient contributions and conclusions derived out of the present work are given as:

1. Numerous studies have been reported in past on biomass gasification with focus on mathematical and experimental modeling, and characterization of woody biomass. The studies on characterization of MSW/RDF, its utilization in conventional gasifier-engine systems for power generation applications and its impact on environment are scant and disorganized in open literature.
2. MSW quantity is increasing at alarming rate and degrading the environment seriously worldwide. Delhi itself generated 751894 MT of MSW for year 2010-11; the major chunk of which is being dumped in three landfill sites (Gazipur, Okhla and Bhalswa) for disposal forcing them towards saturation.
3. The composition of raw MSW received at landfills varies widely with location and seasons as well. Thus, for utilization of MSW in conventional gasification system, specific characterization is needed.
4. For physical characterization of MSW, Sampling is identified as simplest tool. Salient points from physical characterization are given as:
    a. Organic component is observed to be highest in Season-1 (16 Dec. 2008 to 30 March 2009). Fuel component is observed to be highest in Season-3(1 July 2009 to 30 Sept. 2009), while it minimize in Season-1.

The contribution of inert component is significant (i.e., 24-32%), while recyclables vary within the range of 1-1.8%.

b. Composition pattern of MSW at Okhala site is almost similar to Gazipur landfill site. However, at Gazipur site the recyclable component is relatively high, while the inert component was relatively less than Okhala site. Trends for fuel and organic component form Bhalswa and Gazipur site are similar. At Gazipur, however, the recyclable component is higher but relatively less than Okhla site.

c. "Textile" and "cotton waste" were among the biggest contributor for both the seasons (i.e., Season-1 and Season-3) for all three landfill sites. For Season-1, the sub-components "paper" and "cardboard" are observed to be among the second biggest for all three landfill sites. For Season-3 sub-components "straw" and "hay" are among the second biggest at Gazipur and Okhla, whereas at Bhalswa, the second biggest contributor was "paper" and "cardboard".

d. Amongst organics, the sub-component "green matter" was the main contributor at Gazipur and Okhla, while "vegetables" were observed to be the main contributor at Bhalswa landfills.

5. In raw MSW, the moisture content was observed to be very high (i.e., 36-59%) for all three landfill sites. The bulk density does not display any specific pattern, however, observation at Gazipur site are relatively more uniform (i.e., 594 kg/m^3 for Season-2, 805kg/m^3 for Season-3); at Okhla, they varies from 680kg/m^3 (Season-2) -795kg/m^3 (Season-1). At Bhalswa, the variation was ranging from 801kg/m^3 (Season-2) - 900kg/m^3 (Season-3).
6. In raw MSW the pH value, potassium and sulphur content are obtained to be 7.5, 3830 mg/kg and 430 mg/kg, respectively.
7. The TG and DG thermograms of RDF sample are obtained for conditions that prevailed in the gasifier. The following salient points are noticed from TGA analysis

    a. The initiation, maximization and completion of devolatilisation near 190°C, 225-310°C and at ~523°C have been observed.

b. A sharp weight loss of RDF sample in temperature range of 190-436 °C attributes to primary thermal decomposition, which indicates the presence of hemicellulose and cellulose constituents. The rapid weight loss in range 436-523°C, indicates secondary thermal decomposition of RDF.
c. The volatiles released below 325°C tend to suppress tar formation potential of RDF.

8. Approximate and proximate analysis of MSW gives the moisture content, volatile matter, fixed carbon and ash content to be 40%, 31.9%, 3.00% and 25.1%, while upgraded RDF gives 16 % of moisture content, 56% volatile matter, 8.00% of fixed carbon and 20% of ash content, respectively.
    a. Sulphur content is 0.097% in MSW of Delhi.Fixed carbon content is extremely low than wood, while the ash content is alarmingly high in MSW.
    b. Calorific values of the air-dried MSW and RDF sample were obtained to be 1175 kcal / kg and 2600 kcal/kg, respectively.
9. Materials and compounds containing the impurities have been detected in ash by energy dispersive X-ray spectrometry (EDS). The initial deformation and softening temperature of ash is observed to be 860°C and 950°C, respectively. These are relatively lower than wood.
10. Tests and measurements for characterization of MSW/RDF and residual ash revealed that direct utilization of MSW in conventional gasifiers is very difficult (if not possible) as it may pose operational difficulty. Raw MSW can be upgraded to energy rich RDF by sorting and segregation for inert, recyclables and non-combustibles.
11. The well proportionate mixture of upgraded and compressed RDF pellets and wood chips can be utilized for thermochemical processing in fixed bed gasification systems.
12. The feed of compressed RDF pellets with woody biomass in 1:1 proportion was used in gasifier to supply the gaseous fuel “syngas” to 10 kW, 3-cylinder engine (modified for operation in single fuel mode). This engine was connected to a generator for electrification application. This decentralized

power production system was kept running for more than three hours in order to confirm successful operation with RDF as feedstock.

13. The water pollution (water spray over hot gas for cooling) was measured for pH value of re-circulated water, which was found to be within the limit. The TDS, BOD, Cyanides, dissolved phosphates and phenols, are observed to be on higher side, while "free ammonia" is observed to be highly concentrated, when compared against CPCB norms.
14. On average basis, the exhaust emissions from engine for carbon monoxide, hydrocarbons, carbon dioxide and NO_x for each kW power output were observed to be 0.465 %, 5.82 ppm, 2.028 % and 6.654 ppm, respectively.
15. A thermodynamic model has been developed and predictions were tested with considerable agreement against experiments. Methane content has been observed negligibly small. Gas quality deteriorates with high moisture content and high equivalence ratio.
16. These results also revealed that thermodynamic model may be employed safely for downdraft gasification system.
17. A 2-D numerical model based on CFD Fluent 6.2 has been developed for a 10 kW downdraft gasifier to predict the reaction temperature fields and concentration gradients of species within the reduction zone. The area averaged volumetric percentages of H_2, CO and CH_4 at reactor exit are worked out to be 11.33%, 19.37% and 2.36%, respectively. In reduction zone, the temperature contours are observed to be realistic and predicted composition of Syngas at the exit of reduction zone has been experimentally verified.

18. To estimate the landfill gas generation from the three Landfill sites of Delhi, LandGEM Model was used to compare two typical cases; Case 1: when MSW is being dumped at landfill site till 2020, Case 2: if MSW, instead of getting dumped into landfills (from 2012 onwards), is utilized in gasifier-engine systems to produce electricity.
    a. Case1: The landfill gas emission will be peaking in the year 2021 with peak production rate of methane (i.e., 5.70×10^4 Mg/year), carbon

dioxide (i.e., 1.56×10^5Mg/year) and NMOC (i.e., 2.45×10^3 Mg/year), respectively.

b. Case 2: The methane, carbon dioxides and NMOC generation would be reduced by 368236, 1010354 and 15828Mg, respectively in next 20 years.
c. The production of 55MW electricity from different treatment options of MSW based on 2011, would also reduce the burden on conventional sources like coal and would indirectly reduce the emission of other greenhouse gases.
d. Considering emission reduction in terms of equivalent carbon dioxide for each year and due to production of electricity from the RDF, the saving of methane and overall saving of emissions in terms of equivalent carbon dioxode for the next 20 years would be 19296162 Mg. and is expected to maximize in year 2021.

19. After careful apportionment of RDF and woody biomass feedstock, adequate selection of gasifier design configuration and matching of thermal system response; such coupled gasifier-engine-systems for power production application can be seen as feasible solution for depleting resources of fossil fuel, MSW disposal problem and degrading environment leading to climate change due to MSW management.

Reference

Abushammala F.M.M, Basri N.E.A., Kadhum A.A.H. (2009) Review on landfill gas emission to the atmosphere, *European Journal of Scientific Research*, 30, 427-436.

Advanced Energy Strategies Inc. (2004) Investigation into Municipal Solid Waste, Gasification for Power Generation, Prepared for Alameda Power & Telecom http://oldsite.alamedamp.com/newsroom/reports/gasification.pdf

AIT (Asian Institute of Technology) (1991) Sampling Techniques of Municipal Solid Waste, School of Environment, Resources and Development, Thailand, 04, 5-10.

Akolkar A.B., Choudhury M.K, Selvi P.K. (2008) Assessment of methane emission from Muncipal solid waste disposal site, *Research Journal of Chemistry And Environment*, 12, 49-55.

Alamgir M., Ahsan A. (2007) Characterizations of MSW and nutrient contents of organic component in Bangladesh, *Electronic Journal of Environmental, Agriculture and Food Chemistry*, 6, 1945-1956.

ANSYS FLUENT 12.0 (2009), Theory Guide.

Arena U. (2011) Gasification: an alternative solution for waste treatment with energy recovery, *Waste Management*, 31, 405–406.

Arrhenius S. (1889) Ueber die Reaktionsgeschwindigkeit bei der Inversion von Rohrzucker durch Saeuren, *Z Phys. Chem.*, 4, 226.

Atkins P.W., De P. J. (2006) Physical Chemistry, Oxford University Press.

Babu B.V., Chaurasia A.S. (2003) Modeling for pyrolysis of solid particle: kinetics

and heat transfer effects, *Energy Conversion and Management*, 44, 2251-2275.

Babu B.V., Sheth P.N. (2006) Modeling and simulation of reduction zone of downdraft biomass gasifier: effect of char reactivity factor, *Energy Conversion and Management*, 47, 2602–2611.

Babcock, Wilcox (1992) Steam, 40th ed. Chapter 16: Atmospheric Pressure Fluidized-Bed Boilers, Babcock and Wilcox, Barberton., OH.

Baggio P., Baratieri M., Gasparella A., Longo G.A. (2008) Energy and environmental analysis of innovative system based on municipal Solid waste (MSW) pyrolysis and combined cycle, *Applied Thermal Engineering*, 28, 136-144.

Bain R.L. (2009) Indirectly heated gasification of biomass to produce hydrogen, National Renewable Energy Laboratory (NREL), Annual Progress Report (58-63).

Basu P. (2010) Biomass gasification and pyrolysis: practical design and theory, *Elsevier Academic Press*, Burlington, USA.

Bebar L., Martinak P., Hajek J., Stehlik P., Hajny Z., Oral J. (2002) Waste to energy in the field of thermal processing of waste, *Applied Thermal Engineering*, 22, 897-906.

Bebar L., Stehlik, P., Havlen L., Oral J. (2005) Analysis of using gasification and incineration for thermal processing of wastes, *Applied Thermal Engineering*, 25, 1045-1055.

Belgiorno V., De Feo G., Rocca C.D., Napoli R.M.A. (2003) Energy from gasification of solid wastes, *Waste Management*, 23, 1-15**.**

Bentzen J.D., Henriksen U. (2000) Condensate from a two-stage gasifier, 1st World Conference on Biomass for Energy and Industry, Sevilla.

Bjorklund A. (2001) Hydrogen as a transportation fuel produced from thermal

gasification of municipal solid waste: an examination of two integrated technologies, *International Journal of Hydrogen Energy,* 26, 1209-1221.

Blasi C.D, Signorelli G., Portoricco G. (1999) Countercurrent fixed-bed gasification of biomass at laboratory scale, *Industrial & Engineering Chemistry Research*, 38, 2571-2581.

Blasi C.D. (2008) Modeling chemical and physical processes of wood and biomass pyrolysis, *Progress in Energy and Combustion Science*, 34, 47-90.

Bridgewater A.V. (1995) The technical and economic feasibility of biomass gasification for power generation, *Fuel*, 74, 631-653.

Brunner T., Joller M., Obernberger I. (2004) Aerosol formation in fixed-bed biomass furnaces: results from measurements and modeling. *Proc. Conf. Science in Thermal and Chemical Biomass Conversion*, Sept 2004, Victoria, Canada.

Buragohain B., Mahanta P., Moholkar V.S. (2011) Investigations in gasification of biomass mixtures using thermodynamic equilibrium and semi–equilibrium models, *Energy and Environment*, 2, 551-578.

Burcat A. (1984) Combustion Chemistry, chapter Thermochemical Data for combustion, Springer Verlag.

City Development Plan, Delhi (2006) Department of urban development, government of Delhi, http://jnnurm.nic.in/wp-content/uploads/2010/12/CDP_Delhi.pdf

Consonni S., Vigano F. (2010) A comparative analysis of two waste gasification technologies. 3rd Int. symposium on energy from biomass and waste, Venice, Italy 8 – 11 November 2010. *CISA Publisher*, Italy.

Calaminus B., Stahlberg R. (1998) Continuous in-line gasification/vitrification process for thermal waste treatment: process technology and current status of projects, *Waste Management*, 18, 547-556.

Carlsson P, Wiinikka H., Marklund M., Gronberg C., Pettersson E., Lidman M., Gebart R., (2010) Experimental investigation of an industrial scale black liquor gasifier; the effect of reactor operation parameters on Product gas composition, *Fuel*, 89, 4025-4034.

Carnevale E., Lombardi L., Corti A. (2012) Analysis of energy recovery potential using innovative technology of waste gasification, *Waste Management*, 32, 640-652.

Chakraborty M., Pandey J., Sharma C., Gupta P.K. (2011) Methane emission estimation by different methodologies for Delhi's landfills: a comparative assessment, *Atmospheric Environment*, 45, 7135-7142.

Chalvatzaki E., Lazaridid M. (2010) Estimation of greenhouse gas emissions from land fills application to the Akrotiri land fill site (Chania Greece), *Global NEST Journal*, 12, 108-116.

Chang N.B., Davila E. (2007) Municipal solid waste characterizations and management strategies for the Lower Rio Grande Valley, Texas, *Waste Management*, 28, 776–794.

Chang Y.H., Chang N.B (1998) Optimization analysis for the development of short-term solid waste management strategies using pre-sorting process prior to incinerator, *Resources Conservation and Recycling*, 24, 7–32.

Chang Y.H., Chang N.B., Chen W.C. (1998) Systematic evaluation and uncertainty analysis of the refuse derived fuel process in Taiwan, *Journal Air and Waste Management Association*, 48, 537–544.

Characterization of New York city's solid waste streams (2000) Science Applications Inter. Corporation, lack no 12, 1993, pp 721-725.
http://www.nyc.gov/html/dos/pdf/wprr/wprro6.pdf

Choy K.K.H., Porter J. F., Hui C.W., McKay G. (2004) Process design and feasibility study for small scale MSW gasification, *Chemical Engineering Journal of Environmental Sciences*, 105, 31-41.

Chrigui M. (2005) Eulerian-Lagrangian approach for modeling and simulations of turbulent reactive multi-phase flows under gas turbine combustor conditions. PhD thesis, Technische Universitaet Darmstadt.

Christensen K.A. (1995) The formation of submicron particles from the combustion of straw,Ph.D. Thesis,Department of Chemical Engineering,Technical University of Denmark, Lyngby, Denmark.

Classification of solid waste and monitoring methodology for Hong Kong (2000),http://www.epd.gov.hk/epd/english/environmentinhk/waste/data/monit_sw2000_appendix.html

Cornejo P., Farias O. (2011) Mathematical modeling of coal gasification in a fluidized bed reactor using a eulerian granular description, *International Journal of Chemical Reactor Engineering*, 9,1-13.

Cristo F., Barducci G., Uliveri P., Pike D.C., Mcdonald N., Repetto F. (1999) The Greve in Chanti Project. *Renewable Energy*, 16, 1041-1044.

Crowe M., Carty G. (1996) Municipal waste characterisation procedures, published by the environmental protection agency, Ireland, http://www.epa.ie/downloads/pubs/waste/wastecharacterisation/EPA_municipal_waste_characterisation.pdf

Cunliffe A.M., Williams P.T. (2007) Influence of temperature on pcdd/pcdf from municipal solid waste incinerator flyash under post combustion plant conditions, *Chemosphere*, 68, 1723–1732.

Dalai A.K., Batta N., Eswaramoorthi I., Schoenau G.J. (2009) Gasification of refuse derived fuel in a fixed bed reactor for syngas production, *Waste Management*, 29, 252-258.

Danheux C.B., D'haeyere A., Fontane A., and Laurent P. (1998), Upgrading of waste derived solid fuel by steam gasification, PII:S0016- 2361(97)00170.

Defra (2007) Advanced thermal treatment of municipal solid waste, enviros consulting limited on behalf of *Department for Environment, Food & Rural Affairs* (Defra), available on <www.defra.gov.uk>.

Delhi Pollution Control Committee (DPCC) (2008) Environmental impact assesment of integrated msw processing complex Ghazipur, Delhi.
http://dpcc.delhigovt.nic.in/gdpcc.pdf

Dong C.,Jin B., Zhong Z.,Lan J. (2002) Tests on co-firing of municipal solid waste and coal in a circulating fluidized bed, *Energy Conversion and Management*, 43, 2189-2199.

Dong T.T.T., Lee B.K. (2009) Analysis of potential RDF resources from solid waste and their energy values in the largest industrial city of Korea, *Waste Management*, 29, 1725-31.

Environmental Protection Agency (EPA)Ireland (1996) Municipal waste characterization,
http://www.epa.ie/downloads/pubs/waste/wastecharacterisation/name,11656,en.html

E4tech (2009) Review of technologies for gasification of biomass and wastes, NNFCC project, www.nnfcc.co.uk

Eighmy T.T., Kosson D.S. (1996) U.S.A. National overview on waste management, *Waste Management*, 16, 361-366.

EPA (Environmental Protection Agency) (1996), Characterization of Municipal Solid Waste in the United States: 1995 Update, US EPA 530-R-96-001, PB 96-152 160.

EPA US (1999) Characterization of Municipal Solid Waste in the United States: 1999 Update. http://www.epa.gov/osw/nonhaz/municipal/pubs/msw99.pdf

Ferraris S.M., Milena V.M., Buzzi A., Veglia L., Massimo (2009) Use of vitrified MSWI bottom ashes for concrete production, *Waste Management*, 29, 1041–1047.

Fletcher D.F., Haynes B.S., Christo F.C., Joseph S.D. (2000) A CFD based combustion model of an entrained flow biomass gasifier, *Applied Mathematical Modeling*, 24, 165-182.

Forteza R., Far M., Segu C., Cerda V. (2004) Characterization of bottom ash in municipal solid waste incinerators for its use in road base, *Waste Management*, 24, 899–909.

Fluent 6.2. (2003), User's Guide. Fluent Incorporation.

Gang X., Baosheng J., Zhaoping Z.,Yong C., Mingjiang N., Kefa C., Rui X., Yaji H., He H. (2007) Experimental study on MSW gasification and melting technology, *Journal of Enviromental* Sciences, 19, 1398-1403.

Gang X., Ni M.J., Chi Y., Cen K.F. (2008) Low-temperature gasification of waste tire in a fluidized bed, *Energy Conversion and Management*, 49, 2078-2082.

Garcia A.J., Esteban M.B., Marquez M.C., Ramos P. (2005) Biodegradable municipal solid waste: characterization and potential use as animal feedstuffs, *Waste Management*, 25, 780–787.

Gawaikar V., Deshpande V.P. (2006) Source specific quantification and characterization of Municipal Solid Waste - a Review, *Institution of Engineers (India) Journal*, 86, 33-38.

Gaur A., Park J.W., Maken S., Song H.J., Park J.J. (2010) Landfill gas (LFG) processing via adsorption and alkanolamine absorption, *Fuel Processing Technology*, 91, 635-640.

Gaur A., Park J.W., Jang J.H., Song H.J. (2011) Precipitation of barium carbonate from alkanolamine solution—study of CO_2 absorption from landfill gas (LFG)**,** *Journal of Chemical Technology and Biotechnology,*86,153-156.

Gendebien A., Leavens K., Blackmore A., Godley K., Lewin K., Whiting J., Davis R. (2003), Refuse derived Fuel, current practice and perspective, European commission, 1-229. http://ec.europa.eu/environment/waste/studies/pdf/rdf.pdf

Gerun L., Paraschiv M., Vijeu R., Bellettre J., Tazerout M., Gobel B., Henriksen U. (2008) Numerical investigation of the partial oxidation in a two stage downdraft gasifire, *Fuel*, 87, 1383-1393.

Giddings D. (2000) Investigation into the operation of a cement works precalciner vessel, Ph.D.Thesis, The University of Nottingham, School of Mechanical, Materials, Manufacturing Engineering and Management.

Gil J., Aznar M.P., Caballero M.A., Frances E., Corella, J. (1997) Biomass gasification in fluidized bed at pilot scale with steam-oxygen mixtures: product distribution for different operating conditions, *Energy and Fuels*, 11, 1109-1118.

Gilbert R.G., Luther K., Troe J. (1983) Theory of thermal unimolecular reactions in the fall-off range, *Berichte der Bunsengesellschaft für physikalische Chemie*, 87, 169-177.

Giltrap D.L., McKibbin R., Barnes G.R.G. (2003) A steady state model of gas-char reactions in a down draft biomass gasifier, *Solar Energy*, 74, 85-91.

Gomez B.A., Leckner B. (2010) Modeling of biomass gasification in fluidized bed, *Progress in Energy and Combustion Science*, 36, 444–509.

Gomez E., Rani D.A., Cheeseman C.R., Deegan D., Wise M., Boccaccini A.R. (2009) Thermal plasma technology for the treatment of wastes: A critical review, *Journal of Hazardous materials*, 161, 614-626.

Granatstein D.L. (2003) Case study on waste fuelled gasification project Greve in Chainti,Italy,*IEABioenergy*.http://www.ieabioenergytask36.org/Publications/20012003/Case_Studies/Case_Study_on_Waste-fuelled_Gasification_Project.pdf

Gronli M. (1996) Theoretical and experimental study of the thermal degradation of biomass, Ph. D. Thesis, Norwegian University of Science and Technology.

Grover P.D., Baveja K.K., Rao T.R., Iyer, P.V.R. (1988), Thermochemiocal

characterization of biomass residues for gasification, Biomass Research Laboratory, IIT Delhi.

Gupta S., Prasad M.K., Kansal A. (1998) Solid waste management in India: options and opportunities, *Resources Conservation and Recycling*, 24, 137-154.

Habibi A., Merci B., Heynderickx G.J. (2007) Impact of radiation models in CFD simulations of steam cracking furnaces, *Computers & Chemical Engineering*,31,1389-1406.

Hackbusch W. (1985) Multi-grid methods and applications, *Springer Verlag*.

Frey H.H., Peters B., Hunsinger H., Vehlow J. (2003) Characterization of municipal solid waste combustion in a grate furnace, *Waste Management*, 23, 689-701.

Hackett C., Durbin T.D., Welch W., Pence J. (2004) Evaluation of conversion technology processes and products, California environmental protection agency Integrated Wastes Management Board, www.ciwmb.ca.gov/Publications.

Hamel S., Hasselbach H., Weil S., Krumm W. (2007) Autothermal two-stage gasification of low-density waste-derived fuels, *Energy*,32, 95-107.

Hau J.L., Ray R., Thorpe R.B., Azapagic A. (2008) A Thermodynamic model of the outputs of gasification of solid Waste, *Int. Journal of Chemical Reactor Engineering*, 6, 1-22.

He M., Hu Z., Xiao B., Li J., Guo X., Luo S., Yang F., Feng Y., Yang G., Liu S. (2009) Hydrogen-rich gas from catalytic steam gasification of municipal solid waste (MSW), Influence of catalyst and temperature on yield and product composition, *International Journal of Hydrogen Energy*, 34, 195-203.

He M., Hu Z., Xiao B., Xianjun G.J.L., Siyi L., Fan Y., Yu F., McAsey, Jha M. (1997) Municipal waste management: recycling and landfill space constraints, *Waste Management & Research*, 26, 3-21.

Hermansson S., Thunman H. (2011) CFD modeling of bed shrinkage and channeling

in fixed-bed combustion, *Combustion and Flame*, 158, 988–999.

Higman C., Van Der B.M. (2003) Gasification, gulf professional publishing, *Elsevier Science, Burlington* MA, USA.

Hinze J.O. (1975) Turbulence, McGraw-Hill Publishing Company.

Hollenbacher R.H. (1992) Biomass combustion technologies in the united states, biomass combustion conference, Reno, Nevada, US DOE Western Regional Biomass energy Program.

Holt N. (2005) Gasification technology status – December 2005, EPRI report 1010460, Electric Power Research Institute, Palo Alto CA, http://www.scribd.com/doc/56491930/EPRI-Gasification-Technology-Status-December-2006

Huang H., Buekens A. (2001) Chemical kinetic modeling of de novo synthesis of pcdd/f in municipal waste incinerators, *Chemosphere*, 44, 1505-1510.

Hutchinson B.R., Raithby G.D. (1986) A multigrid method based on additive correction strategy, *Numerical Heat Transfer*, 9, 511–537.

Hyun J.S., Park J.W., Maken S., Park J.J. (2004) Vitrification of fly and bottom ashes from municipal solid waste incinerator using Brown's gas, *Journal of Industrial & Engineering Chemistry*, 10, 361-367

Intergovernmental Penal on Climate Change (IPCC) (2001) Climate change 2001-the scientific basis, *Cambridge Press*, 244-245.

Jarungthammachote S., Dutta A. (2006) Thermodynamic equilibrium model and second law analysis of a downdraft waste gasifier, *Energy*, 32, 1660-1669.

Jayah T.H., Lu A., Fuller R.J., Stewart D.F. (2003) Computer simulation of a downdraft wood gasifier for tea drying, *Biomass and Bioenergy*, 25, 459-469.

Jeevanrao K., Shantaram, M.V. (1993) Physical characteristics of urban solid wastes of Hyderabad, Indian *Journal of Environmental Protection*, 13, 1-11.

Jha A., Sharma K.C., Singh N., Ramesh R., Purvaja R., Gupta P.K. (2007) Greenhouse gas emissions from municipal solid waste management in Indian mega-cities: a case study of Chennai landfill sites, *Chemosphere*, www.elsevier.com/locate/chemosphere.

Jidapa N. (2007) Potential of refuse derived fuel production from Bangkok MSW, Master of Engineering thesis, Asian Institute of Technology School of Environment, Resources and Development,Thailand. http://www.faculty.ait.ac.th/visu/Data/AITThesis/Master%20Thesis%20final/Jidapa%20Thesis%2012-12-07.pdf

Jimbo H.X. (1996) Plasma melting and useful application of molten slag, *Waste Management*, 16, 417-422.

Jung C.H., Masahiro O. (2007) Thermodynamic behaviour of rare metals in the melting process of municipal solid waste (MSW) incineration residues, *Chemosphere*, 69, 279–288.

Kaer S.K., Rosendahl L. (2003) Extending the modeling capacity of CFD codes applied to biomass-fired boilers. *In. Proc. ECOS*, Copenhangen, Denmark, Jun 30-Jul 2, 2003, 251-264.

Kaer S.K., Rosendahl L.A., Baxter L.L. (2006) Towards a CFD-based mechanistic deposit formation model for straw-fired boilers, *Fuel*, 85, 833-848.

Kallio G.A., Reeks M.W. (1989) A Numerical simulation of particle deposition in turbulent boundary layers, *International Journal of Multiphase Flow*, 15, 433-446.

Kawaguchi K., Miyakoshi K., Momonoi K. (2002) Studies on pyrolysis behaviour of gasification and melting system of municipality solid waste *Journal of Material Cycles and Waste Management*, 4, 102-110.

Kee R.J., Rupley F.M., Miller J.A. (1987) Chemical thermodynamic data base, technical report, Sandia Report 87-82153.

Kennan K., Kankyou K. (2006) Emissions Data of JEE Nagasaki plant compliance source test report April- June 2006.

Kerr T. (2008) Turning a liability into an asset: landfill methane utilisation potential in India, *International Energy Agency*, http://www.iea.org/index.asp.

Kiss G.W.M., Riegel J., Stahlberg R. (1994) Thermoselect—recovery of energy and raw materials from waste, *EF-Verlag*, Berlin,F.J. Schweitzer, Editor, 21–55.

Kjeldsen P., Barlaz M.A., Rooker A.P., Baun A., Ledin A., Christensen T.H. (2002) Present and long-term composition of MSW landfill leachate: critical review, *Environmental Science Technology*, 22, 297-336.

Kikuchi R., Sato H., Matsukura Y., Yamamoto T. (2005) Semi-pilot scale test for production of hydrogen-rich fuel gas from different wastes by means of a gasification and smelting process with oxygen multi-blowing, *Fuel Processing Technology*, 86, 1279-1296.

Kim B.H., Lee S., Maken S., Song H.J., Park J.W., Min B. (2007) Removal characteristics of pcdds/fs from municipal solid waste incinerator by dual bag filter (DBF) system, *Fuel*, 86, 813-819

Klee A.J. (1980) Quantitative decision making, design and management for resource and recover series, Vol. 3, Ann Arbor Science, Michigan, USA.

Klein A. (2002) Gasification: An Alternative process for energy recovery and disposal of municipal solid wastes, *MS Thesis*, Columbia University.

Klien A., Themelis N. (2003) Energy recovery from municipal solid wastes by

gasification, north American waste to energy conference (NAWTEC-11), In 11th Proceeds, ASME International, Tampa FL, 241-252.

Kumar S., Gaikwad S.A., Shekdar A.V., Kshirsagar P.S., Singh R.N. (2004) Estimation method for national methane emission from solid waste landfills, *Atmospheric Environment*, 38, 3481–3487.

Kumar S., Gaikwad S.A., Shekdar A.V., Kshirsagar P.S. and Singh R.N. (2004) Estimation method for national methane emission from solid waste landfills, *Atmospheric Environment*, 38, 3481–3487.

Kusar H. (2003) Catalytic combustion of gasified waste, KTH-Kungliga Tekniska Hogskolan department of chemical engineering and technology, chemical technology, Stockholm.

Kwak T.H., Lee S., Maken S., Park J.W., Min B.R., Yoo Y.D. (2006) Environmental aspects of gasification of Korean municipal solid waste in a pilot plant, *Fuel*, 85**,** 2012- 2017.

Kwak T.H., Lee S., Maken S., Shin H.C., Park J.W., Yoo Y.D. (2005) A Study of Gasification of Municipal Solid Waste Using a Double Inverse Diffusion Flame Burner *Energy Fuels*, *19*, 2268–2272.

Kwak T.H., Lee S., Park J.W., Maken S., Yoo Y.D., Lee S.H. (2006) Gasification of Municipal Solid Waste in a Pilot Plant and Its Impact on Environment. *Korean Journal of Chemical Engineering,* 23, 954-960.

Larsona E.D., Worrell E., Chen J.S. (1996) Clean fuels from municipal solid waste for fuel cell buses in metropolitan areas resources, *Conservation and Recycling*, 17, 273-298.

Lasagni M., Collina E., Grandesso E., Piccinelli E., Pitea D. (2009) Kinetics of carbon degradation and pcdd/pcdf formation on MSWI fly ash, *Chemosphere,* 74, 377–383.

Lee S.H., Choi K.B., Lee J.G., Kim J.H. (2006) Clasification characterstics of combustible Wastes in a 5 ton/day fixed bed gasifier, *Korean Journal of Chemical Engineering*, 23, 576-580

Lee S., Park K., Park J.W., Kim B.H. (2005) Characteristics of reducing NO using urea and alkaline additives, *Combustion and Flame*, 141, 200-203.

Lemmens B., Elslander H., Vandereydt I., Peys K., Diels L., Oosterlinck M., Joos M.,(2007) Assessment of Plasma Gasification of high caloric waste streams, *Waste Management*, 27, 1562-1569.

Li X., Grace J.R., Watkinson A.P., Lim C.J., Ergudenler (2001) A Equilibrium modeling of gasification: a free energy minimization approach and its application to a circulating fluidized bed coal gasifier, *Fuel*, 80,195-207.

Littarru P. (2006) Repartition of pcdd and pcdf in the emissions of municipal solid waste incinerators between the particulate and volatile phases, *Waste Management*, 26, 861-868.

Liu G.H., Xiao Q.M., Zhaosheng Y. (2009) Experimental and kinetic modeling of oxygen-enriched air combustion of municipal solid waste, *Waste Management*, 29, 792-796.

Liu Y., Liu Y. (2005) Novel incineration technology integrated with drying, pyrolysis, gasification, and combustion of MSW and ashes vitrification, *Environmental Science & Technology*, 39, 3855-3863.

Lombardi L., Carnevale E., Corti A. (2012) Analysis of energy recovery potential using innovative technology of waste gasification, *Waste Management*, 32, 640-652.

Ludwig C.B., Malkmus W., Reardon J.G., Thomson J.A. (1973) Handbook of infrared radiation from combustion gases, NASA SP-3080.

Luo Z.Y., Wang S.R., Cen K.F. (2005) A model of wood flash pyrolysis in fluidized bed, *Energy*, 30, 377-392.

Ma L., Jones J. M., Pourkashanian M., Williams A. (2007) Modeling the combustion of
pulverized biomass in an industrial combustion test furnace, *Fuel*, 86, 12-13.

Mackie K.R., Cooper C.D. (2009) Landfill gas emission prediction using Voronoi diagrams and importance sampling, *Environmental Modelling and Software*, 24, 1223-1232.

Maclaven Yu, Chang-Ching V.Y., Maclaven V. (1995) A comparison of two waste streams quantification and characterization methodologies, *Journal of Waste Management and Research*, 13, 343-361.

Magnussen B.F. (1981) On the structure of turbulence and a generalized eddy dissipation concept for chemical reaction in turbulent flow. In 19th AIAA Meeting.

Magnussen B.F., Hjertager B.H. (1996) On mathematical models of turbulent combustion with special emphasis on soot formation and combustion, in 16th Symp. (International) on Combustion, the Combustion Institute.

Magnussen B.F., Gran I.R. (1996) A numerical study of a bluff-body stabilized diffusion flame, part 2 influence of combustion modeling and finite-rate chemistry, *Combustion Science and Technology*, 119, 191–217.

Magrinho A., Semiao V. (2008) Estimation of residual MSW heating value as a function of waste component recycling, *Waste Management*, 28, 2675-2683.

Min T.J., Yoshikawa K., Murakami K. (2005) Distributed gasification and power generation from solid wastes, *Energy*, 30, 2219-2228.

Maken S., Jang S.H., Park J.W., Song H.C., Lee S., Chang E.H. (2005) Vitrification of MSWI fly ash using Brown's gas and fate of heavy metals, *Journal of Scientific & Industrial Research (India)*, 64, 198-204.

Malkow T. (2004) Novel and innovative pyrolysis and gasification technologies for energy efficient and environmentally sound MSW disposal, *Waste Management*, 24, 53–79.

Manual on Municipal Solid Waste Management (2000) Expert committee constituted by the government of India, ministry of urban development, central public health and environmental engineering organization and ministry of urban development, government of India, New Delhi.

Marklund M., Tegman R., Gebart R. (2007) CFD modeling of black liquor gasification: identification of important model parameters, *Fuel*, 86, 1918-1926.

Mathieu P., Dubuisson R. (2002) Performance analysis of a biomass gasifier, *Energy Conversion and Management*, 43(10), 1291-1299.

Mathur S.R., Murthy J.Y. (1997) A pressure-based method for unstructured meshes, Numerical Heat Transfer, Part B: Fundamentals, 31, 195-215.

Maughan J.R., Bowen J.H., Cooke D.H., Tuzson J.J. (1994) Reducing gas turbine emissions through hydrogen-enhanced, steam-injected combustion, *ASME Cogen Turbo Power '94. IGTI*, 9, 381-390.

McGowin, C.R., Wiltsee, G.A.,(1996), Strategic analysis of biomass and waste fuels for electric power generation, *Biomass and Bioenergy*,10, 167-175.

McKay (2002) Dioxin characterization formation and minimization during municipal solid waste (MSW) incineration review, *Chemical Engineering Journal*, 86, 343-368.

Murphy J.D., McKeogh E. (2004) Technical, economic and environmental analysis of energy production from municipal solid waste, *Renewable Energy*, 29, 1043-1057.

Murphy J.D., McKeogh E. (2006) The benefits of integrated treatment of wastes for the production of energy, *Energy*, 1, 294-310.

Metin E., Erozturk A., Neyim, C. (2003) Solid waste management practices and review of recovery and recycling operations in Turkey, *Waste Management &*

Research, 23, 425-432.

Milligan J.B. (1994) Downdraft gasification of biomass, Ph.D. Thesis, Aston University, Birmingham, UK.

Milne T.A., Evans R.J., Abatzoglou N. (1998), Biomass gasifier tars, their nature, formation, and conversion, national renewable energy laboratory, US department of energy.

Miltner M., Miltner A., Harasek M., Friedl A. (2007) Process simulation and CFD calculations for the development of an innovative baled biomass-fired combustion chamber, *Applied Thermal Engineering*, 27, 1138-1143.

Mindaugas S., Marija B. (2011) Assessment of green house gasses attributable to the waste management sector in urban planning, Environment Engineering, The 8th International Conference May 19–20, 2011, Vilnius, Lithuania.

Moilanen A. (2006) Thermogravimetric characterisations of biomass and waste for gasification processes Espoo 2006, VTT Publications 607.

Morris M. (1998) Electricity production from solid waste fuels using advanced gasification technologies, TPS termiska processer AB, www.tps.se.

Mor S., Ravindra K., Visscher A.D., Dahiyaa R.P., Chandra A. (2006) Municipal solid waste characterization and its assessment for potential methane generation: a case study, *Science of the Total Environment*, 371, 1-10.

Mountouris A., Voutsas E., Tassios D. (2006) Solid waste plasma gasification: equilibrium model development and exergy analysis. *Energy Conversion and Management*, 47 1723–1737.

Mountouris A., Voutsas E., Tassios D. (2008) Plasma gasification of sewage sludge: process development and energy optimization, *Energy Conversion and Management* 49, 2264-2271.

Murphy J.D., Oduro E.K. (2004) Technical, economic and environmental analysis of

energy production from municipal solid waste, *Renewable Energy*, 29, 1043-1057.

Neilson C.E. (1998) LM2500 gas turbine modifications for biomass fuel operation, *Biomass and Bioenergy*, 15, 269-273.

Niessen W.R., Markes C.H., Sommerlad R.E. (1996) Evaluation of gasification and novel thermal processes for the treatment of municipal solid waste, National Renewable Energy Laboratory,US Department of Energy.
http://www.osti.gov/bridge/product.biblio.jsp?osti_id=378836

Ntshengedzeni S., Edson M., Meyer L. (2010) Evaluation of the conversion efficiency of 180 Nm3/h Johansson biomass gasifier, *International Journal of Energy and Environment*, 1, 113-120.

Oonk H., Oonk, A.Y. (2010) Literature review methane from landfills, methods to quantify generation oxidation and emission, www.sustainablelandfillfoundation.eu

Otoma S., Mori Y., Terazono A., Aso T., Sameshima R. (1997) Estimation of energy recovery and reduction of CO_2 emission in municipal solid waste generation, *Resources Conservation and Recycling*, 20, 95-117.

Pallares J., Arauzo I., Williams A. (2007) Integration of CFD codes and advanced combustion models for quantitative burnout determination, *Fuel*, 86, 2283-2290.

Parikh J., Channiwala S.A., Ghosal G.K.(2005) A correlation for calculating HHV from proximate analysis of solid fuels, *Fuel*, 84, 487-494

Park K., Hyun J., Maken S., Jang S., Park J.W. (2005) Vitrification of Municipal Solid Waste Incinerator Fly Ash Using Brown's Gas, *Energy Fuels*, *19*, 258–262.

Patankar S.V. (1980) Numerical heat transfer and fluid flow, hemisphere, Washington, D.C.

Petrescu M., Batrinescu G., Stanescu B. (2011) Evaluation of gasious emissions from the radauti municipal landfill, *International Journal of Conservation Science*, 2, 45-54

Perkins G., Sahajwalla V. (2007) Modeling of heat and mass transport phenomena and chemical reaction in underground coal gasification, Transaction IChemE, Part A, *Chemical Engineering Research and Design*, 85, 329–343.

Perry R.H., Green D.W. (1998) Perry's Chemical Engineers Handbook', 7th MGH Int. Ed., NY.

Phan A.N., Changkook R., Sharifi V.N., Swithenbank J. (2008) Characterization of slow pyrolysis products from segregated wastes for energy production, *Journal of Analylical and Applied Pyrolysis*, 81, 65-71.

Piquet J. (1999) Turbulent Flows - Models and Physics, Springer Verlag

Pinto F., Lopes H., Andre R.N., Gulyurtlu I., Cabrita I. (2001) Effect of catalysts in the quality of syngas and by-products obtained by co-gasification of coal and wastes, tars and nitrogen compounds abatement, *Fuel*, 86, 2052–2063.

Porteiro J., Joaquin C., David P., Enrique G., Jorge C., Gonzalez M., Miguez J.L. (2009) Numerical modeling of a biomass pellet domestic boiler, *Energy & Fuels*, 23, 1067–1075.

Porteous A. (2001) Energy from waste incineration - a state of the art emissions review with an emphasis on public acceptability, *Applied Energy*, 70, 157-167.

Ragland K.W., Arts D.J., Baker A.J. (1991) Properties of wood for combustion analysis, *Bioresource Technology*, 37, 161-168.

Rao M.S., Singh S.P., Sodha M.S., Dubey A.K., Shyam M. (2004) Stoichiometric, mass, energy and exergy balance analysis of countercurrent fixed-bed gasification of post-consumer residues, *Biomass and Bioenergy*, 27, 155-171.

Ratnadhariya J.K., Channiwala S.A. (2003) Parametric sensitivity of downdraft Gasifier as predicted by three zone KF model, International Conference on Mechanical Engineering 2003 (ICME2003) 26- 28 December 2003, Dhaka.

Ratnadhariya J.K., Channiwala S.A. (2009) Three zone equilibrium and kinetic free modeling of biomass gasifier – a novel approach, *Renewable energy*, 34, 1050-1058.

Ravelli S., Perdichizzi A., Barigozzi G. (2008) Descriptions, application and numerical modelling of bubbling fluidized bed combustion in waste-to-energy plants. *Progress in Energy and Combustion Science*, 34, 224–253.

Rehm M., Seifert P., Meyer B. (2009) Theoretical and numerical investigation on the EDC-model for turbulence–chemistry interaction at gasification conditions, *Computers and Chemical Engineering*, 33, 402–407.

Rhie C.M., Chow W.L. (1983) Numerical study of the turbulent flow past an airfoil with trailing edge separation, *AIAA Journal*, 21, 1525–1532.

Schlichting H., Gersten K. (2000) Boundary Layer Theory, 8th Edition, Springer.

Sanchez M.E., Cuetos M.J., Martinez O., Moran A. (2007) Pilot scale thermolysis of municipal solid waste combustibility of the products of the process and gas cleaning treatment of the combustion gases, *Journal of Analytical and Applied Pyrolysis*, 78**,** 125-132.

Sangtongam K., Gmurczyk J., Gupta A.K. (2007) Parameters influencing clean syngas production from biomass, solid waste, and coal during steam gasification, Proceedings of International Symposium on Eco. Topia Science(SETS07).

Santisirisomboon J., Bundit L., Supachart (2003) Least cost electricity generation options based on environmental impact abatement, *Environmental Science & Policy* 6, 533-541.

Stege A. (2006) Modeling Landfill biogas generation for different countries, *Landfil lMethane to Markets Workshop*,
http://www.globalmethane.org/documents/events_land_20060309_stege.pdf

Shafizadeh F. (1982) Pyrolytic reactions and products of biomass, *Journal of Analytical and Applied Pyrolysis*, 3, 283-305.

Sharholy M., Ahmad K., Mahmood G., Trivedi R.C. (2007) Municipal solid waste management in Indian cities – A review, *Waste Management*, 28, 459–467.

Sharma A.K. (2006) Simulation of biomass gasifer-engine systems, Ph.D. Thesis, Mechanical Engineering Department, IIT, Delhi.

Sharma A.K. (2008a) Experimental study on 75 kWth downdraft (biomass) gasifier system. *Renewable Energy*, 34, 1726–1733.

Sharma A.K. (2008b) Equilibrium & kinetic modeling of reduction reactions in the char bed of a downdraft (biomass) gasifier: a comparison, *International Journal of Solar Energy*, 82: 918-928.

Sharma A.K. (2007) Modeling fluid and heat transport in the reactive, porous bed o downdraft (biomass) Gasifier, *International Journal of Heat and Fluid Flow*, 28, 1518-1530.

Shen B., Qinlei (2006) Study on MSW catalytic combustion by TGA, *Energy Conversion and Management*, 47, 1429-1437.

Shin H.C., Kim H.S., Shin E.S. (2005) Environmental and economic assessment of landfill gas electricity generation in Korea using LEAP model, *Energy Policy*, 33, 1261-1270.

Shin H.C., Park J.W., Kim H.S., Shin E.S. (2005) Environmental and economic assessment of landfill gas electricity generation in Korea using LEAP model, *Energy Policy*, 33, 1261-1270.

Siegel R., Howell J.R. (1992) Thermal radiation heat transfer, *Hemisphere Publishing Corporation*.

Silaen A., Wang T. (2010) Effect of turbulence and devolatilization models on coal gasification simulation in an entrained-flow gasifier, *International Journal of Heat and Mass Transfer*, 53, 2074–2091.

Sivakumar S., Pitchandi K., Natrajan E. (2008) Modelling and simulation of down draft wood Gasifier, *Journal of Applied Sciences*, 8, 271-279.

Smith T.F., Shen Z.F., Friedman J.N. (1982) Evaluation of co-efficients for the weighted sum of gray gases model, *Journal of Heat Transfer*, 104, 602–608.

Staniunas M., Burinskiene M. (2011) Assessment of green house gasses attributable to the waste management sector in urban planning, Environment Engineering, The 8th International Conference May 19–20, 2011, Vilnius, Lithuania.

Stehlik P. (2009) Contribution to advances in waste to energy technologies, *Journal of Cleaner Production*, 17, 1-13.

Sumio Y., Masuto S., Fumihiro M. (2004 July) Thermoselect waste gasification and reforming process, *JFE Technical Report*, 3, 21-26.

Talyan V., Dahiya R.P., Anand S., Sreekrishnanent T.R. (2006) Quantification of methane emission from municipal solid waste disposal in Delhi, *Resources, Conservation and Recycling*, 50, 240–259.

Tchobanoglous G., Theisen H., Virgil S. (1993) Integrated solid waste management, McGraw-Hill, New York.

Thamavithya M., Dutta A. (2008) An investigation of MSW gasification in a spout-fluid bed reactor, *Fuel Processing Technology*, 89, 948-957.

Tilmans A., Jeanmart H. (2007) Investigation of combustion of pyrolysis gases in a downdraft gasifier, Third European Combustion Meeting ECM.

Turns S.R. (2000) Introduction to Combustion, 2nd Edition, McGraw Hill.

Visvanathan C., Trankler J., Gongming Z., Joseph K., Basnayake B.F.A., Chiemchaisri C., Kuruparan P., Norbu T., Shapkota P. (2004) Municipal solid waste management in Asia, 31-56. Asian Regional Research Program on Environmental Technology (ARRPET), AIT, Thailand.

Wang Y., Kinoshita C.M. (1993) Kinetic model of biomass gasification, *Solar Energy*, 51 19-25.

Wang Y., Yan L. (2008) CFD modeling of a fluidized bed sewage sludge gasifier for syngas, *Asia-Pacific Journal of Chemical Engineering,* 3, 161–170.

Wang Q., Yan J., Tu X., Chi Y., Li X., Lu S., Cen K. (2009) Thermal treatment of municipal solid waste incinerator fly ash using DC double arc argon plasma, *Fuel*, 88, 955–958.

Warnatz J., Mass U., Dibble R.W. (2006) Combustion, Heidelberg, Springer Verlag.

Wesseling P. (2000) Principles of Computational Fluid Dynamics. Springer Verlag.

Willcox D. (1998) Turbulence Modeling for CFD, DCW Industries, California.

Xiu S.N., Wang N.N., Yi W.M., Li B.M., Shahbazi G. (2008) Validation of kinetic parameter values for prediction of pyrolysis behaviour of corn stalks in a horizontal entrained-flow reactor, *Biosystems Engineering*, 100, 79-85.

Yan W., Shuting Z., Yufeng Z., Hui X., Na D., Guanyi C. (2005) Experimental studies on low-temperature pyrolysis of municipal household garbage-temperature influence on pyrolysis product distribution, *Renewable Energy*,30, 1133-1142.

Yang Y.B., Phan A.N., Ryu C., Sharifi V., Swithenbank J. (2007) Mathematical modelling of slow pyrolysis of segregated solid wastes in a packed-bed pyrolyser, *Fuel*, 86, 169–180.

Yang Y. B., Swithenbank J. (2008) Mathematical modelling of particle mixing effect on the combustion of municipal solid wastes in a packed-bed furnace, *Waste*

Management, 28, 1290–1300.

Yassina L., Lettieri P., Simons S.J.R., Germana A. (2009), Techno-economic performance of energy-from-waste fluidized bed combustion and gasification processes in the UK context, *Chemical Engineering Journal* 146, 315-327.

Yokohama N., Otaka H., Minato I., Nakata M. (2008) Evaluation of gas-particle partition of dioxins in flue gas I: evaluation of gasification behavior of polychlorionated dibenzo-p-dioxins and polychlorinated dibenzofurans in fly ash by thermal treatment, *Journal of Hazardous Materials*, 153, 395-403.

Yoshikawa K. (2004), Commercial demonstration of a small –scale gasification and power generation from MSW, 2nd International Energy Conversion Engineering Conference 16-19 August 2004 Providence, Rhode Island, AIAA -5649.

Zainal Z.A., Ali R., Lean C.H., Seetharamu K.N. (2001) Prediction of the performance of a downdraft gasifier using equilibrium modelling for different biomass materials, *Energy Conversion and Management*, 42, 1499-1515.

Zhang P., Law C.K. (2009) A fitting formula for the falloff curves of unimolecular reactions, *International Journal of Chemical Kinetics*, 41, 727–734.

Zhang Y., Chen Y., Meng A., Li Q., Cheng H. (2008) Experimental and thermodynamic investigation on transfer of cadmium influenced by sulfur and chlorine during municipal solid waste (MSW) incineration, *Journal of Hazardous Materials*, 153, 309–319

Zhou H., Jensen P.A., Flemming J.F. (2007) Dynamic mechanistic model of superheater deposit growth and shedding in a biomass fired grate boiler, *Fuel*, 86, 1519-1533.

Zubtsov V.M., Pian C.C.P., Yoshikawa K. (2005) Potential applications of high-temperatureair/steam-blowngasification and pyrolysis systems, *Energy*, 30, 2229–2242.

Appendix-I

Fluent models set up and inputs summary

FLUENT
Version: 2d, pbns, spe, ske (2d, pressure-based, species, standard k-epsilon)
Release: 6.3.26
Title:

Models

Model	Settings
Space	2D
Time	Steady
Viscous	Standard k-epsilon turbulence model
Wall Treatment	Standard Wall Functions
Heat Transfer	Enabled
Solidification and Melting	Disabled
Radiation	P1 Model
Species Transport	Reacting (6 species)
Coupled Dispersed Phase	Enabled
Pollutants	Disabled
Pollutants	Disabled
Soot	Disabled

Boundary Conditions

Zones

name	id	type
fluid	2	fluid
outle	3	pressure-outlet
symm_axis	4	symmetry
redn_wall	5	wall
fuel_inlet	6	mass-flow-inlet
default-interior	8	interior

Boundary Conditions

fluid

Condition	Value
Material Name	mixture-template
Specify source terms?	no
Source Terms	((mass) (x-momentum) (y-momentum) (k) (epsilon) (species-0) (species-1) (species-2) (species-3) (species-4) (energy) (p1))
Specify fixed values?	no
Fixed Values	((x-velocity (inactive . #f) (constant . 0) (profile)) (y-velocity (inactive . #f) (constant . 0) (profile)) (k (inactive . #f) (constant . 0) (profile)) (epsilon (inactive . #f) (constant . 0) (profile)) (species-0 (inactive . #f) (constant . 0) (profile)) (species-1 (inactive . #f) (constant . 0) (profile)) (species-2 (inactive . #f) (constant . 0) (profile)) (species-3 (inactive . #f) (constant . 0) (profile)) (species-4 (inactive . #f) (constant . 0) (profile)) (temperature (inactive . #f) (constant . 0) (profile)))
Motion Type	0
X-Velocity Of Zone (m/s)	0
Y-Velocity Of Zone (m/s)	0
Rotation speed (rad/s)	0
X-Origin of Rotation-Axis (m)	0
Y-Origin of Rotation-Axis (m)	0
Deactivated Thread	no
Laminar zone?	no
Set Turbulent Viscosity to zero within laminar zone?	yes
Porous zone?	yes
X-Component of Direction-1 Vector	1
Y-Component of Direction-1 Vector	0
Relative Velocity Resistance Formulation?	yes
Direction-1 Viscous Resistance (1/m2)	0
Direction-2 Viscous Resistance (1/m2)	0
Choose alternative formulation for inertial resistance?	no
Direction-1 Inertial Resistance (1/m)	0
Direction-2 Inertial Resistance (1/m)	0
C0 Coefficient for Power-Law	0
C1 Coefficient for Power-Law	0
Porosity	0.5
Solid Material Name	char
Reaction Mechanism	0
Activate reaction mechanisms?	yes
Surface-Volume-Ratio (1/m)	0

outle

Condition	Value

Gauge Pressure (pascal) -10
Backflow Total Temperature (k) 900
Backflow Direction Specification Method 1
X-Component of Flow Direction 1
Y-Component of Flow Direction 0
X-Component of Axis Direction 1
Y-Component of Axis Direction 0
Z-Component of Axis Direction 0
X-Coordinate of Axis Origin (m) 0
Y-Coordinate of Axis Origin (m) 0
Z-Coordinate of Axis Origin (m) 0
Turbulent Specification Method 3
Backflow Turbulent Kinetic Energy (m2/s2) 1
Backflow Turbulent Dissipation Rate (m2/s3) 1
Backflow Turbulent Intensity (%) 0.099999994
Backflow Turbulent Length Scale (m) 1
Backflow Hydraulic Diameter (m) 0.17
Backflow Turbulent Viscosity Ratio 10
External Black Body Temperature Method 0
Black Body Temperature (k) 300
Internal Emissivity 1
Backflow (((constant . 0.2) (profile)) ((constant . 0.12) (profile)) ((constant . 0.02) (profile)) ((constant . 0.1) (profile)) ((constant . 0) (profile)))
Discrete Phase BC Type 3
Discrete Phase BC Function none
is zone used in mixing-plane model? no
Specify targeted mass flow rate no
Targeted mass flow (kg/s) 1

symm_axis

Condition Value
---

redn_wall

Condition	Value
Wall Thickness (m)	0
Heat Generation Rate (w/m3)	0
Material Name	aluminum
Thermal BC Type	0
Temperature (k)	700
Heat Flux (w/m2)	0
Convective Heat Transfer Coefficient (w/m2-k)	0
Free Stream Temperature (k)	300
Wall Motion	0
Shear Boundary Condition	0
Define wall motion relative to adjacent cell zone?	yes
Apply a rotational velocity to this wall?	no
Velocity Magnitude (m/s)	0
X-Component of Wall Translation	1
Y-Component of Wall Translation	0
Define wall velocity components?	no
X-Component of Wall Translation (m/s)	0
Y-Component of Wall Translation (m/s)	0
Internal Emissivity	1
External Emissivity	1
External Radiation Temperature (k)	300
Wall Roughness Height (m)	0
Wall Roughness Constant	0.5
Discrete Phase BC Type	2
Normal	((polynomial angle 1))
Tangent	((polynomial angle 1))
Discrete Phase BC Function	none
Impact Angle Function	((polynomial angle 1))
Diameter Function	((polynomial 1.8e-09))
Velocity Exponent Function	((polynomial 0))
	(0 0 0 0 0)
	(((constant . 0) (profile)) ((constant . 0) (profile)) ((constant . 0) (profile)) ((constant . 0) (profile)) ((constant . 0) (profile)))
Rotation Speed (rad/s)	0
X-Position of Rotation-Axis Origin (m)	0
Y-Position of Rotation-Axis Origin (m)	0
X-component of shear stress (pascal)	0
Y-component of shear stress (pascal)	0
Surface tension gradient (n/m-k)	0
Specularity Coefficient	0

fuel_inlet

Condition	Value
Mass Flow Specification Method	0
Mass Flow-Rate (kg/s)	8.2348903e-05
Mass Flux (kg/m2-s)	1
Average Mass Flux (kg/m2-s)	1
Upstream Torque Integral (n-m)	1
Upstream Total Enthalpy Integral (w/m2)	1
Total Temperature (k)	1254
Supersonic/Initial Gauge Pressure (pascal)	0
Direction Specification Method	1
Reference Frame	0
X-Component of Flow Direction	1
Y-Component of Flow Direction	0
X-Component of Axis Direction	1
Y-Component of Axis Direction	0
Z-Component of Axis Direction	0
X-Coordinate of Axis Origin (m)	0
Y-Coordinate of Axis Origin (m)	0
Z-Coordinate of Axis Origin (m)	0
Turbulent Specification Method	3
Turbulent Kinetic Energy (m2/s2)	1
Turbulent Dissipation Rate (m2/s3)	1
Turbulent Intensity (%)	0.099999994
Turbulent Length Scale (m)	1
Hydraulic Diameter (m)	0.22
Turbulent Viscosity Ratio	

10

(((constant . 0.05198) (profile)) ((constant . 0.046999998) (profile)) ((constant . 0.064769998) (profile)) ((constant . 0.061560001) (profile)) ((constant . 0.093450002) (profile)))

External Black Body Temperature Method	0
Black Body Temperature (k)	300
Internal Emissivity	1
Discrete Phase BC Type	2
Discrete Phase BC Function	none
is zone used in mixing-plane model?	no

default-interior

Condition Value

Solver Controls

Equations

Equation	Solved
Flow	no
Turbulence	yes
co	yes
h2	yes
ch4	yes
co2	yes
h2o	yes
Energy	yes
P1	yes

Numerics

Numeric	Enabled
Absolute Velocity Formulation	yes

Relaxation

Variable	Relaxation Factor
Pressure	0.1
Density	0.94999999
Body Forces	1
Momentum	0.1
Turbulent Kinetic Energy	0.80000001
Turbulent Dissipation Rate	0.80000001
Turbulent Viscosity	1
co	0.94999999
h2	0.94999999
ch4	0.94999999
co2	0.94999999
h2o	0.94999999
Energy	1
P1	0.89999998
Discrete Phase Sources	0.5

Linear Solver

Variable	Solver Type	Termination Criterion	Residual Reduction Tolerance
Pressure	V-Cycle	0.1	
X-Momentum	Flexible	0.1	0.7
Y-Momentum	Flexible	0.1	0.7
Turbulent Kinetic Energy	Flexible	0.1	0.7
Turbulent Dissipation Rate	Flexible	0.1	0.7
co	Flexible	0.1	0.7
h2	Flexible	0.1	0.7
ch4	Flexible	0.1	0.7
co2	Flexible	0.1	0.7
h2o	Flexible	0.1	0.7
Energy	Flexible	0.1	0.7
P1	Flexible	0.1	0.7

Pressure-Velocity Coupling

Parameter	Value
Type	SIMPLE

Discretization Scheme

Variable	Scheme
Pressure	Standard
Momentum	First Order Upwind
Turbulent Kinetic Energy	First Order Upwind
Turbulent Dissipation Rate	First Order Upwind
co	First Order Upwind
h2	First Order Upwind
ch4	First Order Upwind
co2	First Order Upwind
h2o	First Order Upwind
Energy	First Order Upwind

Solution Limits

Quantity	Limit
Minimum Absolute Pressure	1
Maximum Absolute Pressure	4.9999999e+10
Minimum Temperature	1
Maximum Temperature	5000
Minimum Turb. Kinetic Energy	9.9999998e-15
Minimum Turb. Dissipation Rate	9.9999997e-21
Maximum Turb. Viscosity Ratio	100000

Material Properties

Material: carbon (combusting-particle)

Property	Units	Method	Value(s)
Density	kg/m3	constant	2000
Cp (Specific Heat)	j/kg-k	constant	1220
Thermal Conductivity	w/m-k	constant	0.045400001
Latent Heat	j/kg	constant	0
Vaporization Temperature	k	constant	400
Volatile Component Fraction	%	constant	0
Binary Diffusivity	m2/s	constant	3.9999999e-05
Particle Emissivity		constant	0.89999998
Particle Scattering Factor		constant	0
Swelling Coefficient		constant	1
Burnout Stoichiometric Ratio		constant	2.67
Combustible Fraction	%	constant	100
Heat of Reaction for Burnout	j/kg	constant	32789000
React. Heat Fraction Absorbed by Solid	%	constant	29.999998
Devolatilization Model	1/s	constant	0
Combustion Model	multiple-surface-reactions		(0 0)

Material: (carbon-solid . mixture-template) (fluid)

Property	Units	Method	Value(s)
Cp (Specific Heat)	j/kg-k	constant	1220
Molecular Weight	kg/kgmol	constant	12.01115
Standard State Enthalpy	j/kgmol	constant	-101.268
Standard State Entropy	j/kgmol-k	constant	5731.747
Reference Temperature	k	constant	298
L-J Characteristic Length	angstrom	constant	0
L-J Energy Parameter	k	constant	0
Degrees of Freedom		constant	0
Speed of Sound	m/s	none	#f

Material: (carbon-dioxide . mixture-template) (fluid)

Property	Units	Method	Value(s)
Cp (Specific Heat)	j/kg-k	constant	840.37
Molecular Weight	kg/kgmol	constant	44.00995
Standard State Enthalpy	j/kgmol	constant	-3.9353235e+08
Standard State Entropy	j/kgmol-k	constant	213720.2
Reference Temperature	k	constant	298.15
L-J Characteristic Length	angstrom	constant	3.941
L-J Energy Parameter	k	constant	195.2
Degrees of Freedom		constant	0
Speed of Sound	m/s	none	#f

Material: (methane . mixture-template) (fluid)

Property	Units	Method	Value(s)
Cp (Specific Heat)	j/kg-k	constant	2222
Molecular Weight	kg/kgmol	constant	16.04303
Standard State Enthalpy	j/kgmol	constant	-74895176
Standard State Entropy	j/kgmol-k	constant	186040.09
Reference Temperature	k	constant	298.15
L-J Characteristic Length	angstrom	constant	3.758
L-J Energy Parameter	k	constant	148.6
Degrees of Freedom		constant	0
Speed of Sound	m/s	none	#f

Material: (hydrogen . mixture-template) (fluid)

Property	Units	Method	Value(s)
Cp (Specific Heat)	j/kg-k	constant	14283
Molecular Weight	kg/kgmol	constant	2.01594
Standard State Enthalpy	j/kgmol	constant	0
Standard State Entropy	j/kgmol-k	constant	130579.06
Reference Temperature	k	constant	298.15
L-J Characteristic Length	angstrom	constant	2.92
L-J Energy Parameter	k	constant	38
Degrees of Freedom		constant	0
Speed of Sound	m/s	none	#f

Material: (carbon-monoxide . mixture-template) (fluid)

Property	Units	Method	Value(s)
Cp (Specific Heat)	j/kg-k	constant	1043
Molecular Weight	kg/kgmol	constant	28.01055
Standard State Enthalpy	j/kgmol	constant	-1.1053956e+08
Standard State Entropy	j/kgmol-k	constant	197531.64
Reference Temperature	k	constant	298.15
L-J Characteristic Length	angstrom	constant	0
L-J Energy Parameter	k	constant	0
Degrees of Freedom		constant	0
Speed of Sound	m/s	none	#f

Material: char (solid)

Property	Units	Method	Value(s)
Density	kg/m3	constant	2000
Cp (Specific Heat)	j/kg-k	constant	1220
Thermal Conductivity	w/m-k	constant	0.17299999

Material: methane (fluid)

Property	Units	Method	Value(s)
Density	kg/m3	constant	0.6679
Cp (Specific Heat)	j/kg-k	constant	2222
Thermal Conductivity	w/m-k	constant	0.0332
Viscosity	kg/m-s	constant	1.087e-05
Molecular Weight	kg/kgmol	constant	16.04303
Standard State Enthalpy	j/kgmol	constant	-74895176
Standard State Entropy	j/kgmol-k	constant	186040.09
Reference Temperature	k	constant	298.15
L-J Characteristic Length	angstrom	constant	3.758
L-J Energy Parameter	k	constant	148.6
Absorption Coefficient	1/m	constant	0.62
Scattering Coefficient	1/m	constant	0
Scattering Phase Function		isotropic	#f
Thermal Expansion Coefficient	1/k	constant	0
Degrees of Freedom		constant	0
Speed of Sound	m/s	none	#f

Material: hydrogen (fluid)

Property	Units	Method	Value(s)
Density	kg/m3	constant	0.08189
Cp (Specific Heat)	j/kg-k	constant	14283
Thermal Conductivity	w/m-k	constant	0.1672
Viscosity	kg/m-s	constant	8.411e-06
Molecular Weight	kg/kgmol	constant	2.01594
Standard State Enthalpy	j/kgmol	constant	0
Standard State Entropy	j/kgmol-k	constant	130579.06
Reference Temperature	k	constant	298.15
L-J Characteristic Length	angstrom	constant	2.92
L-J Energy Parameter	k	constant	38
Absorption Coefficient	1/m	constant	0
Scattering Coefficient	1/m	constant	0
Scattering Phase Function		isotropic	#f
Thermal Expansion Coefficient	1/k	constant	0
Degrees of Freedom		constant	0
Speed of Sound	m/s	none	#f

Material: carbon-dioxide (fluid)

Property	Units	Method	Value(s)
Density	kg/m3	constant	1.7878

Cp (Specific Heat)	j/kg-k	constant	840.37
Thermal Conductivity	w/m-k	constant	0.0145
Viscosity	kg/m-s	constant	1.37e-05
Molecular Weight	kg/kgmol	constant	44.00995
Standard State Enthalpy	j/kgmol	constant	-3.9353235e+08
Standard State Entropy	j/kgmol-k	constant	213720.2
Reference Temperature	k	constant	298.15
L-J Characteristic Length	angstrom	constant	3.941
L-J Energy Parameter	k	constant	195.2
Absorption Coefficient	1/m	constant	0.43
Scattering Coefficient	1/m	constant	0
Scattering Phase Function		isotropic	#f
Thermal Expansion Coefficient	1/k	constant	0
Degrees of Freedom		constant	0
Speed of Sound	m/s	none	#f

Material: carbon-monoxide (fluid)

Property	Units	Method	Value(s)
Density	kg/m3	constant	1.1233
Cp (Specific Heat)	j/kg-k	constant	1043
Thermal Conductivity	w/m-k	constant	0.025
Viscosity	kg/m-s	constant	1.75e-05
Molecular Weight	kg/kgmol	constant	28.01055
Standard State Enthalpy	j/kgmol	constant	-1.1053956e+08
Standard State Entropy	j/kgmol-k	constant	197531.64
Reference Temperature	k	constant	298.15
L-J Characteristic Length	angstrom	constant	0
L-J Energy Parameter	k	constant	0
Absorption Coefficient	1/m	constant	0.17
Scattering Coefficient	1/m	constant	0
Scattering Phase Function		isotropic	#f
Thermal Expansion Coefficient	1/k	constant	0
Degrees of Freedom		constant	0
Speed of Sound	m/s	none	#f

Material: carbon-solid (fluid)

Property	Units	Method	Value(s)
Density	kg/m3	constant	2000
Cp (Specific Heat)	j/kg-k	constant	1220
Thermal Conductivity	w/m-k	constant	0.0454
Viscosity	kg/m-s	constant	1.72e-05
Molecular Weight	kg/kgmol	constant	12.01115
Standard State Enthalpy	j/kgmol	constant	-101.268
Standard State Entropy	j/kgmol-k	constant	5731.747
Reference Temperature	k	constant	298
L-J Characteristic Length	angstrom	constant	0
L-J Energy Parameter	k	constant	0
Absorption Coefficient	1/m	constant	0
Scattering Coefficient	1/m	constant	0
Scattering Phase Function		isotropic	#f
Thermal Expansion Coefficient	1/k	constant	0
Degrees of Freedom		constant	0
Speed of Sound	m/s	none	#f

Material: mixture-template (mixture)

Property	Units	Method	Value(s)
Mixture Species	names		((co h2 ch4 co2 h2o n2) (c<s>) ())
Reaction	finite-rate		((reaction-1 ((c<s> 1 0 1) (co2 1 0.38 1)) ((co 2 0 1)) ((h2 0 1) (ch4 0 1) (h2o 0 1) (n2 0 1)) (stoichiometry 1c<s> + 1co2 --> 2co) (arrhenius 36.16 77390000 0) (mixing-rate 4 0.5) (use-third-body-efficiencies? . #f) (particle-reaction? . #t) (catalyst-species c<s>) (diffusion-species co) (particle-rate 5e-12 1)) (reaction-2 ((c<s> 1 0 1) (h2o 1 0.60000002 1)) ((co 1 0 1) (h2 1 0 1)) ((ch4 0 1) (co2 0 1) (n2 0 1)) (stoichiometry 1c<s> + 1h2o --> 1co + 1h2) (arrhenius 15170 12160000 0) (mixing-rate 4 0.5) (use-third-body-efficiencies? . #f) (particle-reaction? . #t) (catalyst-species c<s>) (diffusion-species co) (particle-rate 5e-12 1)) (reaction-3 ((c<s> 1 0 1) (h2 2 1 1)) ((ch4 1 0 1)) ((co 0 1) (co2 0 1) (h2o 0 1) (n2 0 1)) (stoichiometry 1c<s> + 2h2 --> 1ch4) (arrhenius 0.0040000002 19210000 0) (mixing-rate 4 0.5) (use-third-body-efficiencies? . #f) (particle-reaction? . #t) (catalyst-species c<s>) (diffusion-species co) (particle-rate 5e-12 1)) (reaction-4 ((ch4 1 1 1) (h2o 1 1 1)) ((co 1 1 1) (h2 3 3 1)) ((co2 0 1) (n2 0 1)) (stoichiometry 1ch4 + 1h2o --> 1co + 3h2) (arrhenius 0.072999999 36000000 0) (mixing-rate 4 0.5) (use-third-body-efficiencies? . #f) (backward-reaction? . #t)) (reaction-5 ((co 1 1 1) (h2o 1 1 1)) ((co2 1 0 1) (h2 1 1 1)) ((ch4 0 1) (n2 0 1)) (stoichiometry 1co + 1h2o --> 1co2 + 1h2)

(arrhenius 0.27779999 12000000 0) (mixing-rate 4 0.5) (use-third-body-efficiencies? . #f) (backward-reaction? . #t)))

Mechanism reaction-mechs ((mechanism-1 (reaction-type . all) (reaction-list reaction-1 reaction-2 reaction-3 reaction-4 reaction-5) (site-info)))

Density	kg/m3	incompressible-ideal-gas	#f
Cp (Specific Heat)	j/kg-k	mixing-law	#f
Thermal Conductivity	w/m-k	constant	0.045400001
Viscosity	kg/m-s	constant	1.72e-05
Mass Diffusivity	m2/s	constant-dilute-appx	(2.88e-05)
Thermal Diffusion Coefficient	kg/m-s	kinetic-theory	#f
Absorption Coefficient	1/m	wsggm-cell-based	#f
Scattering Coefficient	1/m	constant	0.89999998
Scattering Phase Function		isotropic	#f
Thermal Expansion Coefficient	1/k	constant	0
Speed of Sound	m/s	none	#f

Material: (nitrogen . mixture-template) (fluid)

Property	Units	Method	Value(s)
Cp (Specific Heat)	j/kg-k	constant	1040.67
Molecular Weight	kg/kgmol	constant	28.0134
Standard State Enthalpy	j/kgmol	constant	0
Standard State Entropy	j/kgmol-k	constant	191494.78
Reference Temperature	k	constant	298.15
L-J Characteristic Length	angstrom	constant	3.621
L-J Energy Parameter	k	constant	97.53
Degrees of Freedom		constant	0
Speed of Sound	m/s	none	#f

Material: nitrogen (fluid)

Property	Units	Method	Value(s)
Density	kg/m3	constant	1.138
Cp (Specific Heat)	j/kg-k	constant	1040.67
Thermal Conductivity	w/m-k	constant	0.0242
Viscosity	kg/m-s	constant	1.663e-05
Molecular Weight	kg/kgmol	constant	28.0134
Standard State Enthalpy	j/kgmol	constant	0
Standard State Entropy	j/kgmol-k	constant	191494.78
Reference Temperature	k	constant	298.15
L-J Characteristic Length	angstrom	constant	3.621
L-J Energy Parameter	k	constant	97.53
Absorption Coefficient	1/m	constant	0
Scattering Coefficient	1/m	constant	0
Scattering Phase Function		isotropic	#f
Thermal Expansion Coefficient	1/k	constant	0
Degrees of Freedom		constant	0
Speed of Sound	m/s	none	#f

Material: oxygen (fluid)

Property	Units	Method	Value(s)
Density	kg/m3	constant	1.2999
Cp (Specific Heat)	j/kg-k	constant	919.31
Thermal Conductivity	w/m-k	constant	0.0246
Viscosity	kg/m-s	constant	1.919e-05
Molecular Weight	kg/kgmol	constant	31.9988
Standard State Enthalpy	j/kgmol	constant	0
Standard State Entropy	j/kgmol-k	constant	205026.86
Reference Temperature	k	constant	298.15
L-J Characteristic Length	angstrom	constant	3.458
L-J Energy Parameter	k	constant	107.4
Absorption Coefficient	1/m	constant	0
Scattering Coefficient	1/m	constant	0
Scattering Phase Function		isotropic	#f
Thermal Expansion Coefficient	1/k	constant	0
Degrees of Freedom		constant	0
Speed of Sound	m/s	none	#f

Material: (water-vapor . mixture-template) (fluid)

Property	Units	Method	Value(s)
Cp (Specific Heat)	j/kg-k	constant	2014
Molecular Weight	kg/kgmol	constant	18.01534
Standard State Enthalpy	j/kgmol	constant	-2.418379e+08
Standard State Entropy	j/kgmol-k	constant	188696.44
Reference Temperature	k	constant	298.15
L-J Characteristic Length	angstrom	constant	2.605
L-J Energy Parameter	k	constant	572.4
Degrees of Freedom		constant	0
Speed of Sound	m/s	none	#f

Material: water-vapor (fluid)

Property	Units	Method	Value(s)
Density	kg/m3	constant	0.5542
Cp (Specific Heat)	j/kg-k	constant	2014
Thermal Conductivity	w/m-k	constant	0.0261
Viscosity	kg/m-s	constant	1.34e-05
Molecular Weight	kg/kgmol	constant	18.01534
Standard State Enthalpy	j/kgmol	constant	-2.418379e+08
Standard State Entropy	j/kgmol-k	constant	188696.44
Reference Temperature	k	constant	298.15
L-J Characteristic Length	angstrom	constant	2.605
L-J Energy Parameter	k	constant	572.4
Absorption Coefficient	1/m	constant	0.54
Scattering Coefficient	1/m	constant	0
Scattering Phase Function		isotropic	#f
Thermal Expansion Coefficient	1/k	constant	0
Degrees of Freedom		constant	0
Speed of Sound	m/s	none	#f

Material: air (fluid)

Property	Units	Method	Value(s)
Density	kg/m3	constant	1.225
Cp (Specific Heat)	j/kg-k	constant	1006.43
Thermal Conductivity	w/m-k	constant	0.0242
Viscosity	kg/m-s	constant	1.7894e-05
Molecular Weight	kg/kgmol	constant	28.966
Standard State Enthalpy	j/kgmol	constant	0
Standard State Entropy	j/kgmol-k	constant	0
Reference Temperature	k	constant	298.15
L-J Characteristic Length	angstrom	constant	3.711
L-J Energy Parameter	k	constant	78.6
Absorption Coefficient	1/m	constant	0
Scattering Coefficient	1/m	constant	0
Scattering Phase Function		isotropic	#f
Thermal Expansion Coefficient	1/k	constant	0
Degrees of Freedom		constant	0
Speed of Sound	m/s	none	#f

Material: aluminum (solid)

Property	Units	Method	Value(s)
Density	kg/m3	constant	2719
Cp (Specific Heat)	j/kg-k	constant	871
Thermal Conductivity	w/m-k	constant	202.4

Appendix-II

Accuracies and Uncertainties in the Measurement

Exhaust Gases	Measurement range	Resolution	Accuracy	Uncertainty
CO	$0-10$ vol%	0.01 vol%	$< 0.6\% \, vol +/- \, 0.03\%$vol.	2.0%
			>0.6% vol. +/- 0.5% of indicated Value	
HC	$0-20000$ ppm	<2000: 1 ppm vol.	<200 ppm vol.+/- 10ppm	$\pm$ 0. 06%
		>2000:20ppm vol.	vol>200ppm vol. +/- 5% of ind. Val.	
CO_2	$0-20 \, vol.\%$	0.1 vol.%	<10% vol.+/-5% vol.>10%	
			vol. +/- 5% of Val. M	
O_2	$0-22 \, vol.\%$	0.01 vol.%	<2% vol.+/-0.1% vol.>2%	
			vol. +/- 5% of Val. M	
NO_x	$\Delta 0-5000$ppm	1ppm vol.	<500ppm vol.: +/- 50 ppm vol. >500ppm vol.:+/- 10% of ind. Val.	$\pm$0. 02%
Smoke	0-500	0.01%	+/- 5% of indicated Value	$\pm$0. 02%

Sample Calculation for NOx Measurement

(a) Fixed error

Maximum capacity of Multi Gas Analyser (MGA) = 5000ppm

Minimum measurement = 1ppm

Divisioning = 0.002%

Least count of M G A= 1ppm

NOx = 84 (for an illustration)

(b) Confidence limit

Probable measurement error (P_e) = $\pm$ (1ppm)= $\pm$ 0.002%

Probable value of a single measurement = (84 $\pm$ 0.5)=84.5

(c) Propagation of uncertainty

Relative uncertainty (U_r) = $\pm$ (P_e / W_o) = $\pm$ (0.002/ 84) = $\pm$ 0.00002

U_r in terms of percentage = $\pm$ U_r X 100 = $\pm$(0.0208) X 100 = $\pm$ 0.002%

Appendix-III

Calibration Report of Thermocouple (K-type) provided by Manufacturer

Indicator-UNICAL 3001m, ambient temperature 33°C

S.No.	Source temperature (°C)	Instrument temperature (°C)
1.	100	99.8
2.	300	299.4
3.	500	298.9
4.	700	698.9
5.	900	896.8

List of publications from the research

Papers Published in Journals

- "ENERGY AND EXERGY ANALYSIS OF THE REDUCTION ZONE IN A DOWNDRAFT(BIOMASS) GASIFIER"

  Published in International Journal of Chemical Reactor Engineering. Volume 8, 2010, Article A88.

- "A 2-D NON PREMIXED COMBUSTION MODELING OF A DOWNDRAFT BIOMASS GASIFIER"

  Published in Global Journal of mechanical Engineering and Computational science – ISSN 2249-3468, Vol. 1 (3).

- "THERMODYNAMIC MODELING OF DOWNDRAFT GASIFICATION OF RDF"

  International Journal of Applied Engineering Research (IJAER) (2011).

Papers Presented in Conferences

- "EXERGY ANALYSIS OF PYROLYTIC DECOMPOSITION OF BIOMASS AT SLOW HEATING RATES"

  Presented at the National Conference on Recent Advances in mechanical and Production Engineering, Pantnagar. February 12-14, 2009.

- "SUITABILITY OF GASIFICATION TECHNOLOGIES FOR TREATING MUNICIPAL SOLID WASTE OF DELHI"

  Presented at the National Conference on Recent Advances in Mechanical and Production Engineering Pantnagar, February 12-14, 2009.

Bio Data

Mr. Rajkumar singh was born in 1966. He did his graduation in mechanical engineering with First division Honours from government engineering college Rani Durgavati Vishwavidyalay, Jabalpur, Madhya Pradesh. He did his post graduation (first division) in Applied Mechanics from IIT Delhi in 1990. Subsequently he joined ChotuRam State college of Engineering Murthal, Sonipat, Hariyana in 1990, where he taught till 2004. Subsequently he joined Delhi College of Engineering and engaged in teaching UG and PG level Mechanical Enginering.His area of interest is Fluid Mechanics and Solid Mechanics.